National Defence / Défense nationale


# AN ANALYSIS OF THE EXPERIMENTAL DATA MEASURED WITH THE MODIFIED HF SURFACE-WAVE RADAR AT CAPE BONAVISTA

by

Hank W.H. Leong



DEFENCE RESEARCH ESTABLISHMENT OTTAWA
REPORT NO. 1312



Canada

July 1997
Ottawa

National Défense
Defence nationale

# AN ANALYSIS OF THE EXPERIMENTAL DATA MEASURED WITH THE MODIFIED HF SURFACE-WAVE RADAR AT CAPE BONAVISTA

by

**Hank W.H. Leong**
*Surface Radar Section*

**DEFENCE RESEARCH ESTABLISHMENT OTTAWA**
REPORT NO. 1312

PROJECT
05AB11

July 1997
Ottawa

# An Analysis of the Experimental Data Measured with the Modified HF Surface-Wave Radar at Cape Bonavista

## Abstract

This report presents the results of an analysis of the data measured with the experimental High-Frequency Surface-Wave Radar (HFSWR) at Cape Bonavista, after a major modification in the radar receiver. The radar was evaluated at four different radio frequencies (4.3, 10.62, 18.65 and 27.8 MHz) and a target was detected at each of the frequencies. Specifically, a low-flying Beechcraft Kingair was detected beyond the line of sight to a distance of about 110 km when the radar operated at 4.3 MHz with an average transmitter power of about 40 Watts. A low-flying Piper Navajo was detected within the line of sight up to a range of 26 km when the radar operated at 27.8 MHz. Half-wavelength long copper wires (#18 AWG) were used as test targets at the radio frequencies of 10.62 and 18.65 MHz. Each wire was attached to a helium balloon, which was then carried away by a strong outward wind. Some of these targets were tracked to a range of about 101 km at 10.62 MHz, and to a range of about 66 km at 18.65 MHz.

The detection of the Kingair by the HFSWR at 4.3 MHz was also studied by simulation. The simulation results showed that the radar could detect the Kingair up to a distance of 95 km. By comparing the simulation results with the experimental results at 4.3 MHz, we found that the measured performance of the radar agreed well with the theoretical performance in the range interval from 35 to 95 km, when the target was detected beyond the line of sight. The measured target signal-to-noise ratio (SNR) and the theoretical target SNR showed almost the same range dependence in the specified range interval, with the measured SNR approximately proportional to $R^{-4.71}$, where R is the target range.

# Analyse des données expérimentales mesurées à l'aide du radar haute-fréquence à ondes de surface modifié du Cap Bonavista

## Résumé

Ce rapport présente les résultats d'une analyse des données mesurées à l'aide du radar haute-fréquence à ondes de surface (HFSWR) expérimental du Cap Bonavista, dont le récepteur radar a subi des modifications majeures. Le radar a été testé à quatre différentes fréquences radio (4.3, 10.62, 18.65, 27.8 MHz); pour chacune de ces fréquences une cible a été détectée. Notamment, un Kingair de Beechcraft volant à basse altitude a été détecté au-delà de la portée optique, à une distance d'environ 110 km lorsque le radar opérait à 4.3 MHz et que la puissance moyenne de son transmetteur était d'environ 40 watts. Un Navajo de Piper volant lui aussi à basse altitude a été détecté dans un rayon allant jusqu'à 26 km; le radar opérait alors à 27.8 MHz. Des fils de cuivre d'une demi-longueur d'onde (n° 18 AWG) ont servi de cibles d'essai pour les fréquences radio de 10.62 et 18.65 MHz. Chaque fil était attaché à un ballon gonflé à l'hélium qui, par la suite, était poussé au large par un vent fort. Quelques-unes des cibles ont été poursuivies jusqu'à environ 101 km pour une fréquence de 10.62 MHz, tandis que d'autres cibles l'ont été jusqu'à environ 66 km pour une fréquence de 18.65 MHz.

De plus, la détection du Kingair par le HFSWR à une fréquence de 4.3 MHz a fait l'objet d'une étude par simulation. Les résultats de la simulation démontrent que le radar peut détecter le Kingair dans un rayon atteignant jusqu'à 95 km. En comparant les résultats expérimentaux de 4.3 MHz et de la simulation, nous pouvons conclure que la performance mesurée du radar correspond de manière assez juste à la performance théorique, et ce pour un intervalle de portée de 35 à 95 km, lorsque la cible était détectée au-delà de la portée optique. Le rapport du signal au bruit (SNR) de la cible mesurée et celui de la cible théorique ont presque la même dépendance de portée dans l'intervalle de portée mentionné, le SNR mesuré étant approximativement proportionnel à $R^{-4.71}$, R représentant la distance de la cible.

# Executive Summary

The High-Frequency Surface-Wave Radar (HFSWR) at Cape Bonavista was modified in 1991 and 1992 to include an on-board receiver preprocessor and a solid-state transmitter [5,6]. Following the modification, a sequence of trials were carried out over a four-day period to evaluate the operation of the HFSWR over a wide range of radio frequencies (RFs) in the HF band (3-30 MHz). This report presents the results of an analysis of the data collected in the trials. The focus of the analysis is on the detection of targets deployed for the HFSWR. By detecting the deployed targets, we then demonstrate the successful operation of the radar at the various RFs.

Two types of targets were used. The first was low-flying aircraft, and the second was vertical, half-wavelength long, #18 AWG copper wire. The aircraft targets included a C-GMWR Beechcraft Kingair and a C-GWLW Piper Navajo Chieftain. The Kingair flew at an altitude of about 50 feet and the Navajo flew at about 100 feet. With the algorithm in [3], the Kingair was detected beyond the line of sight out to a range of about 110 km, when the radar operated at the RF of 4.3 MHz and the average transmit power was about 40 Watts. The detection of the Navajo was carried out at 27.8 MHz. Here, the maximum detectable range was about 26 km only. Each one of the thin wires was attached to a helium balloon, which was then carried away by a strong outward wind. Four balloons were used at each RF, attached with the wires cut to the length of 14.12 m at 10.62 MHz and the length of 8.04 m at 18.65 MHz. Three were detected at each one of these RFs. Some of them were tracked in range from 54 km to 101 km at 10.62 MHz, and from 44 km to 66 km at 18.65 MHz.

The detection of the Kingair by the HFSWR at 4.3 MHz was also studied by simulation. The simulation results showed that the radar could detect the Kingair up to a range of 95 km. By comparing the simulation results with the experimental results at 4.3 MHz, we found that the measured performance of the radar agreed well with the theoretical performance in the range interval between 35 and 95 km, when the target was detected beyond the line of sight. The measured target signal-to-noise ratio (SNR) and the theoretical target SNR showed almost the same range dependence in the specified range interval, with the measured SNR approximately proportional to $R^{-4.71}$, where R is the target range.

Three types of interference were observed in the radar data. The first type was present in the 4.3-MHz radar data. It was localised in range and Doppler, and was caused by a reflection of the

transmitted signal by the F1 layer of the ionosphere. The second type was observed occasionally in the radar data containing signals of the thin wire targets. The interference showed up as bursts in the time series. Each burst produced five equally spaced signals in the Doppler spectrum. The third type of interference was noted in the experiments with the Navajo aircraft, when the radar operated at the RFs of 18.65 and 10.62 MHz. This interference originated from other transmitters in the same frequency band. The presence of the interference made it impossible to detect targets from the two sets of radar data.

The results from the aircraft detection show that our models predict the range performance of the HFSWR adequately. For long range over-the-horizon detection of ship and aircraft targets, lower frequencies, e.g., 4 MHz, are preferred. Ranges greater than 100 km were obtained on the Kingair with a modest transmit power of only about 40 Watts average and with small transmitting and receiving antenna apertures. An operational radar system would use a higher power and larger antenna apertures, and therefore provide better range performance. However, the detection performance can be much worse if interference is present. Techniques to avoid or mitigate co-channel interference are being developed at DREO and will be the subject of future reports.

The signal strengths of the detected thin wires are not discussed in this report. However, we would like to point out that the lengths of the thin wires were at resonance with the transmitted radar signal. Hence, the detection results of the thin wires provide some indications of the optimum performance of the HF radar in the detection of tactical ballistic missiles (TBM), which is currently considered as an option for cueing the TBMs in air defence. The target signals can also be compared with the sea echoes of the radar to provide an estimation of the sea scattering coefficient at HF. This estimation will be reported shortly.

# Table of Contents

# List of Figures

# 1. Introduction

Aided by a relatively high conductivity of sea water (typically 4 mho/m), vertically polarized electromagnetic waves in the upper MF band and in the HF band (~2 - 30 MHz) can propagate along an ocean surface to distances far beyond the line of sight. A HF Surface-Wave Radar (HFSWR) takes advantage of this surface mode of propagation to provide surveillance of air and surface targets over the entire volume of airspace above the sea water. Since the late 1980s, the Surface Radar Section of DREO has been undertaking a research and development program in HFSWRs. Encouraging detection results were obtained in 1989 using an experimental 1.95-MHz HFSWR system at Cape Bonavista, Newfoundland [1]; ocean-going ships were detected at ranges up to 500 km [2], and trans-Atlantic aircraft were detected at ranges up to 280 km [3].

The above detection, however, could not be made on-line because a radar preprocessor was not available, and the radar data had to be preprocessed on a different computer [1,4]. Under a contract to the Department of National Defence, Raytheon Canada Limited then developed an on-board preprocessor for the radar receiver [5] and subsequently modified the HFSWR to incorporate the preprocessor into the radar system [6]. Included in the modifications were also a solid-state transmitter as well as new transmitting and receiving antenna arrays. The ANALOGIC solid-state transmitter replaced the LORAN-A transmitter that had previously been used in the HFSWR at Cape Bonavista, thus permitting the operation of the radar throughout the HF band. After the modification, a number of trials were conducted to evaluate the operation of the new HFSWR system at the radio frequencies (RFs) of 4.3, 10.62, 18.65 and 27.8 MHz.

This report presents the results of an analysis of the data collected in the trials. The focus of the analysis is on the detection of the targets deployed in the trials. Two types of targets were used. The first was low-flying aircraft and the objective was to demonstrate the radar's capability to detect the target beyond the line of sight. The second was vertical, half-wavelength long, #18 AWG copper wire. Each one of the thin wires was carried by a helium balloon; one end of the wire was attached to the balloon and the other was hung freely down from the balloon. The thin wires were at resonance with the transmitted radar signal and they have known radar cross-sections in free space. One objective of the trials was to use the signals from the thin wires to measure the first-order scattering coefficient of the sea at HF. However, in this report, we only treat them as another type of target used to evaluate the operation of the HFSWR. The measurement of the sea-scattering coefficient will be presented in another report. The algorithm in [3] was used to detect the aircraft, and an empirical and graphical method described in this report was used to detect the wire targets.

The organization of this report is as follows. Section 2 provides a general description of the radar facility and the radar experiments. Section 3 presents a preliminary analysis of the radar data. Sections 4 and 5 show the detection results. In Section 6 are the concluding remarks.

# 2. The Experimental HFSWR

## 2.1 The Radar Facility

The modified HFSWR employed an ANALOGIC solid-state transmitter, capable of operation throughout the HF band of 3-30 MHz. Trains of 50-μs pulses were emitted at the pulse repetition frequencies (PRFs) of 50, 100 or 250 Hz. The radar transmitter had a peak output power of about 8 kW. At the above PRFs, the average power of the radar transmitter was about 20, 40 or 100 Watts, respectively.

Two sets of transmit and receive antennas were installed for operation in two different frequency bands: the first set was for operation at around 4 MHz, and the second set was for operation in the frequency band of 15-20 MHz. On transmit at around 4 MHz, an array of two doublets was used. The two doublet elements were spaced at a distance of 37.5 m, or one half of a wavelength at 4 MHz. Each doublet consisted of two whip antennas (16.5 m, Valcom) separated at a distance of 18.75 m, or one quarter of the wavelength. On receive at around 4 MHz, a linear array of four doublets was used. The receiving doublets also had an adjacent element spacing of 37.5 m and an inter-element separation of 18.75 m. The other set of transmit and receive antennas was developed at DREO. They consisted of whip antennas with adjustable lengths for resonance at different radio frequencies. On transmit, a single doublet was used. For receive, a linear array of 16 whip antennas (singlets) was installed. The spacing between the adjacent singlets was equal to 5 m. In some of the current experiments, however, only the alternate elements, i.e., only eight of the 16 elements, were used on receive. Hence, the spacing between the adjacent elements being used could be equal to 10 m. Specific set-ups of the transmit and receive antennas for the individual experiments will be described further in the next subsection. The arrays were all oriented towards the sea with their boresights at an angle of 110° clockwise from the true north direction.

The radar modification included a new receiver with an on-board preprocessor. The design of the receiver is described in [5]. The signal processing aspects of the receiver are as follows. Initially, the radar signals from the individual antenna elements are summed at RF. Next, the summed signal is down-converted to an Intermediate Frequency (IF) of 25 kHz. Then, the IF signal is sampled at a rate of 125 kHz with a 16-bit Analog-to-Digital Converter (ADC). Finally, the

sampled output is fed into the on-board preprocessor and digitally down-converted into the baseband. In-phase and Quadrature mixing (I and Q channels) are used in the preprocessor to output a complex discrete-time signal. The ADC has a theoretical dynamic range of 96 dB.

The simple sum used in the receive array implies that the radar receives echoes from the boresight direction. The samples of the discrete-time signal are called range samples because they represent the radar echoes from different ranges. The spacing between the adjacent ranges is 1.2 km and is given by $c\,\Delta t/2$, where c is the speed of light ($c=3\times10^8$ m/s) and $\Delta t$ is the sampling period of the ADC ($\Delta t=8$ μs). The radar has a range resolution of 7.5 km, as defined by $c\tau/2$, where $\tau$ is the pulse width (50 μs). Hence, the radar return from a stationary point target is over-sampled by the radar receiver, and the target echo would appear in six or more consecutive range samples (50μs/8μs, or 7.5km/1.2km). The relative amplitudes of this target echo in the range samples, however, depend on the shape of the transmitted pulse. The transmitted pulse has the shape of the first half cycle of a raised cosine so that one can interpolate the target signals in range to locate the maximum. The range at which this maximum signal occurs is considered as the target range of the radar.

## 2.2 The Radar Trials

The radar experiments were carried out during the day on August 15-18, 1992. Two aircraft targets, supplied by the Provincial Airlines Ltd. (PAL) of St. John's, Newfoundland, were used during the experiments. These included a C-GMWR Beechcraft Kingair and a C-GWLW Piper Navajo Chieftain[1]. The Kingair flew one run on August 15 at an altitude of 50 feet, and the Navajo flew two runs on August 17 both at an altitude of 100 feet. The thin wires, cut to the lengths of 8.04 and 14.12 metres, were used as test targets on August 16. These were straight #18 AWG copper wires. Below is a summary of the radar operation and the target deployment during the experiments:

August 15 - Detection of C-GMWR Beechcraft Kingair

The radar operated at a RF of 4.3 MHz, and the PRF was 100 Hz. The first set of transmit and receive antennas was used: the transmit antenna was an array of two doublets and the receive antenna was an array of four doublets.

The Kingair flew along the boresight direction of the receive array. It flew towards the array, turned around and then flew away from the radar. At the end of this flight path, the aircraft

[1] The Beechcraft Kingair is bigger than the Piper Navajo. The Kingair has a wingspan of 16.8 m and an overall length of 13.3 m, and the Navajo has a wingspan of 12.5 m and an overall length of 10.6 m.

also zigzagged along the boresight direction, starting at a range of about 74 km (40 n. mi.). This flight information was provided by PAL of St. John's, Newfoundland.

August 16 - Detection of Half-Wavelength Long Copper Wires attached to Helium Balloons

The half-wavelength long wires were used as test targets when the radar operated at 10.62 and 18.65 MHz. Each one of the thin wires was carried by a helium balloon, with one end of the wire attached to the balloon and the other hung freely down from the balloon. The PRF was 250 Hz. The second set of antennas was used on transmit and receive: the transmit antenna was a single doublet and the receive antenna was a uniform and linear array consisting of eight elements spaced at 10 m, i.e., the alternate eight of the 16 elements.

The balloons were launched from a small boat named Bonni Pauline, which sometimes went away from the radar at a speed of approximately 4.6 m/s (9 knots). The balloons were carried away from the radar by a strong outward wind, and the wind was mostly steady, with a wind speed estimated at 7.7 m/s (15 knots) from the boat near the ocean surface.

Four balloons were released at each radar frequency, and the time interval between the releases was between 5 and 10 minutes. When properly inflated, the balloons rose up to an altitude of about 100 feet at 10.62 MHz and to an altitude of about 200 feet at 18.65 MHz. The first balloon was released at a range of about 39 km (21 n. mi.) from the radar.

August 17 - Detection of C-GWLW Piper Navajo Chieftain

The radar operated successively at RFs of 18.65, 10.62 and 27.8 MHz, and the PRF was 100 Hz at all RFs. The second set of antennas was used on transmit and receive: the transmit antenna was a single doublet and the receive antenna was a uniform and linear array with all the 16 elements.

The Navajo flew two runs along the boresight of the receive array. The flight paths were the same on both runs, and were similar to that of the Kingair. In the first run, the radar operated at 18.65 MHz, and in the second run, it operated briefly at 10.62 MHz when the aircraft approached the radar, and then at 27.8 MHz when the aircraft receded from the radar.

August 17 & 18 - Various tests, mostly at a RF of 4.3 MHz and at a PRF of 50 Hz.

The radar returns, i.e., the complex discrete-time signals from the preprocessor in the receiver, were recorded contiguously for 200 or 300 seconds (depending on the PRF) before they were transferred as a data file onto an 8mm Exabyte tape. A total of ten Exabyte tapes were used to store the data files. A data log of the files on the tapes is shown in Appendix A. For each data file, the information in the log includes: start time and finish time, radar dwell time, radar transmitter frequency, radar PRF and radar range coverage. The range coverage is indicated by the start and end range sample numbers of the radar. For the detection of the aircraft, the range coverage was between 12 and 172.8 km, corresponding to the range sample numbers of 10 and 144. For the detection of the thin wires, the range coverage was between 12 and 106.8 km, corresponding to the range sample numbers of 10 and 89. Note that some files also contain brief comments on the antenna configuration and the target deployment during the time of the data collection.

# 3. Preliminary Data Analysis

## 3.1 HFSWR Time Series

Figure 1 shows the I-channel outputs of four HFSWR time series at the ranges of 69.6, 46.8, 34.8 and 28.8 km, obtained over consecutive radar pulses. The radar frequencies were 4.3, 10.62, 18.65 and 27.8 MHz, respectively, for the four time series. The effective sampling rate of the time series was equal to the PRF of the radar, which was 100 Hz at 4.3 and 27.8 MHz, and 250 Hz at 10.62 and 18.65 MHz. These time series are generally free of interference.

## 3.2 Spectral Analysis

The Discrete Fourier Transform (DFT) was used to analyse the spectral content of the time series. A Blackman window [7] was used before the DFT, and the DFT was computed by using the Fast Fourier Transform (FFT) algorithm. Figure 2 shows the Doppler power spectral densities (PSD), or simply called the Doppler spectra, of the time series in Figure 1. These are, respectively, the squared amplitude outputs of the FFTs applied to the first 4096 points of the time series in Figures 1a and 1d, and to the first 16384 points of the time series in Figures 1b and 1c. At the PRFs chosen for the different RFs, the durations of the data segments are, respectively, equal to 40.96 seconds in Figures 1a and 1d, and 65.54 seconds in Figures 1b and 1c. These are the coherent integration times (CITs) of the radar at the different RFs.

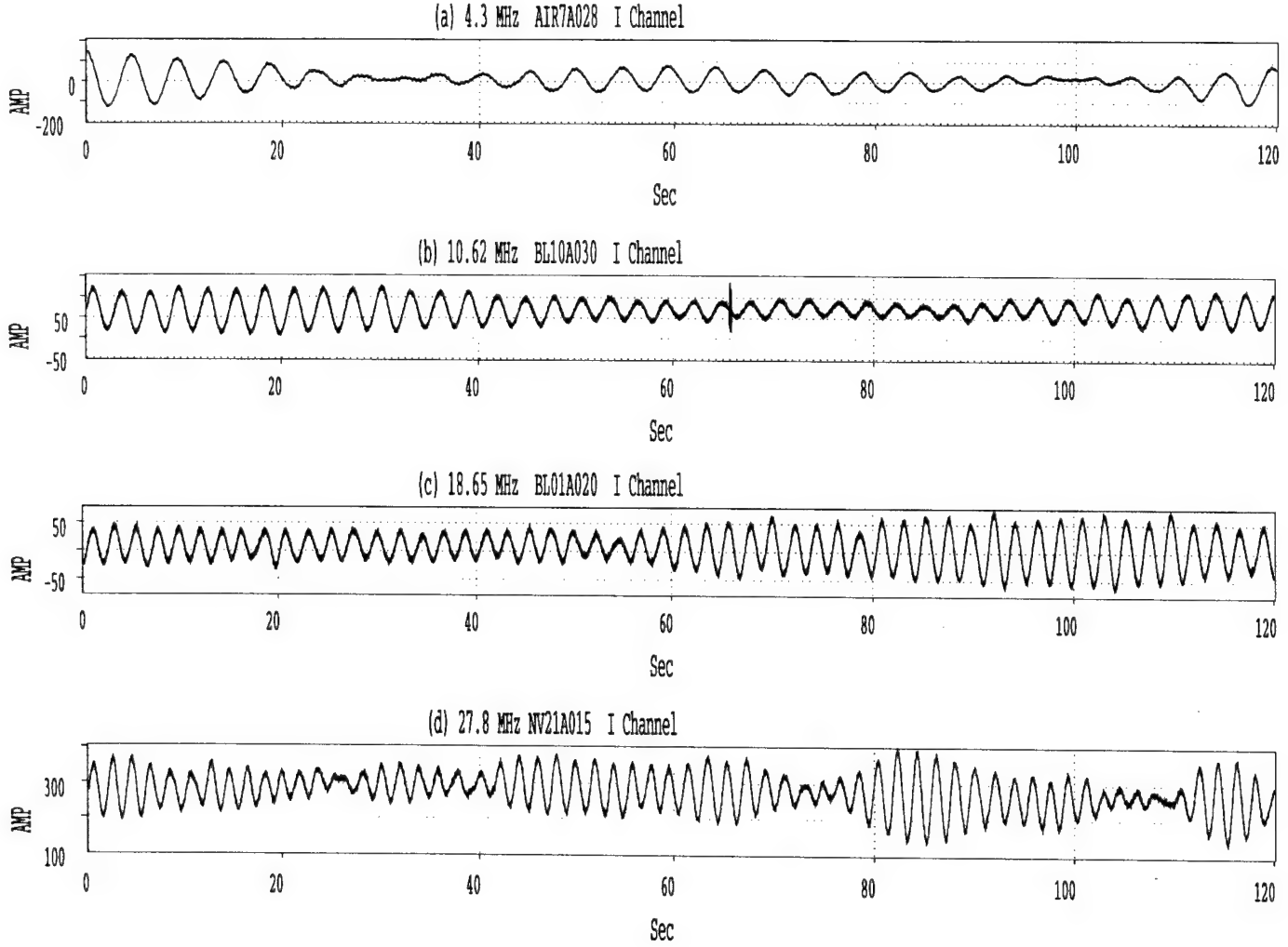


Figure 1 HFSWR Time Series at 4.3, 10.62, 18.65 and 27.8 MHz (only I channel is shown)

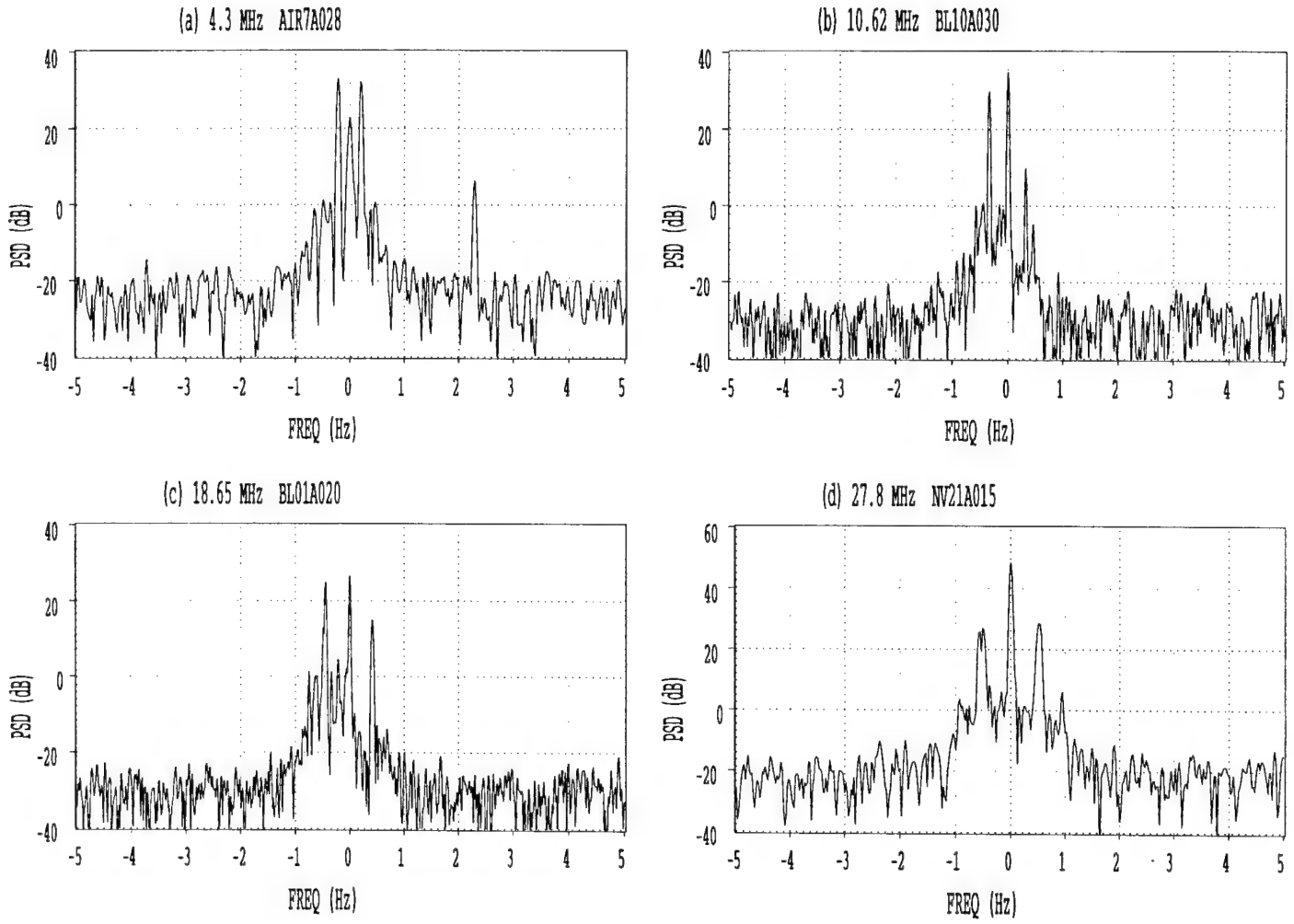


Figure 2 HFSWR Doppler Spectra at 4.3, 10.62, 18.65 and 27.8 MHz

Figure 2 shows the typical characteristics of HFSWR Doppler spectra at relatively close ranges. Assuming that there is no DC bias in the radar receiving system, the spectral power at zero Hertz represents the echo from stationary objects in the selected range bin. This is the ground clutter of the radar, which is mostly picked up through the sidelobes of the receiving antenna array. The two sharp lines on the left and right sides of the ground clutter are the first-order sea echoes scattered back, at near-zero grazing angles, from ocean waves that have a radial spacing exactly equal to one half of the radar wavelength [8]. This is a resonant scattering of the transmitted radar signal. It is similar to the Bragg scattering of X rays in crystals, and hence, the two sharp lines in Figure 2 are referred to as the Bragg lines of the radar. There are two Bragg lines, because the resonant ocean waves are perceived as either advancing or receding from the radar. If there is no ocean current in the radial direction, the Bragg lines have unique Doppler frequencies given by [8]

$$f_B = \pm \sqrt{\frac{g}{\pi\lambda}} \tag{1}$$

where g is the gravitational acceleration (g=9.81 m/s$^2$), and $\lambda$ is the wavelength of the radar. The radar wavelength is given by $\lambda$=c/f, where c is the speed of light and f is the radar operating frequency. Table I lists the Doppler frequencies of the Bragg lines for the four radio frequencies used in the radar experiments.

Table I Bragg Resonant Frequencies in the Radar Experiments

| Radar Frequency (MHz) | Wavelength (m) | Bragg Frequencies (Hz) |
|---|---|---|
| 4.3 | 69.77 | ± 0.211 |
| 10.62 | 28.25 | ± 0.332 |
| 18.65 | 16.09 | ± 0.441 |
| 27.8 | 10.79 | ± 0.538 |

There are other discrete components around the Bragg lines. This is particularly evident in Figures 2b and 2c when the radar operated at 10.62 and 18.65 MHz, respectively. These fine, but less dominant, features result from various second-order scattering processes [9,10]. Collectively, they are referred to as the second-order sea clutter continuum.

The sea clutter continuum is superimposed on a noise spectrum. As the magnitude of the Doppler frequency increases, the level of the sea clutter continuum decays rapidly down to the noise floor of the Doppler spectrum. When the radar operates at 4.3 MHz, for example, the sea-clutter level is below the noise level already when the Doppler frequency is either below -1.0 Hz or above 1.0 Hz. Slow targets such as ships and icebergs are detected against the sea clutter continuum. Fast targets such as aircraft and missiles are detected against the background noise. In Figure 2a, for example, an aircraft signal is shown at the Doppler frequency of about 2.27 Hz, corresponding to a radial velocity of -285 km/hour (-156 knots). This signal is visibly present outside the dominant sea clutter region of -1 and 1 Hz.

Because of the dominance of the Bragg lines, the time series in Figure 1 has a sinusoidal appearance. The magnitude of the Bragg frequencies increases with the radar operating frequency. With the duration of the time series set to 2 minutes (120 seconds) at each of the four operating frequencies, more and more cycles of the dominant sinusoids can be observed in the time series as the radar frequency increases.

### 3.3 Interference in the Data

As for any radar system, the HFSWR is susceptible to interference, either from the radar's own transmissions or from external sources. Unlike microwave radar systems, however, the HFSWR is affected by the ionosphere. During day-time operation, typically in the lower end of HF, the radar's own transmission can be reflected off the ionosphere and returned to the radar receiver. In the upper end of HF, the HFSWR is susceptible to interference from other users of the same frequency band, typically scattered off the ionosphere and propagated from very long distances.

Three types of interference were observed in the experimental HFSWR data. The first type was self-generated, and the others originated from external sources. In the following, the observed interference is described and the effect of the interference on the target detection is discussed.

The first type of interference was observed in the 4.3-MHz radar data. The interference is confined to a range interval between 120 and 173 km; the latter was the maximum instrumentation range of the radar in the experiment. The interference occupies the same Doppler interval as the sea clutter, and hence is also confined in Doppler frequency. One way to detect the interference is to display the spectral power of the Doppler interval from -1 to 1 Hz as a function of range. The spectral power can be obtained by summing the power of the samples in that Doppler interval. This

summation excludes the Bragg lines and the ground clutter at 0 Hz as they are normally dominant in the Doppler spectrum. In the absence of any interference, this sum represents the spectral power of the sea clutter continuum. Figure 3 displays this sum as a function of range for the sixth integration period of data file, AIR6. Normally, this sum attenuates almost monotonically with range. However, as shown in Figure 3, a strong peak is observed at a range of 136 km. The Doppler spectrum of the radar data at 136 km is shown in Figure 4. By comparing the Doppler spectrum in Figure 4 with the Doppler spectra in Figure 2, one can easily observe that the radar data at 136 km was contaminated by the interference.

The level of interference varied with time and it became much stronger in the data collected after 12:30 PM local time (LT). The radar operated at 4.3 MHz from 11:56 AM to 13:25 PM on August 15, 1992. Figure 5 traces out the spectral power of the Doppler interval from -1 to 1 Hz for the first integration period of all the data files collected at 4.3 MHz on August 15, 1992. In Figure 5a are the spectral powers from the data files collected before 12:30 PM, and in Figure 5b are the spectral powers from the data files collected after 12:30 PM. As shown in Figure 5, the levels of interference are considerably higher in the data files collected after 12:30 PM than in those collected before 12:30 PM. The interference in the data collected after 12:30 PM is also observed over the entire range interval of 120 and 173 km.

Figure 6 shows two Doppler spectra of the data from the same range of 155 km. Figure 6a is computed with the data collected before 12:30 PM. The interference is almost non-existent and the sea clutter continuum dominates over the interval of -1 and 1 Hz. Figure 6b is a spectrum of the data collected after 12:30 PM. The sea clutter is now masked by the interference. Only the larger one of the two Bragg lines is observable in the Doppler spectrum. Note that the change from Figure 6a to Figure 6b occurred over a span of about 11 minutes only, with the data shown in Figure 4 being collected at the critical time of the change. The spectral plots of the data collected before 12:30 PM are mostly similar to that shown in Figure 6a, and the spectral plots collected after 12:30 PM are mostly similar to that shown in Figure 6b.

The interference observed in the 4.3-MHz radar data was due to a leakage of the transmitted signal in the vertical direction. The upward radar signal bounced off the ionosphere and returned to the radar receiver. The range interval over which the interference appeared corresponds to the F layer of the ionosphere. The fact that the interference became stronger after 12:30 PM indicates that there was a formation of the F1 layer. The F1 layer is between 130 and 200 km above the earth, and its formation depends on solar radiation, which reaches maximum intensity at about one hour after noon local time [11].

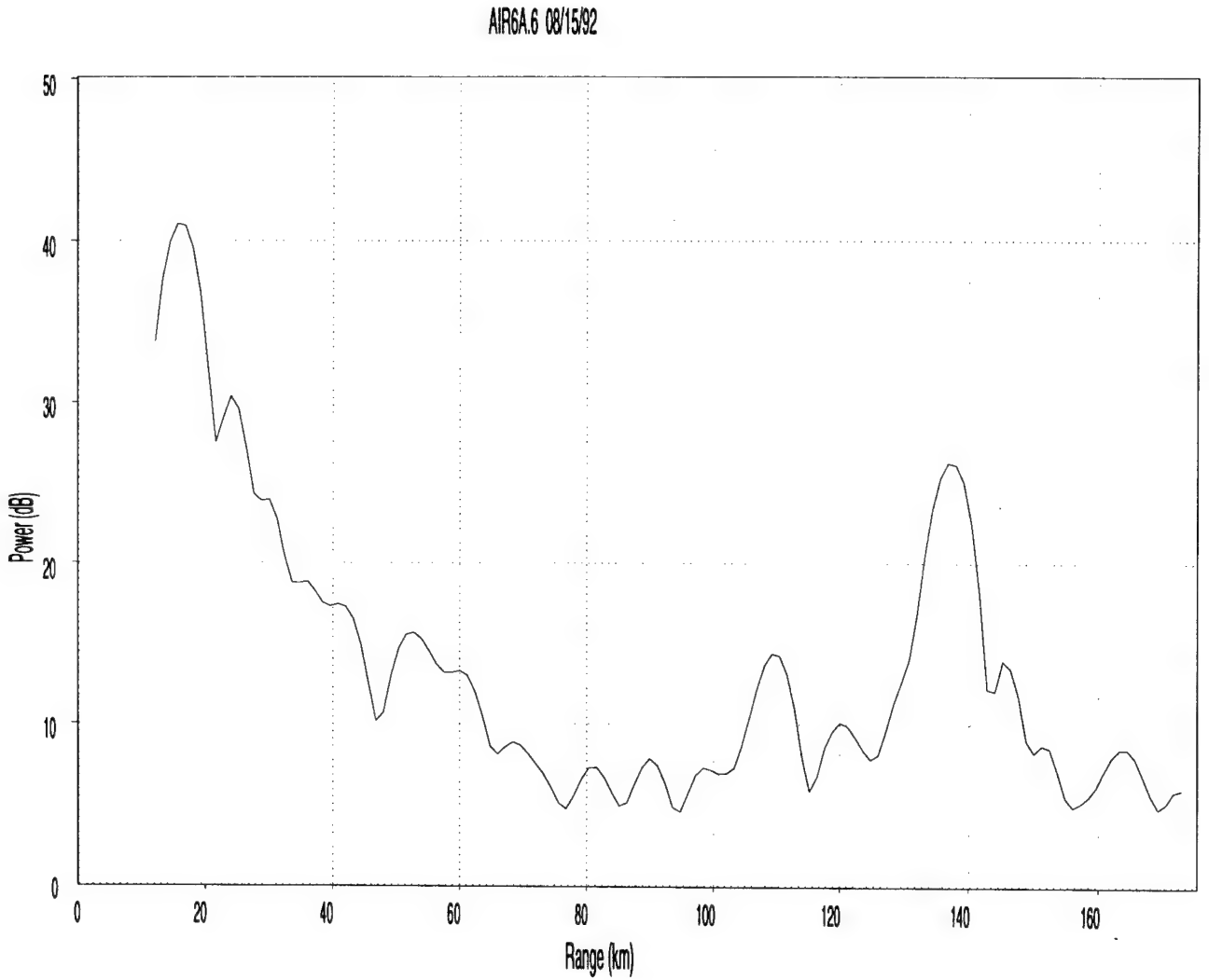


Figure 3 The Spectral Powers of Sea Clutter Continuum at 4.3 MHz from Different Ranges, Showing a Strong Peak at the Range of about 136 km

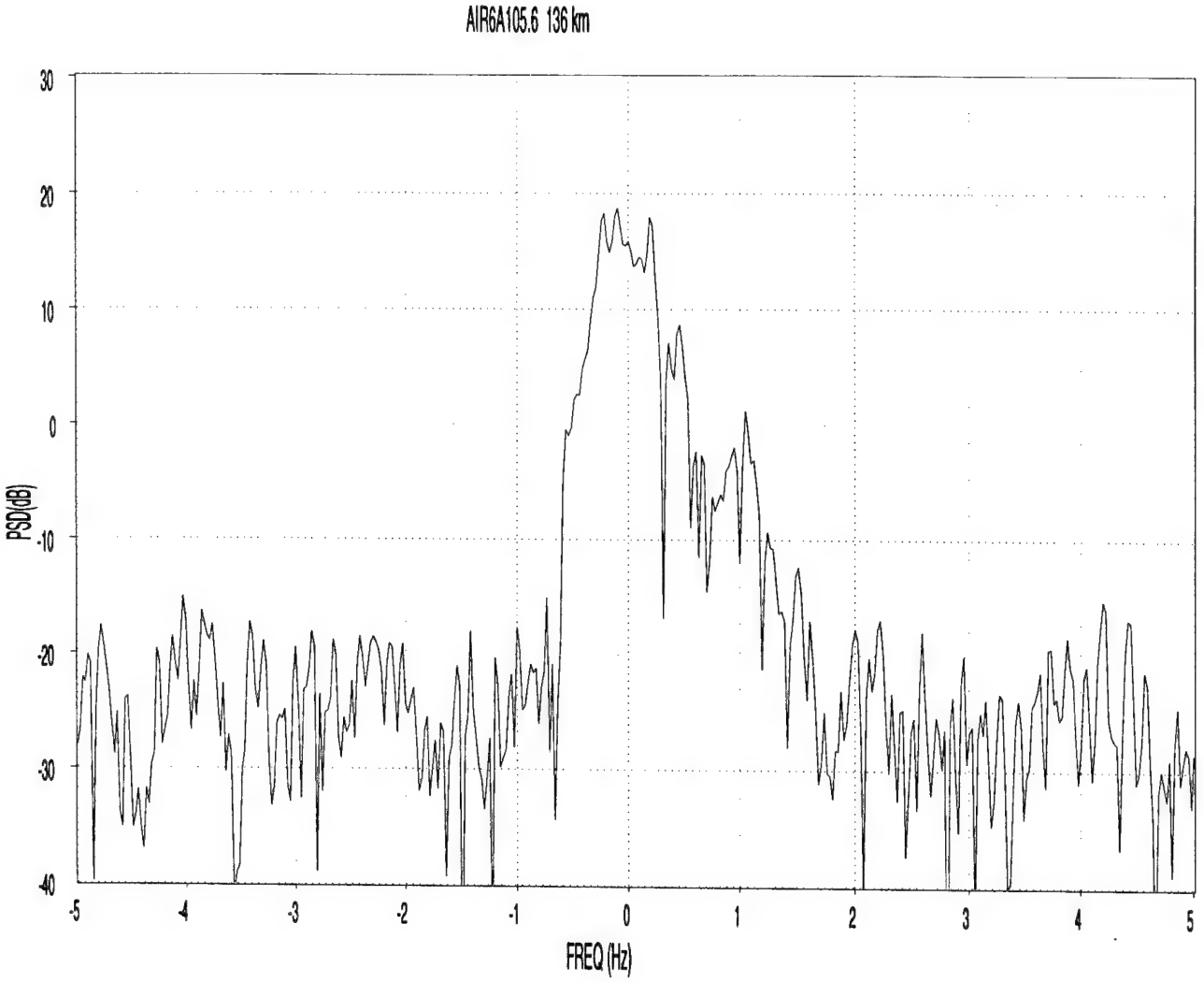


Figure 4 HFSWR Doppler Spectrum at 4.3 MHz Contaminated with Self-Generated Interference

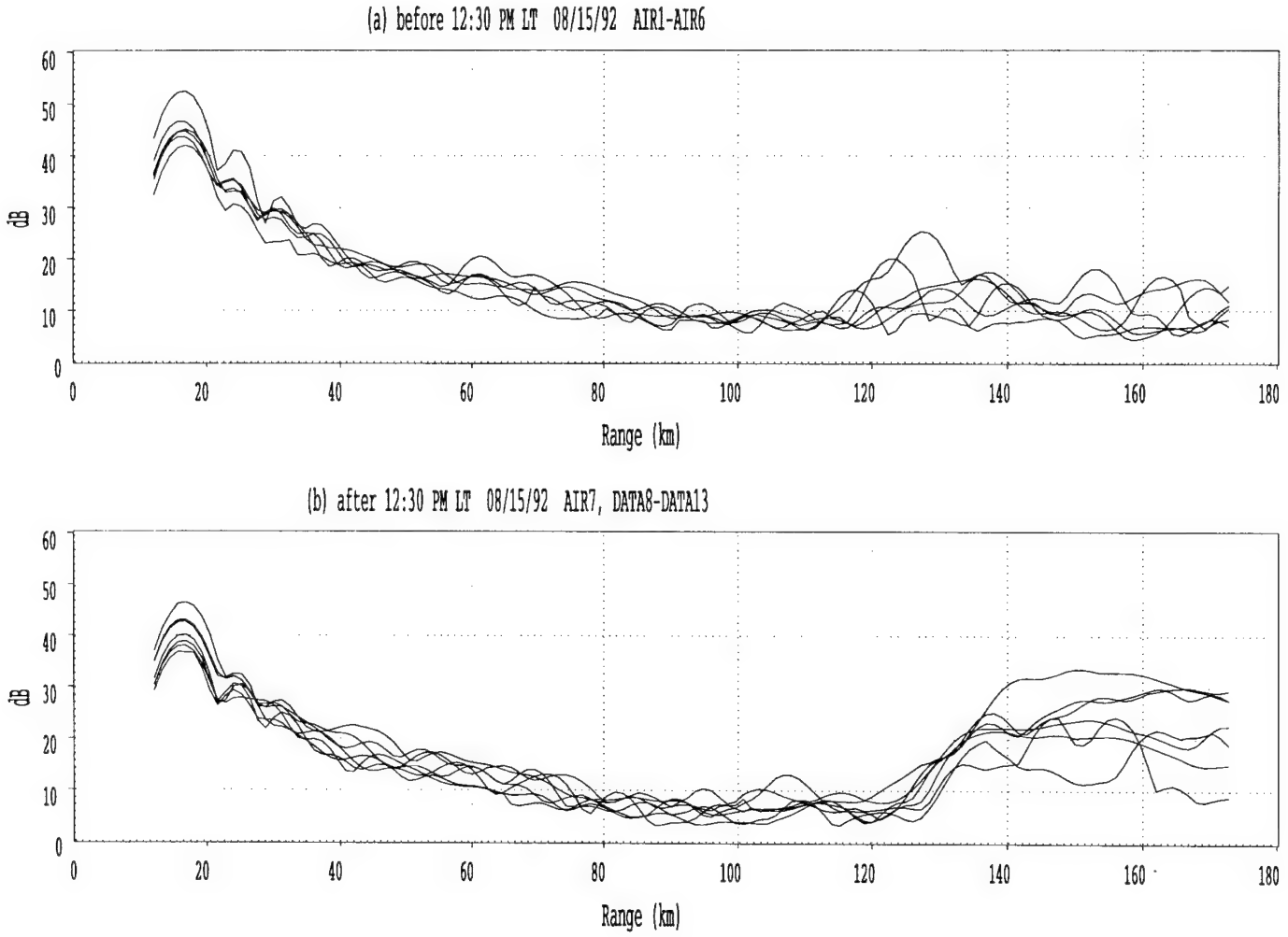


Figure 5 The Spectral Powers of Sea Clutter Continuum at 4.3 MHz from Different Ranges, Showing Signs of Interference between 120 and 173 km before and after 12:30 PM Local Time

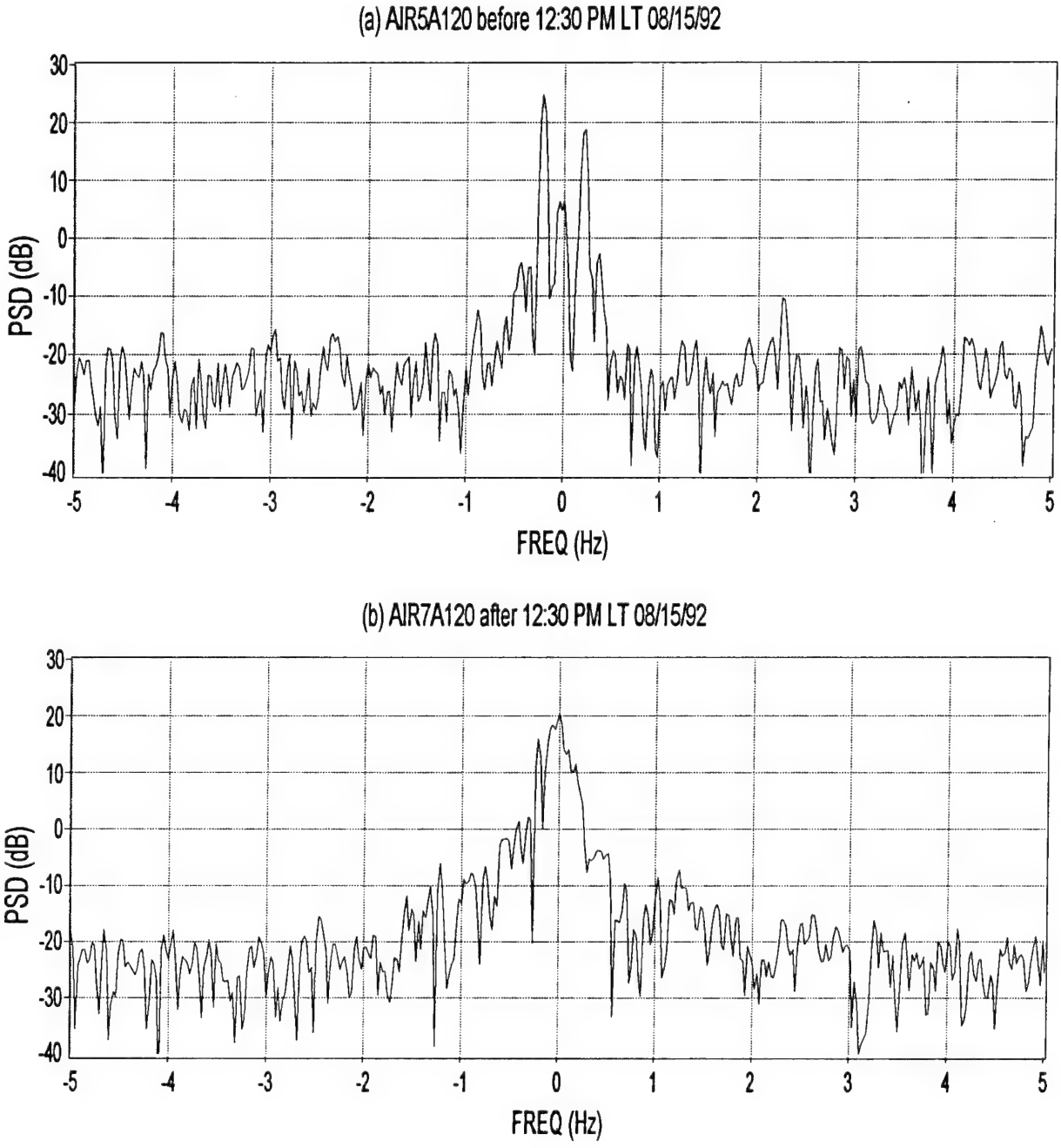


Figure 6 HFSWR Doppler Spectra at 4.3 MHz before and after 12:30 PM LT

The second type of interference was observed occasionally in the radar data collected on August 16 at the radio frequencies of 10.62 and 18.65 MHz. The interference appeared as a burst in the time series and produced five spectral peaks in the Doppler spectrum. The spectral peaks resemble one another and are equally spaced in Doppler frequency. An example of the interference is shown in Figure 7. In Figures 7a and 7b are the I and Q channels of the time series at 10.62 MHz, and in Figure 7c is the Doppler spectrum of the time series. The interference can be observed in the time series for about one second at the time of 115 second, and in the Doppler spectrum at the frequencies of about -115, -65, -15, 35, and 85 Hz. The origin of this interference is unknown.

The third type of interference showed up in the data collected on August 17 in the radar experiments with the Navajo aircraft. The presence of the interference was noted during the radar trials. The radar operated initially at 18.65 MHz, and then at 10.62 MHz. No target could be detected from these two sets of radar data because of the interference.

The first two types of interference can also have detrimental effects on the detection of targets in the radar data. The self-generated interference in the 4.3-MHz radar data could pose severe problems in the detection of slow targets such as ships and icebergs. The burst-like interference in the 10.62-MHz and 18.65-MHz radar data could be excised in the time series, but it must be detected before a proper excision algorithm can be employed. If the bursts are not properly excised, then the spectral peaks in the Doppler spectrum could result in false alarms in the target detection.

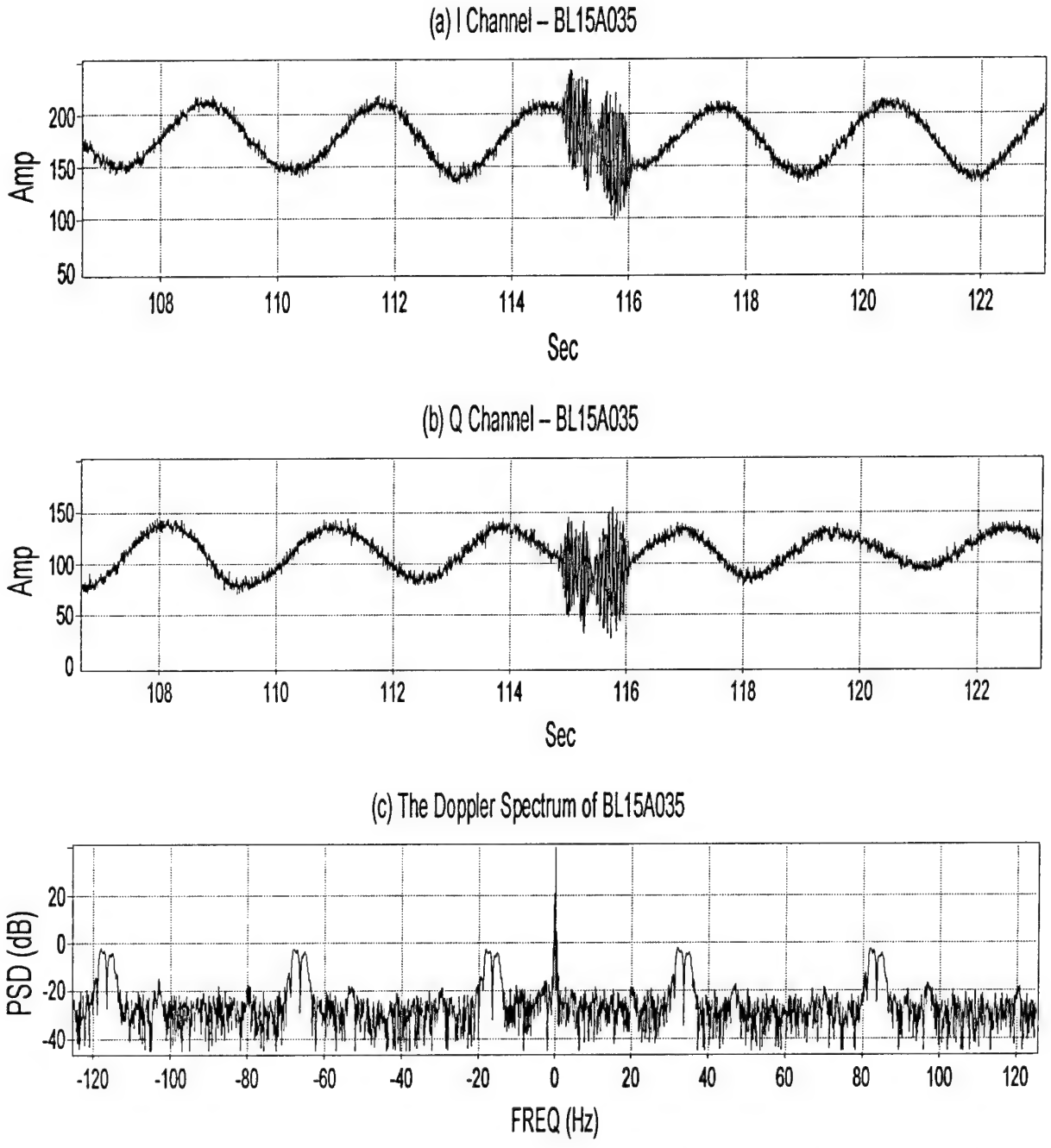


Figure 7 Burst-like Interference in I and Q Channels (a,b), and Corresponding Doppler Spectrum (c) at 10.62 MHz

# 4. Detection of Aircraft

The maximum line-of-sight distance (MLOSD) between a radar and a target is given by

$$d = \sqrt{2kR}\left(\sqrt{h_r} + \sqrt{h_t}\right) \tag{2}$$

where kR is the effective radius of the earth (R=6400 km, k=4/3 [12, p. 449]), and $h_r$ and $h_t$ are the respective heights of the radar and the target. For convenient calculations, the MLOSD can be written as

$$d = 2.27\left(\sqrt{h_r} + \sqrt{h_t}\right) \tag{3}$$

where d is given in kilometres, and $h_r$ and $h_t$ are in feet.

The radar at Cape Bonavista was approximately at 50 feet above the sea level. During the trials, the Kingair and the Navajo flew at the altitudes of about 50 and 100 feet respectively. At these altitudes, the MLOSDs were respectively equal to 32 and 39 km. One objective of the trials was to demonstrate the capability of the radar to detect these targets beyond their respective MLOSDs[2].

The aircraft flew towards and away from the radar along the boresight direction of the receiving antenna array. Hence, the performance of the HFSWR against the targets can be indicated by the signal-to-noise ratio (SNR) of the target as measured along the target tracks. The radar performance, however, can also be predicted by modelling the HFSWR system with HFRADAR [13]. HFRADAR is a HFSWR simulator which comprises a number of modules for propagation attenuation, sea clutter and external noise in the HF band. Agreements of the measured performance with the predicted performance would give a certain degree of confidence in both the HFSWR simulator and the experimental HFSWR system.

The algorithm in [3] is used to detect the aircraft in the radar data. This algorithm employs the conventional Constant-False-Alarm-Rate (CFAR) detection technique [14] and detects signals of high-speed targets against background noise in the Doppler spectrum. The results from the target detection are presented in the following two subsections for the Kingair and the Navajo aircraft.

---

[2] The MLOSD is generally longer than the radar horizon, which is given by

$$d_0 = \sqrt{2kR}\left(\sqrt{h_r}\right) \quad \text{or} \quad d_0 = 2.27\left(\sqrt{h_r}\right)$$

if $d_0$ is given in kilometres, and $h_r$ is in feet. At $h_r$ = 50 feet, for example, $d_0$ = 16 km.

## 4.1 Detection of Beechcraft Kingair

Figures 8 and 9 show the ranges and the radial velocities of the Kingair target along the target track, estimated with the 4.3-MHz radar data. During approach, the aircraft was tracked from a range of about 110 km, and the radial velocity of the aircraft was about 285 km/hour. While the aircraft was receding, the radar operation was interrupted for about 15 minutes to replace the Exabyte tape in the receiving system. When the radar operation resumed, the aircraft was about 72 km away from the radar. As shown in Figure 8, the target was then detected continuously for about 4 minutes. The aircraft began to zigzag along the boresight direction at the range of 74 km, and the aircraft slowed down during the first leg of the zigzag. As shown in Figure 9, the radial velocity of the aircraft decreased from 312 to 297 km/hour during the 4-minute period. The aircraft was last detected at the range of about 100 km, when the radial velocity was equal to 276 km/hour. The detection of the aircraft was made in the noise-dominated intervals between -4 and -1 Hz and between 1 and 4 Hz in the Doppler spectrum. A CIT of 41 seconds was used for the radar data and a detection threshold of 10 dB was assumed for the target SNR. The detection threshold of 10 dB corresponds to a probability of false alarm of $4.5 \times 10^{-5}$, at each point of the target track, if the samples in the two Doppler intervals are Gaussian (Rayleigh in amplitude).

Figure 10 shows four Doppler spectra of the radar data. Signals of the aircraft target can be observed at the Doppler frequency of about 2.27 Hz in all four Doppler spectra. These signals were from the ranges of about 110, 92, 70 and 44 km, corresponding to the range sample numbers of 92, 77, 58 and 37 respectively. At these ranges, the aircraft was detected beyond the MLOSD of 32 km.

The measured SNR of the approaching Kingair is shown in a log-log plot in Figure 11 with respect to the target range, R. A marked difference is observed in the range dependence of the measured SNR before and after the range of about 35 km. A logarithmic fit of the SNR with respect to $\mathrm{Log}_{10}R$ in the range interval between 20 and 35 km indicates that the SNR is proportional to $R^{-6.03}$. A logarithmic fit of the SNR with respect to $\mathrm{Log}_{10}R$ in the range interval between 35 and 95 km, however, indicates that the SNR is proportional to $R^{-4.71}$. The difference in slopes is not unexpected because the target is either within or beyond the line of sight at about 32 km. It is surprising, however, that the SNRs at the close ranges attenuate more quickly than those at the far ranges.

Normally, the signal power of a target detected within the line of sight is proportional to $R^{-4}$, and the signal power of a target detected beyond the line of sight is proportional to $F^4 R^{-4}$, where F is the Norton attenuation factor between the radar and the target and is used to account for additional losses in surface waves [9, p.12-10]. The attenuation of $R^{-4.71}$ in the interval between 35 and 95 km

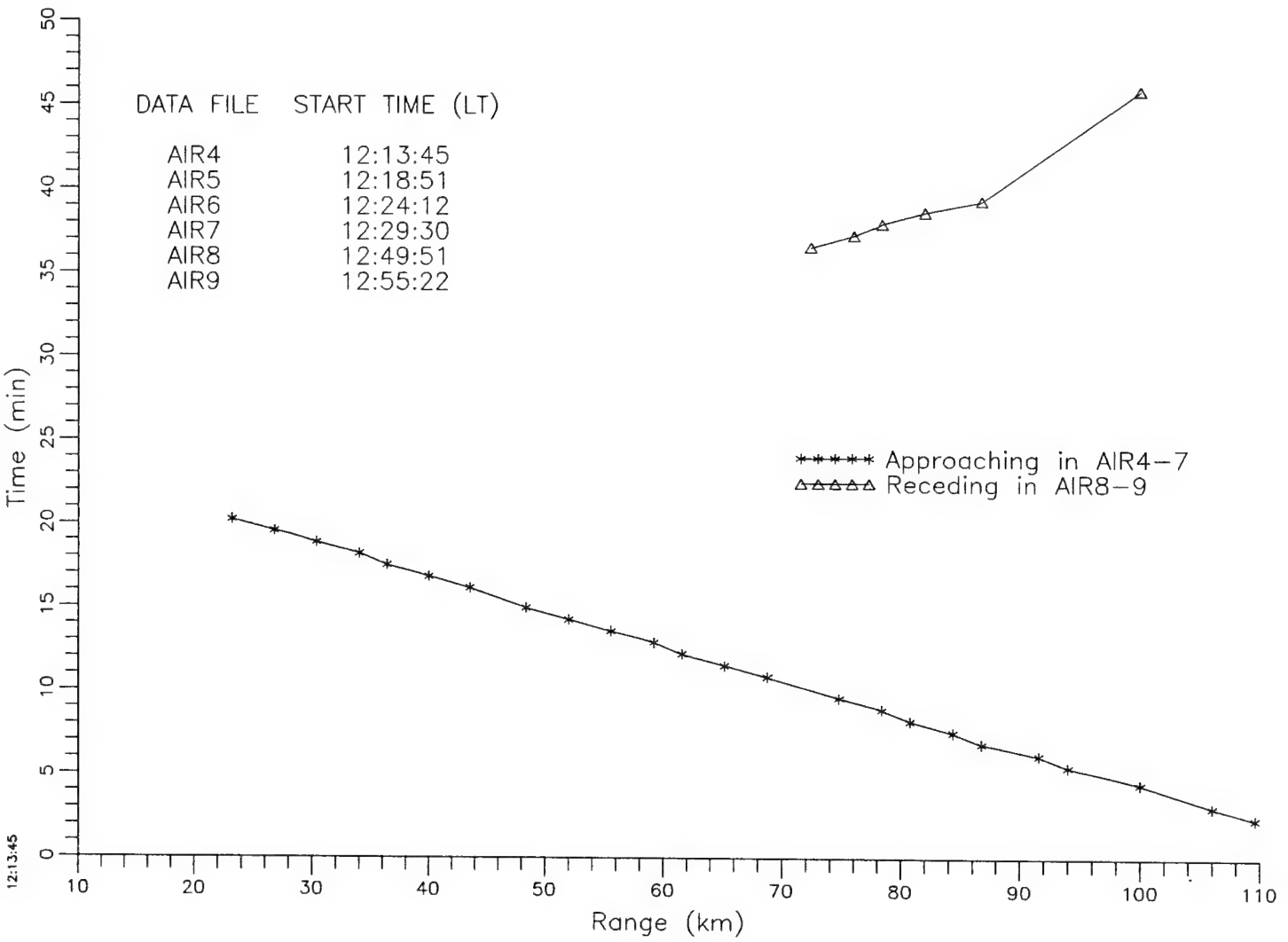


Figure 8 Track of Beechcraft Kingair Detected at 4.3 MHz

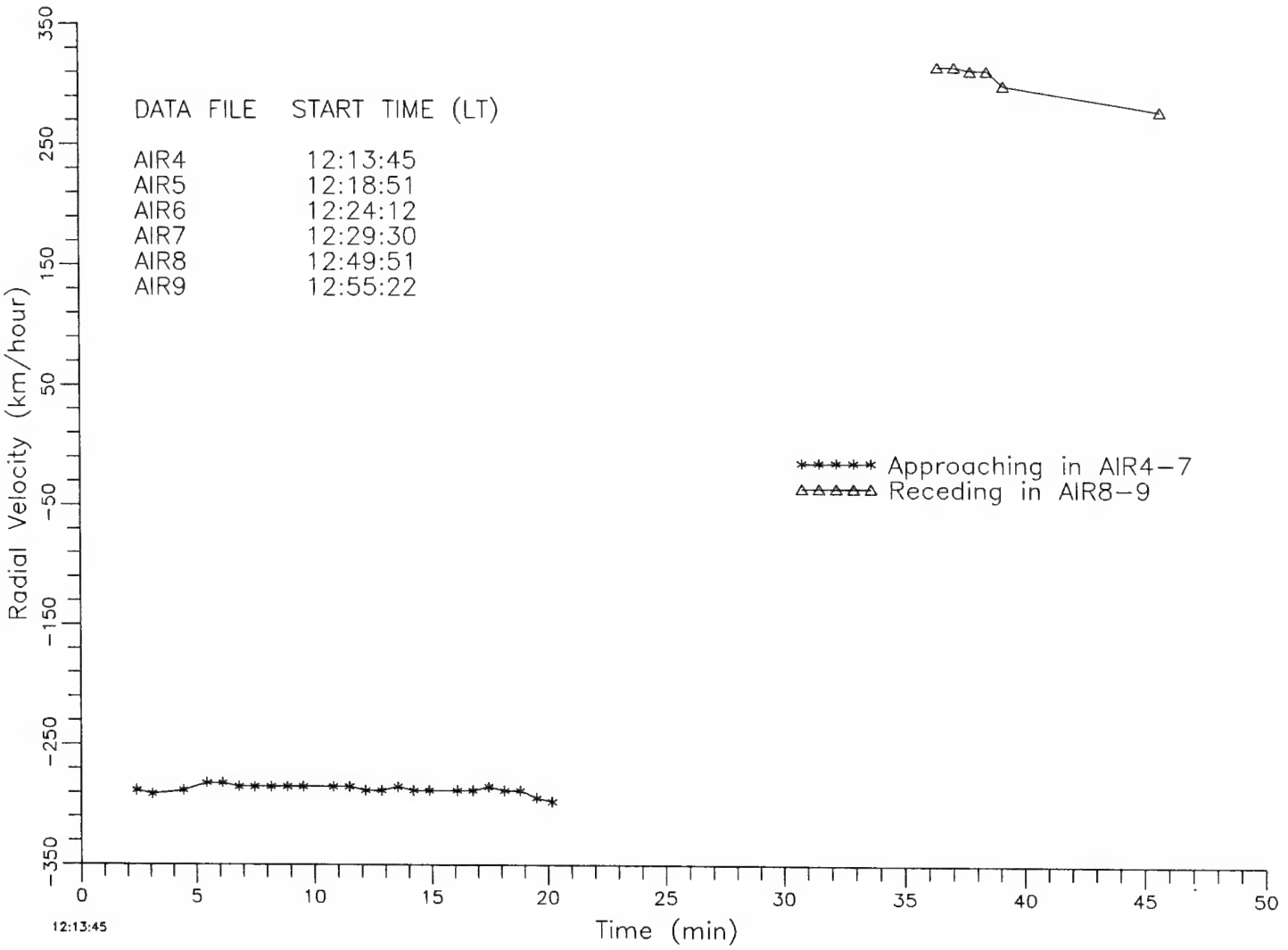


Figure 9 Radial Velocity of Beechcraft Kingair Detected at 4.3 MHz

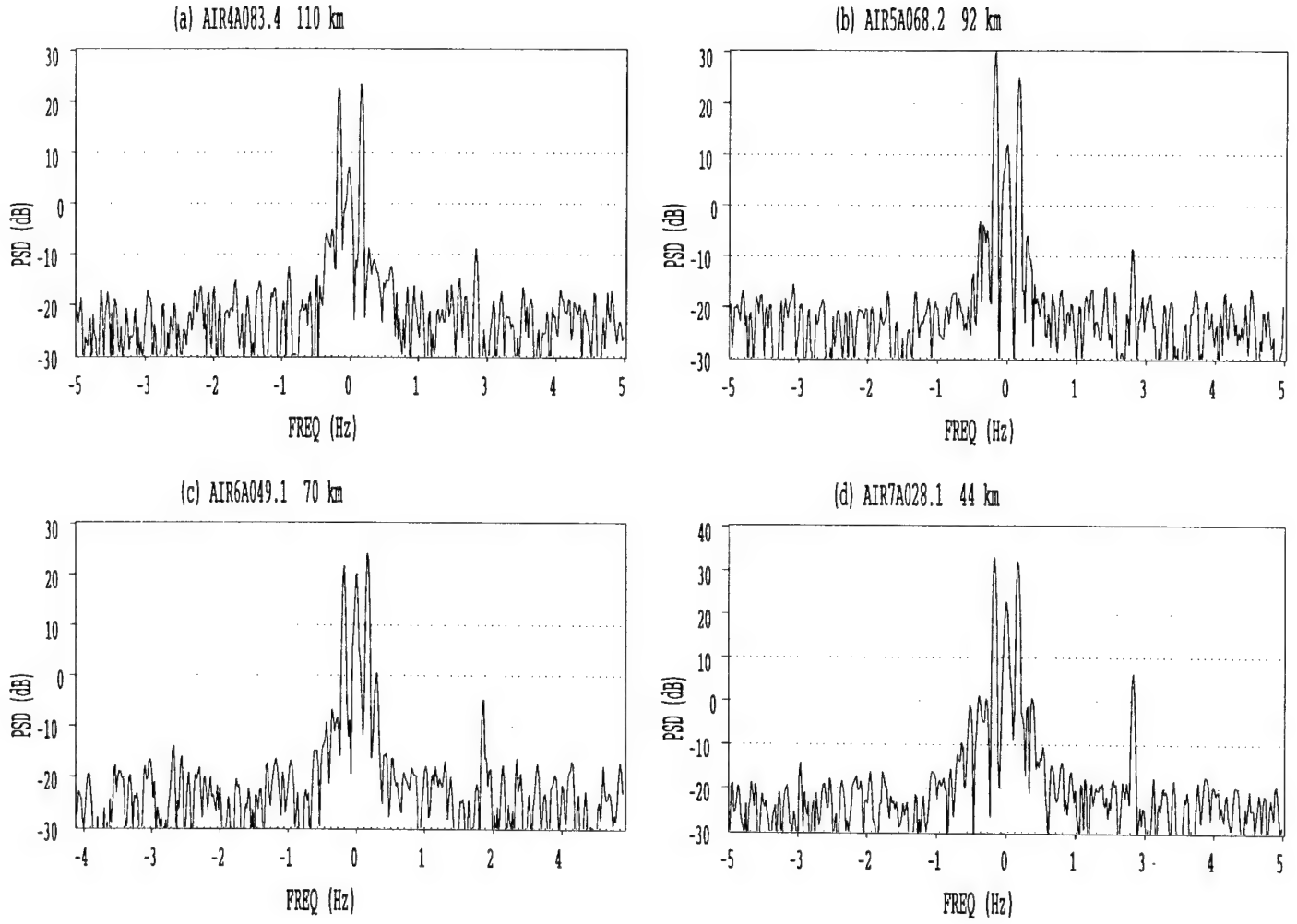


Figure 10 HFSWR Doppler Spectra at 4.3 MHz Showing Signals of Kingair at 2.27 Hz

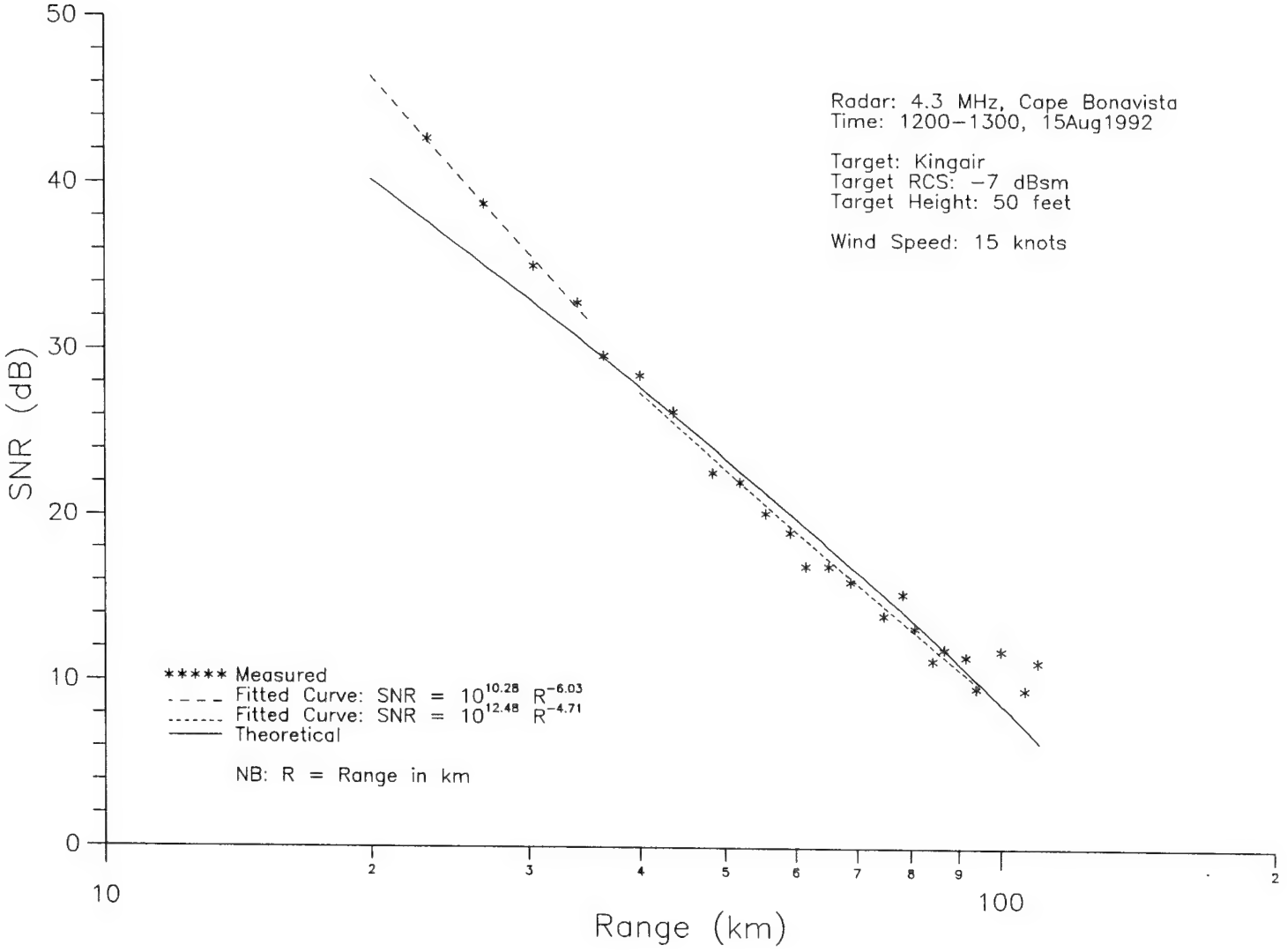


Figure 11 Comparison of Theoretical and Experimental HFSWR Performance in the Detection of Beechcraft Kingair

seems to agree with what is expected, but the attenuation of $R^{-6.03}$ at the close ranges deviates significantly. The reason for this deviation is not clearly understood. One possible explanation is that the strong attenuation at the close ranges was not genuine and that the target signal was actually enhanced by an increase in the radar cross-section of the target due to a change of the aspect angle to the aircraft. The aircraft was getting close to the shoreline and was preparing to make a 180° turn. Hence, it was likely that the aircraft pitched and rolled a little as the aircraft approached the radar.

Figure 11 shows the theoretical SNR of the Kingair, flying along the boresight at a constant altitude of 50 feet. In calculating the SNR, the HFSWR was modelled with the following system parameters:

| | |
|---|---|
| Radar Frequency | 4.3 MHz |
| Average transmit power | 40 Watts |
| Transmitting antenna gain | 11 dBi |
| Receiving antenna gain | 14 dBi |
| Coherent Integration Time | 41 seconds |
| System Loss | 6 dB |

The average transmit power was calculated from the peak transmitter power rated by the manufacturer (8 kW ANALOGIC) and from the duty cycle of the radar during the radar experiment (PRF = 100 Hz and pulse width = 50 μs; duty cycle = 0.50%). The antenna gains were calculated from the element gains and array factors of the transmit and receive antennas by using the conventional theory of linear arrays (refer to [12, p. 281], for example). An element gain of 5.15 dBi was assumed for the monopole (i.e., one of the whip antennas) transmitting or receiving on a conducting plane (A metallic ground screen is typically employed in HFSWR). The array factors were calculated to be 6 and 9 dB, respectively for the transmitting and receiving antenna arrays. The system loss of 6 dB was assumed to account for the signal processing loss and any other losses in the receiving system. It was also assumed that the radar operates under the similar environmental conditions as those in the experiment (quiet noise site; 15 knot wind). The radar cross-section (RCS) of the Kingair is computed in [15] by using the Numerical Electromagnetic Code (NEC). The RCS of the Kingair in level flight is equal to -7 dBsm at 4.3 MHz (aspect: nose-on). This RCS was also used in the SNR calculation.

The measured SNRs deviate from the theoretical SNRs at ranges closer than 35 km, perhaps for the reasons described above. In the range interval between 35 and 95 km, however, the measured SNR and the theoretical SNR agree well with each other. The theoretical SNR concaves

down gently in the range interval, but the concavity is so small than there is very little change in the slope of the curve in the interval. The range dependence of the theoretical SNR ranges from $R^{-4.48}$ at the range of 35 km to $R^{-5.29}$ at the range of 95 km. This is consistent with the measured SNRs ( $R^{-4.71}$ ) in the same range interval. Both the measured SNR and the theoretical SNR decrease to about 10 dB at the range of 95 km. Beyond 95 km, only three more hits of the aircraft were available and the measured SNRs at the three points do not seem to follow any clear pattern of range attenuation. Allowing for the possible variation of the target RCS at the close ranges, we conclude that the theoretical performance of the radar agrees well with the measured performance.

## 4.2 Detection of Navajo Aircraft

The detection of the Navajo was carried out on August 17, using radar frequencies of 18.65, 10.62 and 27.8 MHz. The aircraft flew two runs on that day, both at an altitude of 100 ft. The first run was carried out when the radar operated at 18.65 MHz. Unfortunately, a high level of interference was present during the radar trial, and the Navajo could not be detected from this set of radar data. The second run was carried out at about a half of an hour after the first run. The radar operated briefly at 10.62 MHz and then switched to 27.8 MHz. However, there was also interference in the 10.62-MHz radar data, and the Navajo could not be detected in the data collected at this frequency.

The only possible detection of the aircraft was from the 27.8-MHz radar data. Using a CIT of 41 second and a detection threshold of 10 dB, three consecutive hits of the aircraft target were made in the data file of NAV21 at the ranges of about 19, 23 and 26 km, corresponding to the range sample numbers of 16, 19 and 22 respectively. Figure 12 shows the Doppler spectrum of the radar data at the range of 23 km. The signal of the aircraft appears at the Doppler frequency of -14.33 Hz, corresponding to a radial velocity of 281 km/hour (152 knots). Note that another target-like signal is present at about 6.6 Hz, but the origin of this signal is unknown.

The ranges above are all within the MLOSD of 39 km. The performance of the radar at 27.8 MHz is severely limited by the propagation attenuation at the radio frequency. Modelled results from HFRADAR indicate that the 27.8-MHz radar can detect the Navajo aircraft up to a range of about 30 km only. The radar had an average power of about 40 Watts, and transmitting and receiving antenna gains of about 8 dBi and 17 dBi (theoretical gains). Considering the low power aperture of the radar and the strong propagation attenuation at the radar frequency, it is not surprising that the target could not be detected beyond the MLOSD.

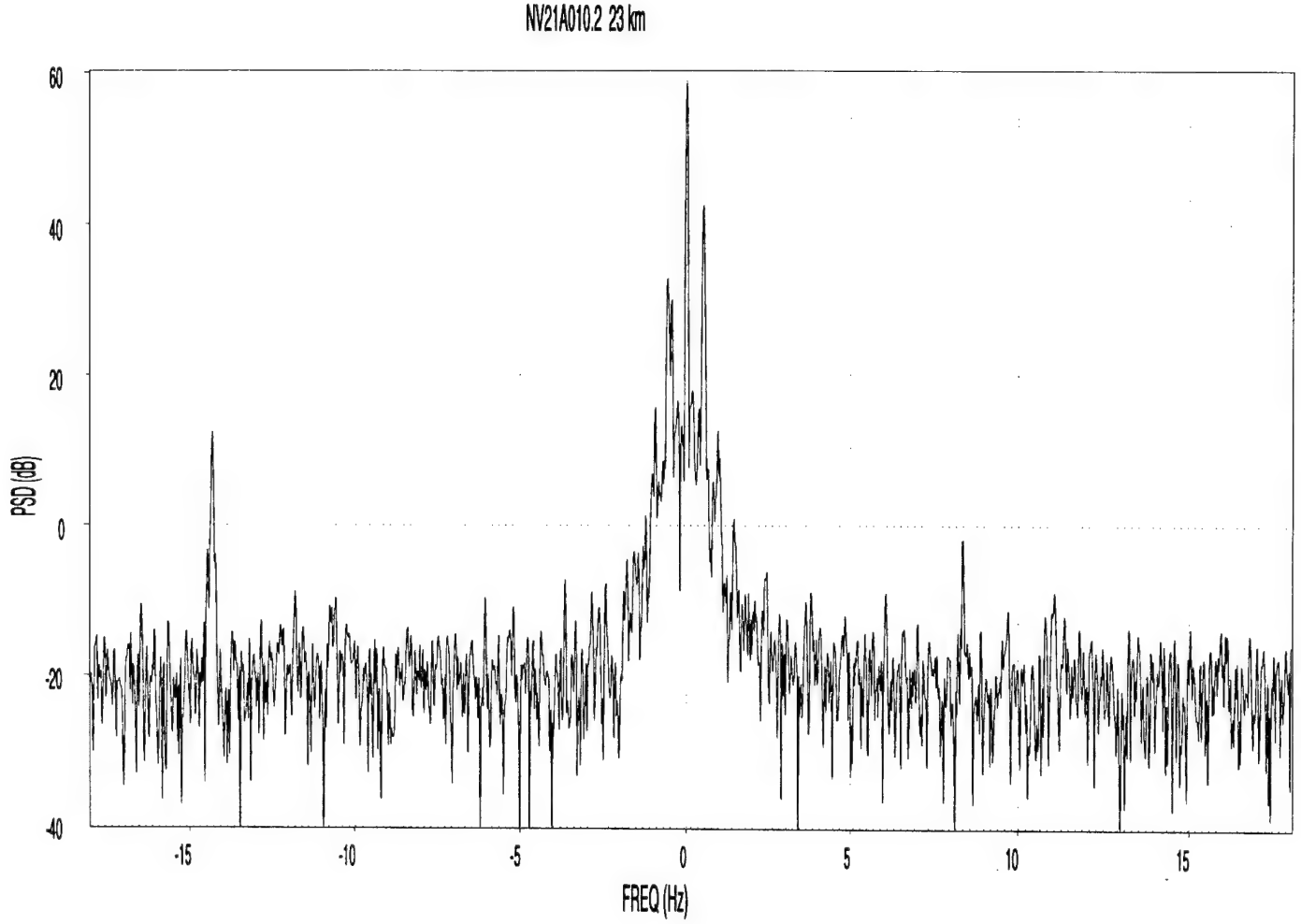


Figure 12 HFSWR Doppler Spectrum at 27.8 MHz Showing Signal of Navajo Aircraft at -14.33 Hz

# 5. Detection of Half-Wavelength Wires

Vertical, half-wavelength long, thin copper wires (#18 AWG) were used as test targets when the radar operated at the frequencies of 10.62 and 18.65 MHz. One end of the wire was attached to a helium balloon and the other end was hung freely down from the balloon. The balloons were released from a small boat named Bonni Pauline and were carried away from the radar by a strong outward wind. The wind speed was estimated to be 7.7 m/s (15 knots) from the boat near the ocean surface. Four balloons were released at each frequency, and the time interval between the releases was between 5 and 10 minutes.

## 5.1 Detection Method

Several factors had to be considered in the search of the wire targets in the radar data:

1) Since the balloons were carried away by the wind, the targets should have the same velocities as the wind. The radial velocity of the wind close to the ocean surface was approximately 7.7 m/s (15 knots), in a direction away from the radar. Hence, the targets upon their releases should have the approximate Doppler frequency of -0.54 Hz at 10.62 MHz, and -0.95 Hz at 18.65 MHz.

2) The target speed, however, would not be fixed at 7.7 m/s because of the random nature of the wind. The fluctuation of the wind would cause the target signal to broaden in the Doppler spectrum. To obtain the target signal power, one had to sum the samples over a relatively large interval around the estimated Doppler frequencies.

3) At the approximate Doppler frequencies above, the target signals could still be detected against the sea clutter continuum. The broadening of the target signal made it difficult to detect the target against the sea clutter.

4) Multiple targets could appear in the same range cell at the same time because of the wind-speed fluctuation. Here, the range cell refers to the width defined by the range resolution of the radar, i.e., 7.5 km. The radar relies on the interpolation of target signals across range to refine the range accuracy. The proximity of the targets could cause problems in locating the target ranges.

In view of these factors, we devised an empirical and graphical scheme for the detection of these targets: we summed the Doppler samples over a relatively large interval around the estimated Doppler frequency, and we displayed the sums as a function of range to search for the target locations. A few iterations of the process were needed in order to properly choose the size and position of the Doppler interval. Initially, we assumed that the targets had a radial velocity of 7.7 m/s, and we choose a Doppler interval, e.g., between -2.00 and -0.50 Hz at 10.62 MHz, and between -2.20 and -0.80 Hz at 18.65 MHz. We detected the peak signal in the chosen Doppler interval for each radar frequency. If the Doppler frequency of the peak signal was found to be larger in magnitude, we then moved the Doppler interval further away from 0 Hz, i.e., away from the region dominated by the clutter components of the radar.

A 16384-point FFT was used along with a Blackman Window to process the radar data. The radar operated at a PRF of 250 Hz at the radio frequencies of 10.62 and 18.65 MHz. Hence, a coherent integration time of 65.54 seconds was used for the data.

Figure 13 illustrates the detection scheme for the half-wavelength wire targets at 10.62 MHz. Here, the Doppler interval chosen is between -2.00 Hz and -0.62 Hz. The Doppler samples in that interval were summed from the data file BL18, and the sums were then displayed as a function of range. Figure 13 clearly shows the presence of three target signals, located at the ranges of about 65, 80 and 101 km, corresponding to the range sample numbers of 45, 58 and 75 respectively. The peaks of the three signals appear at the Doppler frequencies of -0.90, -1.04 and -1.11 Hz, corresponding to the radial velocities of 12.7, 14.7 and 15.7 m/s respectively. This confirms that the targets moved away from the radar, all at speeds greater than anticipated. To track the movements of the targets, we processed the data from BL18 contiguously over three consecutive integration periods, using the data processing scheme above. As shown in Figure 13, all the targets advanced in range over the three integration periods.

Figure 14 shows the results for the half-wavelength wire targets at 18.65 MHz. Here, the Doppler interval chosen is between -2.20 Hz and -1.20 Hz. The Doppler samples in that interval were summed from data file BL04, and the sums were then displayed as functions of range. Again, this process was repeated in time over three consecutive integration periods. Figure 14 shows the presence of at least two targets, located at the ranges of 45 and 53 km, corresponding to the range sample numbers of 29 and 35 respectively. The target at 53 km was detected in all three integration periods. The signal of this target has a Doppler frequency of -1.73 Hz, corresponding to a radial velocity of 13.9 m/s. Figure 14 shows that this target was moving away from the radar. The target at 45 km was detected in the third integration period of the data file only. This target corresponds

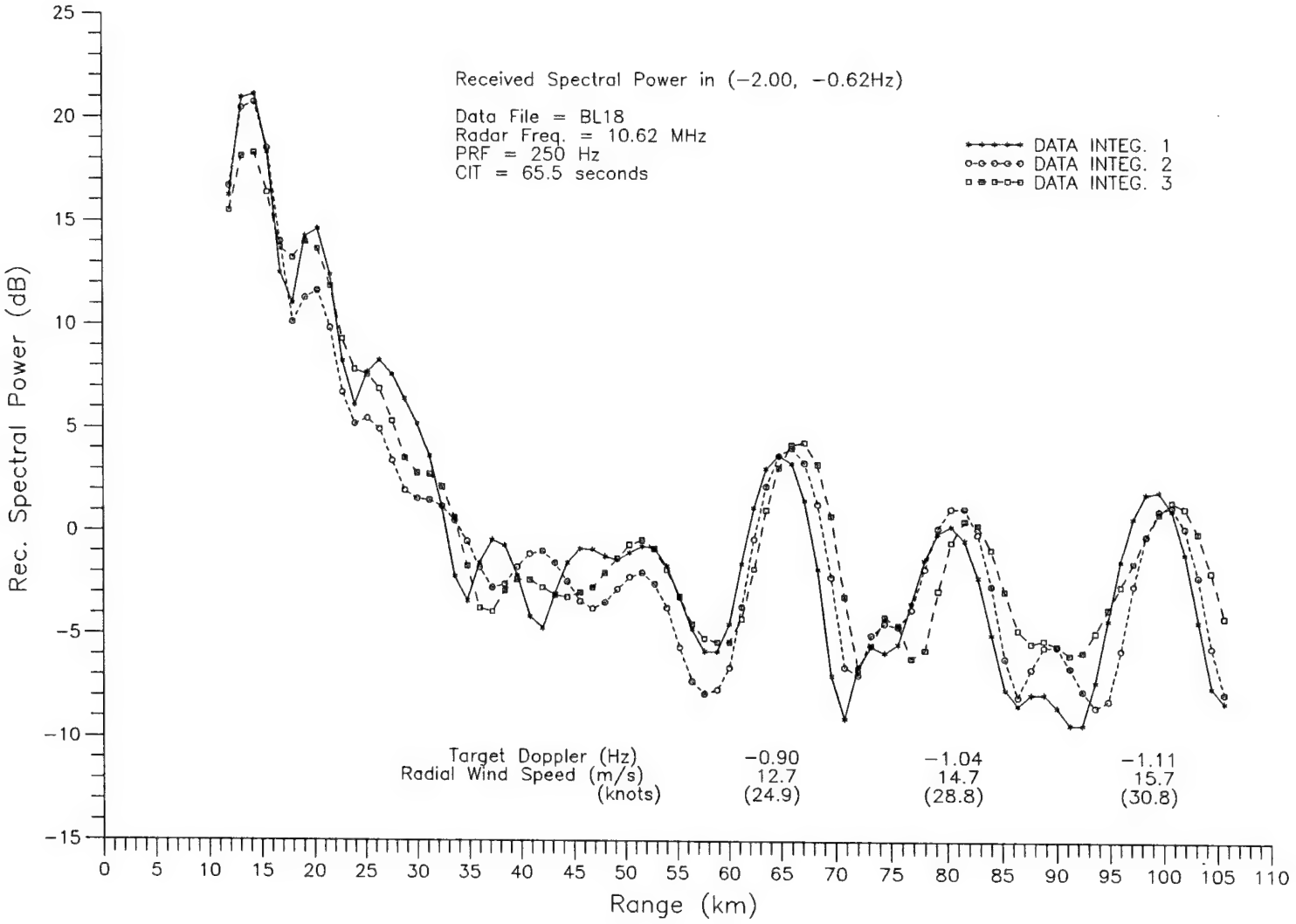


Figure 13 Detection of Half−Wavelength Long Copper Wires at 10.62 MHz

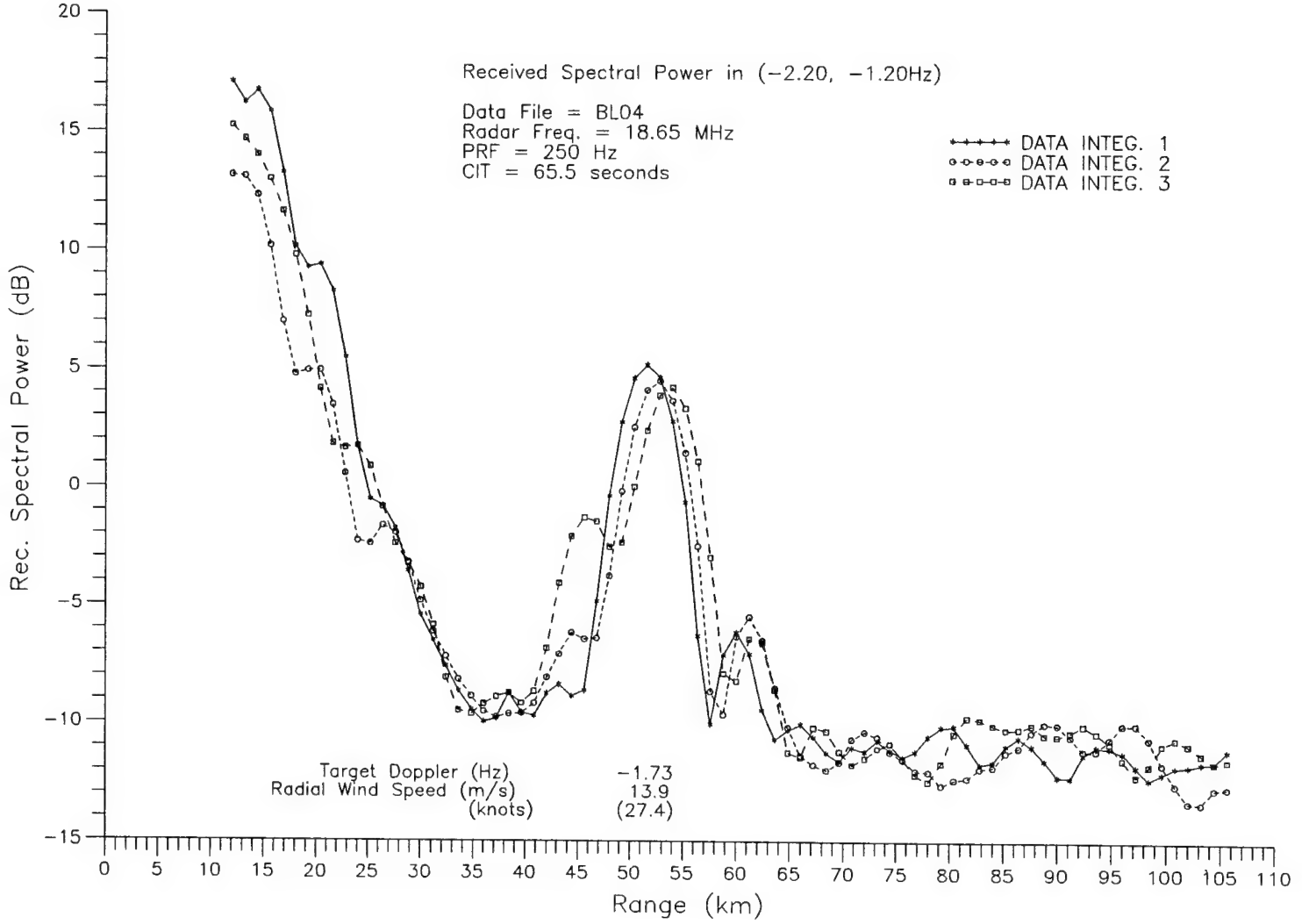


Figure 14 Detection of Half−Wavelength Long Copper Wires at 18.65 MHz

to Balloon 2, which was launched at about the same time as the data file BL04 was collected. Both targets were detected again in the data files collected after BL04.

Figure 14 appears to show that there was another target signal at the range of about 60 km, corresponding to the range sample number of 41. This could be due to the very first balloon target released at 18.65 MHz. This target was not labelled, and was seen dragging across the water during the trial. The signal in Figure 14 is rather weak, and is not always seen in all the data files. Hence, the detection of the unlabelled target is inconclusive from the radar data.

From the Doppler frequencies of the detected targets, one can obtain better estimates of the radial wind velocities at the target locations. Figures 13 and 14 include the wind speeds estimated from the frequencies of the peak target signals in the chosen Doppler intervals. These are the average wind speeds within the data-integration period of 65.5 seconds. They are higher than the estimated wind speed of 15 knots, likely because the targets were at higher altitudes.

## 5.2 Target Signals

The detection method described above was applied to all the data files collected on August 16, at the radio frequencies of 18.65 and 10.62 MHz. Appendices B and C show the detection results from the radar data for the targets deployed at 18.65 and 10.62 MHz, respectively. The radar operated initially at 18.65 MHz for about two hours, and then at 10.62 MHz for another one hour.

Three targets were detected at each radio frequency. These targets are simply re-labelled as BT1, BT2, BT3, BT4, BT5 and BT6. The first three were detected from the 18.65-MHz radar data, and the second three were detected from the 10.62-MHz radar data. A brief summary of the detection results is given at the beginning of each Appendix. Note that not all the released targets were successfully deployed and not all the deployed targets were detected from the radar data.

Figure 15 shows two Doppler spectra of the 10.62-MHz radar data. Two types of target signals are present. In Figure 15a, the target signal has fairly well-defined features in the Doppler spectrum. It consists of three spectral lines: a strong line at the frequency of -1.28 Hz and two weak lines at the frequencies of -1.45 and -1.14 Hz. The sharp features of the signal indicates that the target moved away from the radar at a constant radial speed. As the target moved away, the thin wire attached to the balloon might have oscillated and caused the two weak lines in the Doppler spectrum. Figure 15b shows a more typical signal of the targets. Centred at the frequency of about -1.16 Hz, this signal spreads out in many Doppler bins, due to the fluctuation of the target's radial velocity.

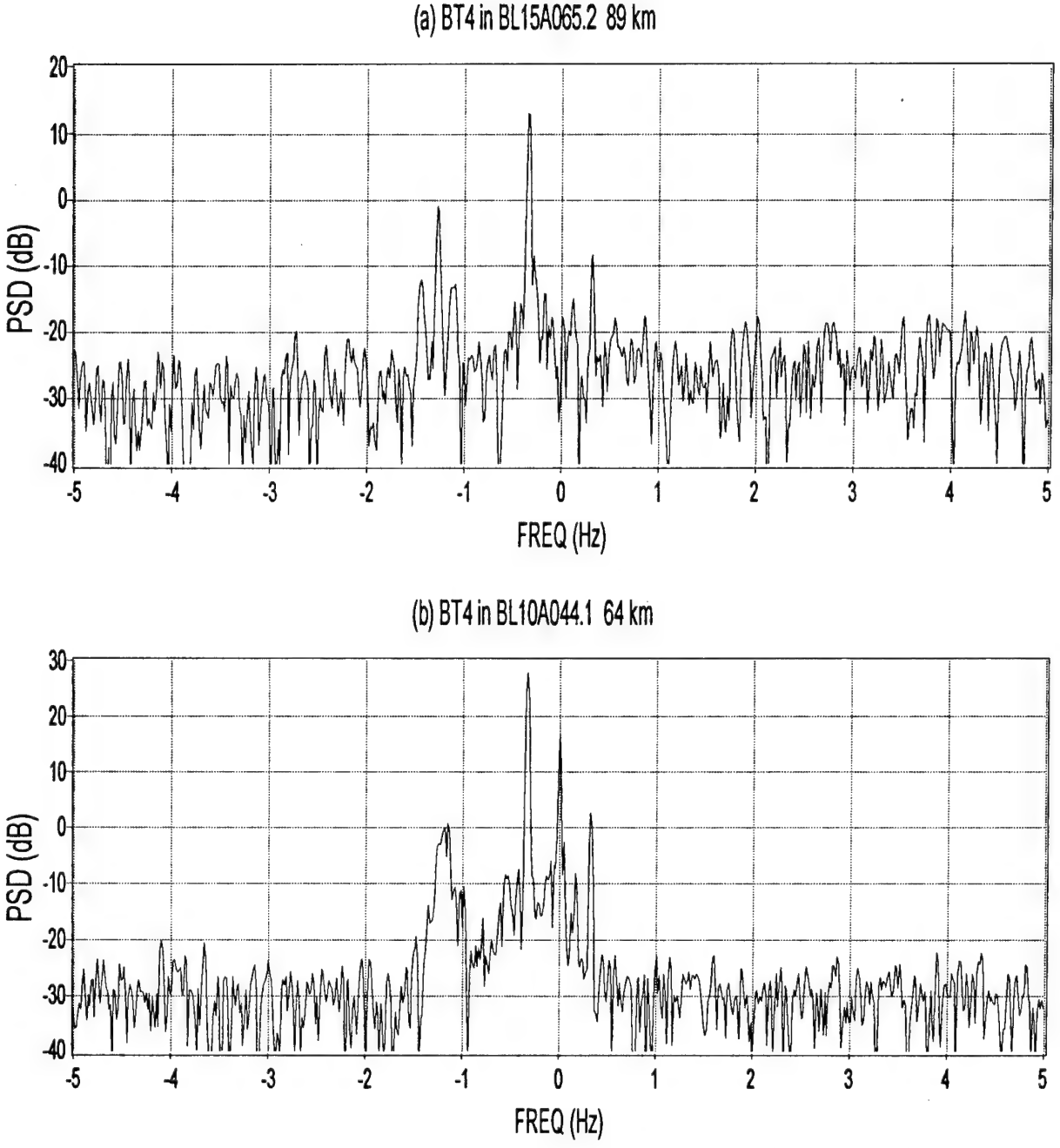


Figure 15 HFSWR Doppler Spectra at 10.62 MHz Showing Signals of Thin Wire Targets at around -1.28 and -1.16 Hz

Figure 16 shows two Doppler spectra of the 18.65-MHz radar data with signals of the detected targets. The dominant features of the signal in Figure 16a also are similar to the target signal in Figure 15a: a strong line at the Doppler frequency of -1.57 Hz plus two weak ones at the frequencies of -1.71 and -1.43 Hz. However, this target signal also includes other less dominant features, located further away from the centre frequency of -1.57 Hz. The target signal in Figure 16b is similar to the signal in Figure 15b: this signal also spreads out in many Doppler bins, almost over the entire interval of -2 to -1 Hz. Note that the spectral peaks at about ±0.97 Hz seemed to always exist in the Doppler spectrum, whether or not there is a target signal. These spectral peaks were not included in the Doppler interval chosen for the target detection.

The boat Bonni Pauline sometimes travelled at a radial velocity of 4.6 m/s, which corresponds to the Doppler frequencies of -0.32 Hz at 10.62 MHz and -0.57 Hz at 18.65 MHz. These Doppler frequencies are at the outside of the chosen Doppler intervals of -2.00 to -0.62 Hz for 10.62 MHz and -2.20 to -1.20 Hz for 18.65 MHz. Hence, the radar signal of the boat was not among the detected target signals.

## 5.3 Target Tracks

Figures 17 and 18 show the ranges and radial velocities of the detected targets at 18.65 MHz along the target tracks, respectively as functions of time with a reference to the beginning of data file BL01. In Figure 17, all the targets moved away from the radar. The first target, BT1, was, in particular, tracked up to a range of about 66 km. In Figure 18, the radial velocities of the targets fluctuated between 11 and 15 m/s (about 22 and 30 knots). The fluctuating wind velocities caused BT2 and BT3 to drift closer and closer to each other in range. As shown in Figure 17, the two targets were effectively located within 7.5 km of each other at the ends of the target tracks. This lead to a degradation in the accuracy of the estimated target ranges.

Figures 19 and 20 show the ranges and radial velocities of the detected targets at 10.62 MHz along the target tracks, respectively as functions of time with a reference to the start of data file BL10. In Figure 19, the targets also moved away from the radar, and in Figure 20, the radial velocities of the targets fluctuated between 9 and 19 m/s (about 17 and 36 knots). The longest track was formed for BT4: it was detected from a range of about 53 km up to a range of about 101 km. Note that the radial speed of BT4 was consistently higher than the speeds of the other two targets, likely because it was at a higher altitude.

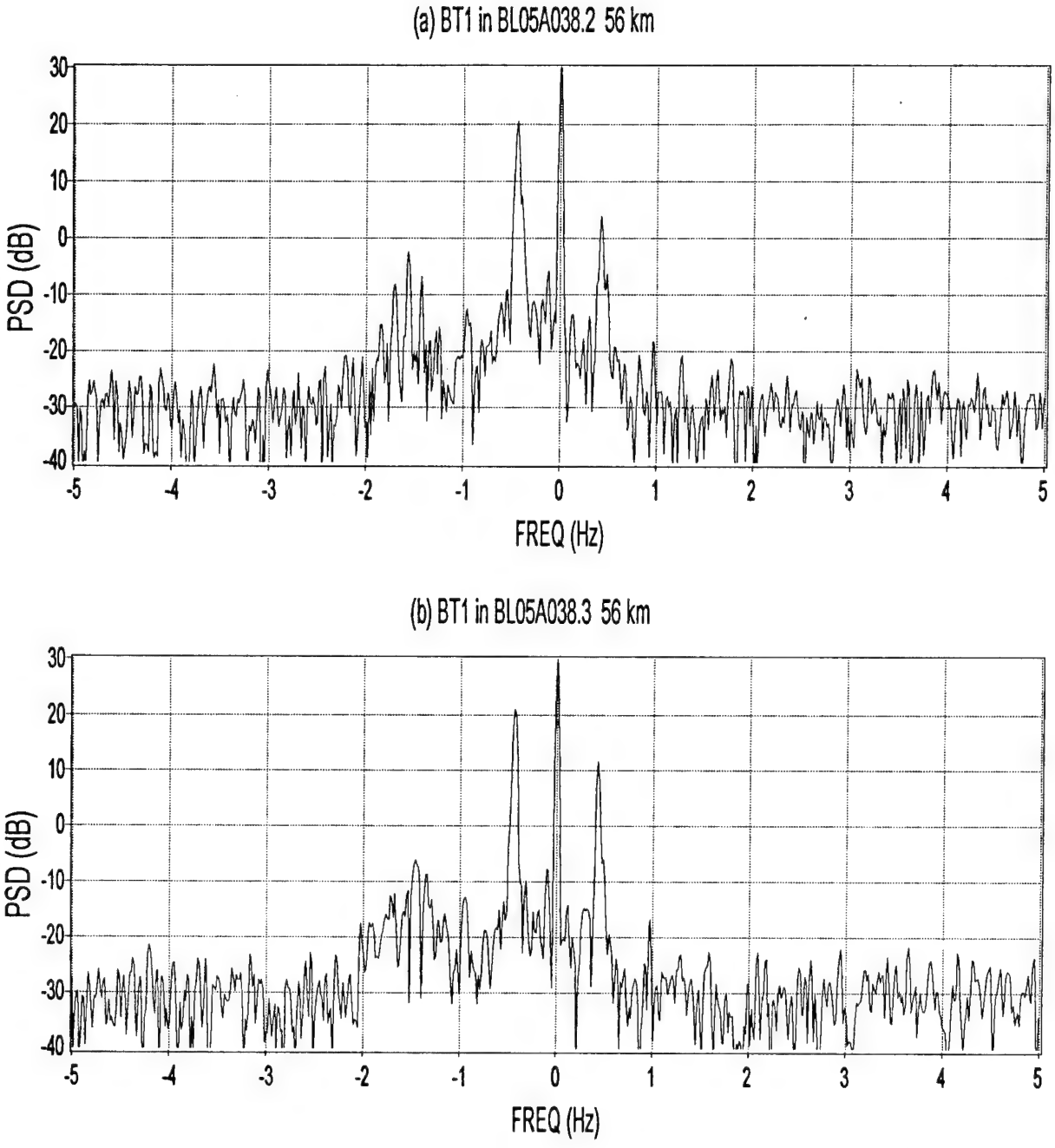


Figure 16 HFSWR Doppler Spectra at 18.65 MHz Showing Signals of Thin Wire Targets at around -1.57 and -1.47 Hz

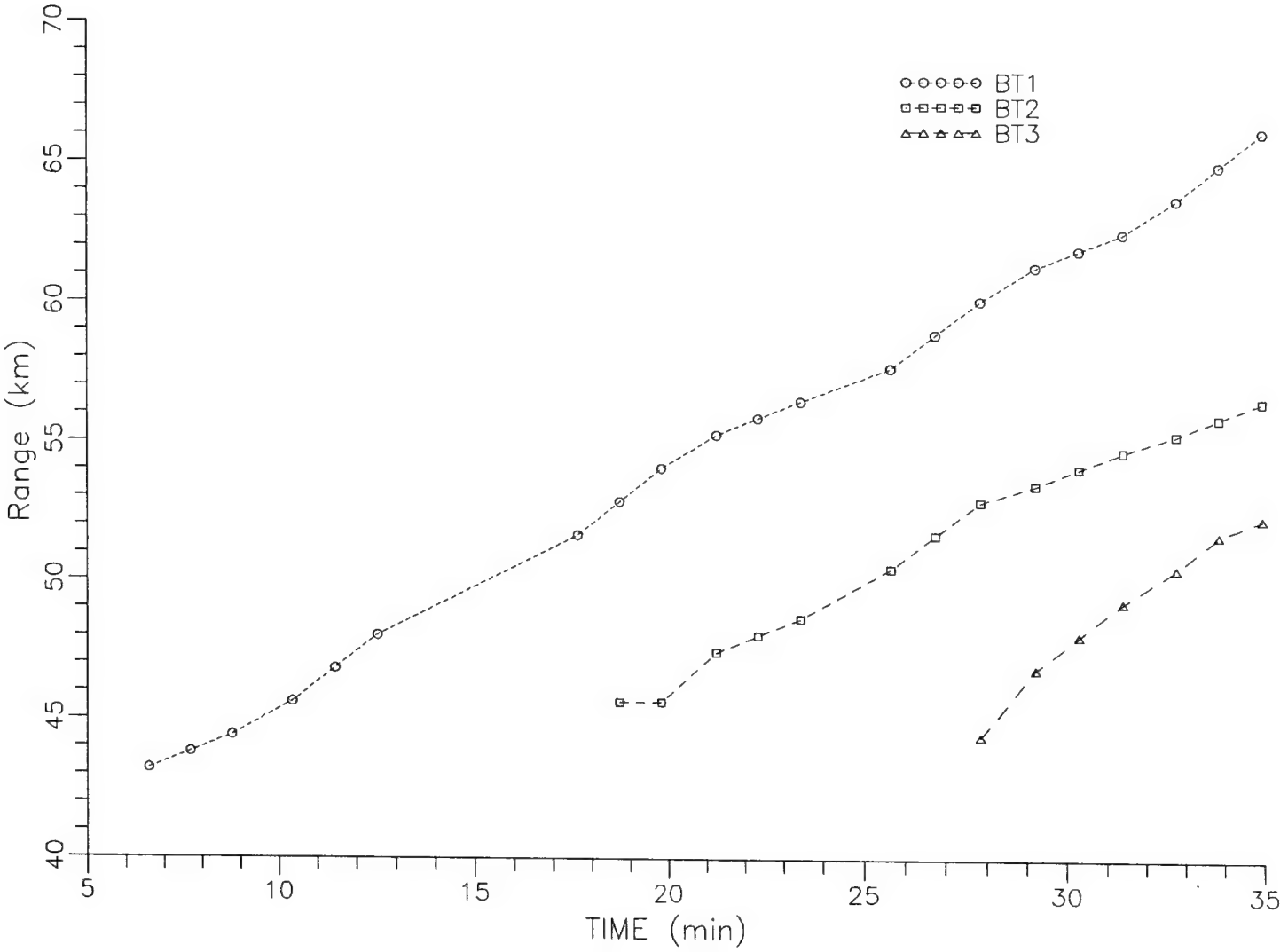


Figure 17 Tracks of Balloons Carrying Half-Wavelength Long Copper Wires at 18.65 MHz

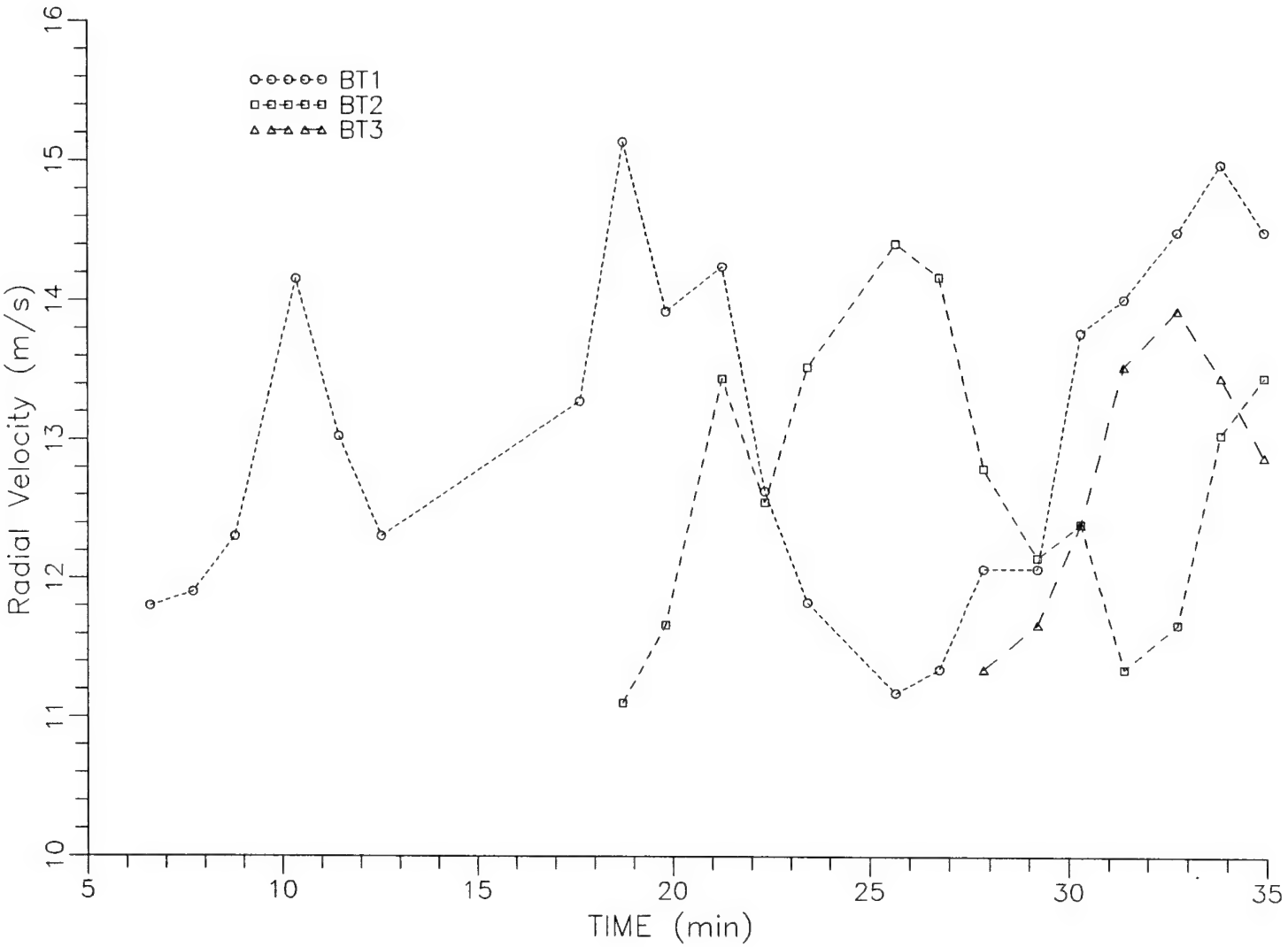


Figure 18 Radial Velocities of Balloons Carrying Half-Wavelength Long Copper Wires at 18.65 MHz

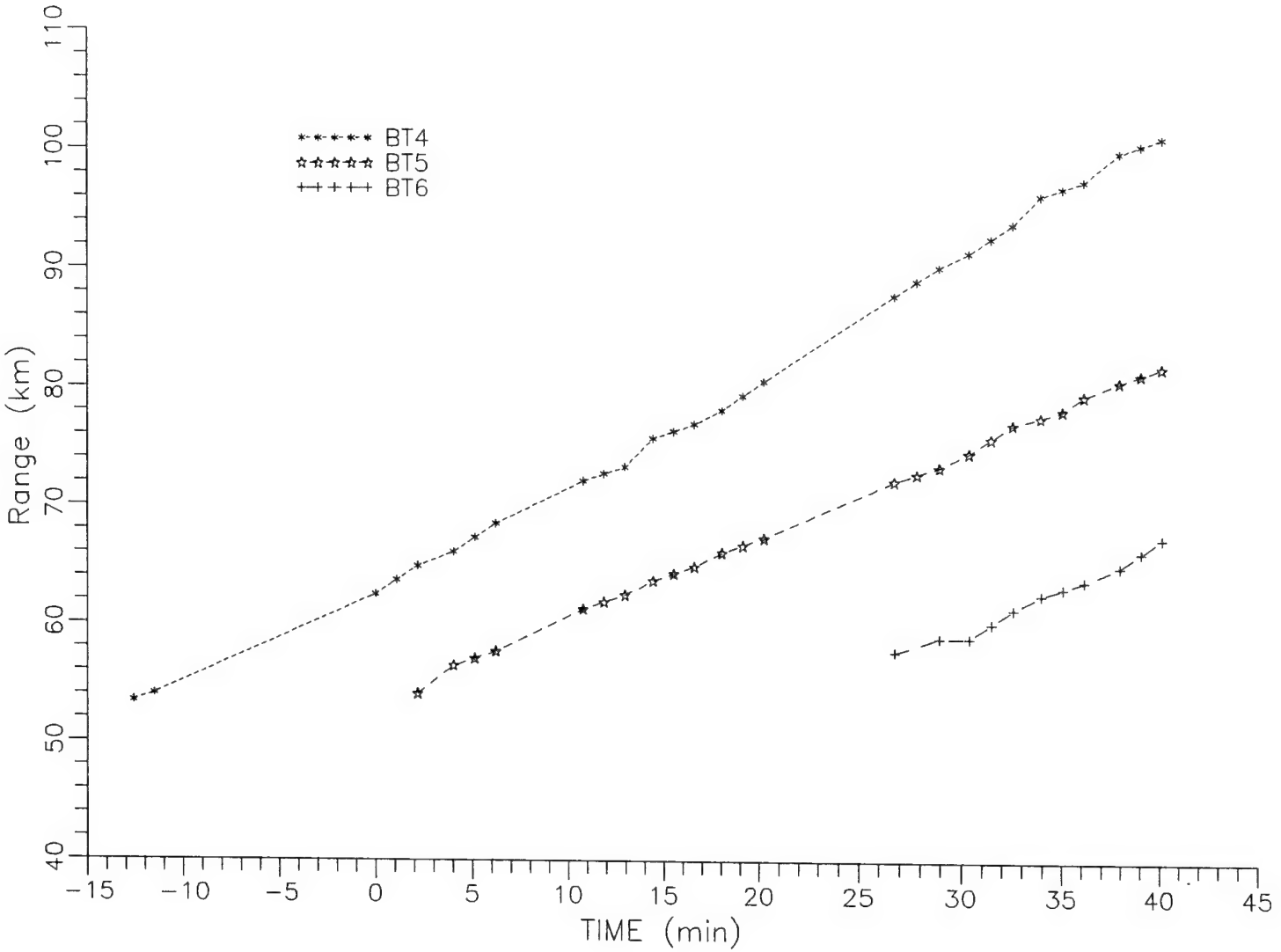


Figure 19 Tracks of Balloons Carrying Half–Wavelength Long Copper Wires at 10.62 MHz

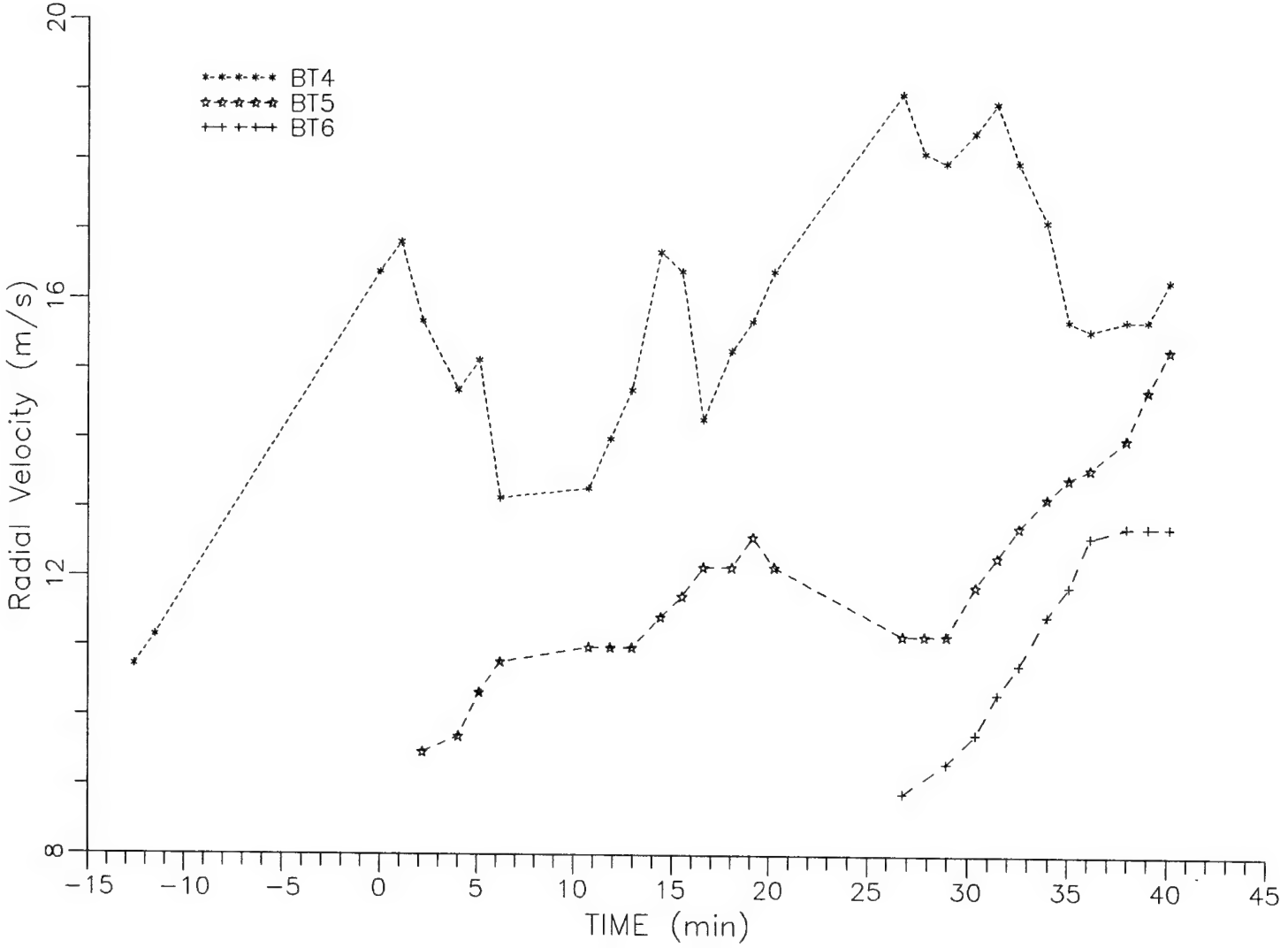


Figure 20 Radial Velocities of Balloons Carrying Half–Wavelength Long Copper Wires at 10.62 MHz

# 6. Conclusions and Recommendations

The data analysed in this report verified that the HFSWR at Cape Bonavista could detect targets at all radio frequencies used in the experiments. At 4.3 MHz, the low-flying Kingair was detected beyond the line of sight up to a range of about 110 km. At 27.8 MHz, the Piper Navajo was detected up to a range of about 26 km. The half-wavelength long thin wires were detected at 10.62 and 18.65 MHz when they were carried away by helium balloons. Some of these targets were tracked in range from about 44 to 66 km at 18.65 MHz, and from about 54 to 101 km at 10.62 MHz.

The detection of the Kingair by the HFSWR at 4.3 MHz was also studied by simulation. The simulation results showed that the radar could detect the Kingair up to a range of 95 km. These simulation results were compared with the experimental results at 4.3 MHz. It was found that the measured performance of the radar agreed well with the theoretical performance in the range interval between 35 and 95 km. The measured SNR and the theoretical SNR showed almost the same range dependence in this interval, with the measured SNR approximately proportional to $R^{-4.71}$. The target was detected beyond the line of sight throughout the interval.

Three types of interference signals were observed in the radar data. The first type was self-generated, and the others originated from external sources. The interference in the 4.3-MHz radar data was localised in range and Doppler frequency, and was likely caused by a reflection of the transmitted signal off the F1 layer of the ionosphere. The second type of interference appeared in the data collected on August 16 at the radio frequencies of 10.62 and 18.65 MHz. The interference caused a brief interruption in the time series and introduced five equally spaced peaks in the Doppler spectrum. This interference could result in false alarms in target detection. The third type of interference was noted in the experiments with the Navajo on August 17 when the radar operated at 18.65 and 10.62 MHz. This type of interference originated from external transmitters. No targets could be detected from the two sets of data because of the interference.

A number of options are available to mitigate the effects of interference on target detection. The best available option is to avoid having the interference in the same frequency channel as the radar signal. This can be achieved by monitoring the HF band continuously during the radar operation. For experimental purposes, a real-time frequency monitor may be sufficient. For an operational radar system, however, it is also desirable to have the information on channel occupancy or channel availability in the HF band. This requires continuous measurements of the external noise and interference level in narrowband steps (e.g., 5-10 kHz) over the frequency bands of interest. The measurements should be carried out continuously over time to build up a database to show the

diurnal and seasonal veriations of the noise and interference level. Information on channel occupancy or availability at any given time of the day can then be extracted from the database to aid the radar operator to select the best available frequency channel. In the event that a clear channel is not available, other techniques such as spatial nulling or polarimetric nulling can be employed. Currently, these techniques are being developed at DREO to facilitate the future operations of the HFSWR systems that are installed along the coast of Newfoundland.

The experiments involving the half-wavelength copper wires proved to be an inexpensive, but useful, way to evaluate the HFSWR. The thin wires were at resonance with the transmitted radar signal. Hence, the detection results of the thin wires provide some indications of the optimum performance of the HF radar in the detection of tactical ballistic missiles (TBM), which is currently considered as an option for cueing the TBMs in air defence. The target signals can also be compared with the sea echoes of the radar to provide an estimation of the first-order sea scattering coefficient at HF. This estimation will be reported shortly.

## Acknowledgements

The author would like to thank Dr. A.M. Ponsford of Raytheon Canada Limited for supplying the HFSWR data. The radar trials were conducted under the Scientific Authority of Dr. Tim Coyne, who past away after a long battle with cancer. Dr. Coyne and Jim Lundy of Star Tech. Ltd. sailed on Bonni Pauline under heavy wind conditions to launch the balloon targets.

## References

1. A.M. Ponsford and S.K. Srivastava, "Ground Wave Radar Development at NORDCO Limited - Phase 1", NORDCO Contract Report, 1990.

2. H.C. Chan, "Long Range Ship Detection Using High Frequency Surface Wave Radar", DREO Report No. 1184, Defence Research Establishment Ottawa, Sept. 1993.

3. H. Leong, "Long Range Aircraft Detection Using High-Frequency Surface-Wave Radar", DREO Report No. 1245, Defence Research Establishment Ottawa, Dec. 1994.

4. H.C. Chan, "Development of Software and Preliminary Analysis of High Frequency Surface Wave Radar Data", DREO Report No. 1153, Defence Research Establishment Ottawa, Dec. 1992.

5. Raytheon Canada 1991, "Design and Development of a Prototype Instrumentation for HF Surface Wave Radar Applications", Final Report DSS File #W7714-0-9446/01-ST, Raytheon Ref. ASD-148.

6. Raytheon Canada 1992, "Radar Site Modifications and Trials", Final Report DSS File #W7714-1-9508/01-QF, Raytheon Ref. ASD-149.

7. F.J. Harris, "On the Use of Windows for Harmonic Analysis with the Discrete Fourier Transform", Proceedings of the IEEE, Vol. 66, No. 1, pp. 51-83, Jan. 1966.

8. D.D. Crombie, "Doppler Spectrum of Sea Echo at 13.56Mc/s", Nature, 1955, 175, pp.681-682.

9. D. E. Barrick, "Remote Sensing of Sea State by Radar", Chapter 12, in "Remote Sensing of Troposphere", Edited by V. E. Derr, GPO, Washington, DC, 1972.

10. J. Walsh and S.K. Srivastava, "Rough Surface Propagation and Scatter with Applications to Ground Wave Remote Sensing in an Ocean Environment", Proc. AGARD (NATO) EEP Specialists' Meeting on Scattering and Propagation in Random Media, Italy, No. 419, pp. 23.1-23.15, 1988.

11. J.M. Headrick, "HF Over-The-Horizon Radar", in "Radar Handbook", Second Edition, Edited by M. Skolnik, McGraw-Hill Company, 1990.

12. M.I. Skolnik, "Introduction to Radar Systems", 2nd Edition, McGraw-Hill Company, 1980.

13. D. Friend, "The HF Radar Look-up Table Program User's Manual", Version 3-000, DREO Contract Report from Atlantic Scientific, Ottawa, Ontario, March 1995.

14. H.M. Finn and R.S. Johnson, "Adaptive Detection Mode with Threshold Control as a Function of Spatially Sampled Clutter-level Estimates", RCA Review, No. 29, 1968.

15. C.W. Trueman and S.J. Kubina, "HF Ground Wave Radar Studies", Final Report, TN-EMC-94-02, Concordia University, Montreal, Canada, August, 1994.

# Appendix A Data Log

DATA LOG:
DATE: 08/15/92 TAPE NO. 1 EXPERIMENT: Beechcraft Kingair

| FILENAME | START_TIME | FIN_TIME | DWELL (s) | Tx_FREQ (MHz) | PRF (Hz) | ST_RS | END_RS | TOTAL_RS | Comments |
|---|---|---|---|---|---|---|---|---|---|
| AIR1 | 11:56:04 | 12:01:04 | 300 | 4.30 | 100 | 10 | 144 | 135 | Cardioid Tx. |
| AIR2 | 12:01:19 | 12:06:19 | 300 | 4.30 | 100 | 10 | 144 | 135 | |
| CRAP | 12:07:29 | 12:07:32 | 3 | 4.30 | 100 | 10 | 70 | 61 | |
| AIR3 | 12:08:03 | 12:13:03 | 300 | 4.30 | 100 | 10 | 144 | 135 | |
| AIR4 | 12:13:35 | 12:18:35 | 300 | 4.30 | 100 | 10 | 144 | 135 | |
| AIR5 | 12:18:51 | 12:23:51 | 300 | 4.30 | 100 | 10 | 144 | 135 | |
| AIR6 | 12:24:12 | 12:29:12 | 300 | 4.30 | 100 | 10 | 144 | 135 | |
| AIR7 | 12:29:30 | 12:34:30 | 300 | 4.30 | 100 | 10 | 144 | 135 | |

DATA LOG:
DATE: 08/15/92 TAPE NO. 2 EXPERIMENT: Beechcraft Kingair

| FILENAME | START_TIME | FIN_TIME | DWELL (s) | Tx_FREQ (MHz) | PRF (Hz) | ST_RS | END_RS | TOTAL_RS | Comments |
|---|---|---|---|---|---|---|---|---|---|
| DATA8 | 12:49:51 | 12:54:51 | 300 | 4.30 | 100 | 10 | 144 | 135 | Renamed to AIR8 |
| DATA9 | 12:55:22 | 13:00:22 | 300 | 4.30 | 100 | 10 | 144 | 135 | Renamed to AIR9 |
| DATA10 | 13:02:06 | 13:07:06 | 300 | 4.30 | 100 | 10 | 144 | 135 | |
| DATA11 | 13:07:58 | 13:12:58 | 300 | 4.30 | 100 | 10 | 144 | 135 | |
| DATA12 | 13:13:28 | 13:18:28 | 300 | 4.30 | 100 | 10 | 144 | 135 | |
| DATA13 | 13:20:16 | 13:25:16 | 300 | 4.30 | 100 | 10 | 144 | 135 | |

DATA LOG:
DATE: 08/15/92 TAPE NO. 3 EXPERIMENT: Beechcraft Kingair

| FILENAME | START_TIME | FIN_TIME | DWELL (s) | Tx_FREQ (MHz) | PRF (Hz) | ST_RS | END_RS | TOTAL_RS | Comments |
|---|---|---|---|---|---|---|---|---|---|
| DATA14 | 13:36:08 | 13:41:08 | 300 | 18.65 | 100 | 10 | 144 | 135 | |
| DATA15 | 13:41:50 | 13:46:50 | 300 | 18.65 | 100 | 10 | 144 | 135 | |
| DATA16 | 13:48:12 | 13:53:12 | 300 | 18.65 | 100 | 10 | 144 | 135 | |
| DATA17 | 13:53:47 | 13:58:47 | 300 | 18.65 | 100 | 10 | 144 | 135 | |
| DATA18 | 14:00:41 | 14:05:41 | 300 | 18.65 | 100 | 10 | 144 | 135 | |
| DATA19 | 14:06:34 | 14:11:34 | 300 | 18.65 | 100 | 10 | 144 | 135 | |
| DATA20 | 14:11:53 | 14:15:31 | 215 | 18.65 | 100 | 10 | 144 | 135 | |
| NOISE1 | 14:23:08 | 14:28:08 | 300 | 18.65 | 100 | 10 | 144 | 135 | |
| NOISE2 | 14:30:11 | 14:35:11 | 300 | 4.30 | 100 | 10 | 144 | 135 | |

DATA LOG:
DATE: 08/16/92 TAPE NO. 1 EXPERIMENT: Balloon with λ/2 Cu Wire Launched from Bonni Pauline (BP); 8 Element Receive Array

| FILENAME | START_TIME | FIN_TIME | DWELL (s) | Tx_FREQ (MHz) | PRF (Hz) | ST_RS | END_RS | TOTAL_RS | Comments |
|---|---|---|---|---|---|---|---|---|---|
| BP01 | 11:27:26 | 11:30:46 | 200 | 18.65 | 250 | 1 | 79 | 79 | BP @10 n.mi. @9 knots |
| BP02 | 12:14:28 | 12:17:48 | 200 | 18.65 | 250 | 10 | 88 | 79 | BP @18 n.mi. @9 knots |
| BL01 | 12:46:08 | 12:49:28 | 200 | 18.65 | 250 | 10 | 88 | 79 | Balloon dragging across water |
| BL02 | 12:52:44 | 12:56:04 | 200 | 18.65 | 250 | 10 | 88 | 79 | Balloon 1 Due East 15 knots Altitude ~ 200 feet |
| BL03 | 12:56:29 | 12:59:49 | 200 | 18.65 | 250 | 10 | 88 | 79 | |
| BL04 | 13:03:46 | 13:07:06 | 200 | 18.65 | 250 | 10 | 88 | 79 | Balloon 2 |
| BL05 | 13:07:23 | 13:10:43 | 200 | 18.65 | 250 | 10 | 88 | 79 | |
| BL06 | 13:11:48 | 13:15:08 | 200 | 18.65 | 250 | 10 | 88 | 79 | Balloon 3, Not rising as fast same direction; BP 21.7 n.mi. Boresight |
| BL07 | 13:15:21 | 13:18:42 | 200 | 18.65 | 250 | 10 | 88 | 79 | |
| BL08 | 13:18:53 | 13:22:13 | 200 | 18.65 | 250 | 10 | 88 | 79 | |
| NOISE1 | 13:23:27 | 13:26:47 | 200 | 18.65 | 250 | 10 | 88 | 79 | |

DATA LOG:
DATE: 08/16/92 TAPE NO. 2 EXPERIMENT: Balloon with λ/2 Cu Wire, 8 Element Array

| FILENAME | START_TIME | FIN_TIME | DWELL (s) | Tx_FREQ (MHz) | PRF (Hz) | ST_RS | END_RS | TOTAL_RS | Comments |
|---|---|---|---|---|---|---|---|---|---|
| BL09 | 14:15:01 | 14:18:20 | 200 | 10.62 | 249 | 10 | 89 | 80 | Balloon 4 Due East 15 knots, 100 feet |
| BUM1 | 14:18:53 | 14:19:05 | 12 | 10.62 | 250 | 10 | 89 | 80 | |
| BL10 | 14:28:43 | 14:32:03 | 200 | 10.62 | 250 | 10 | 88 | 79 | Balloon 5 |
| BL11 | 14:32:45 | 14:36:05 | 200 | 10.62 | 250 | 10 | 88 | 79 | |
| BL12 | 14:39:30 | 14:42:50 | 200 | 10.62 | 250 | 10 | 88 | 79 | Balloon 6 |
| BL13 | 14:43:09 | 14:46:29 | 200 | 10.62 | 250 | 10 | 88 | 79 | |
| BL14 | 14:46:47 | 14:50:07 | 200 | 10.62 | 250 | 10 | 88 | 79 | |
| BL15 | 14:55:30 | 14:58:50 | 200 | 10.62 | 250 | 10 | 88 | 79 | Balloon 7 |
| BL16 | 14:59:07 | 15:02:27 | 200 | 10.62 | 250 | 10 | 88 | 79 | |
| BL17 | 15:02:42 | 15:06:02 | 200 | 10.62 | 250 | 10 | 88 | 79 | |
| BL18 | 15:06:42 | 15:10:03 | 200 | 10.62 | 250 | 10 | 88 | 79 | |
| NOISE2 | 15:18:55 | 15:22:15 | 200 | 10.62 | 250 | 10 | 88 | 79 | |

DATA LOG:
DATE: 08/17/92 TAPE NO. 1 EXPERIMENT: Piper Navajo

| FILENAME | START_TIME | FIN_TIME | DWELL (s) | Tx_FREQ (MHz) | PRF (Hz) | ST_RS | END_RS | TOTAL_RS | Comments |
|---|---|---|---|---|---|---|---|---|---|
| NAV1 | 11:20:09 | 11:25:09 | 300 | 18.65 | 100 | 10 | 144 | 135 | Rx. Array 16 elements |
| NAV2 | 11:35:57 | 11:40:57 | 300 | 18.65 | 100 | 10 | 144 | 135 | @5m spacing |
| NAV3 | 11:44:44 | 11:49:44 | 300 | 18.65 | 100 | 10 | 144 | 135 | Aircraft not in position |
| nav4 | 11:50:43 | 11:55:43 | 300 | 18.65 | 100 | 10 | 144 | 135 | Interference seen on |
| NAV5 | 11:56:20 | 12:01:20 | 300 | 18.65 | 100 | 10 | 144 | 135 | -ve side of DFT Analyzer |
| NAV6 | 12:02:03 | 12:07:03 | 300 | 18.65 | 100 | 10 | 144 | 135 | |
| NAV7 | 12:07:24 | 12:12:24 | 300 | 18.65 | 100 | 10 | 144 | 135 | |
| NAV8 | 12:13:44 | 12:18:44 | 300 | 18.65 | 100 | 10 | 144 | 135 | |
| NAV9 | 12:26:14 | 12:26:51 | 27 | 18.65 | 100 | 10 | 144 | 135 | |

DATA LOG:
DATE: 08/17/92 TAPE NO. 2 EXPERIMENT: Piper Navajo

| FILENAME | START_TIME | FIN_TIME | DWELL (s) | Tx_FREQ (MHz) | PRF (Hz) | ST_RS | END_RS | TOTAL_RS | Comments |
|---|---|---|---|---|---|---|---|---|---|
| NAV10 | 12:40:42 | 12:45:42 | 300 | 18.65 | 100 | 10 | 144 | 135 | |
| NAV11 | 12:48:13 | 12:53:13 | 300 | 18.65 | 100 | 10 | 144 | 135 | |
| NAV12 | 12:53:42 | 12:58:42 | 300 | 18.65 | 100 | 10 | 144 | 135 | |
| NAV13 | 12:59:17 | 13:04:17 | 300 | 18.65 | 100 | 10 | 144 | 135 | 25 Hz offset |
| NAV14 | 13:05:15 | 13:10:15 | 300 | 18.65 | 100 | 10 | 144 | 135 | Back to normal |
| NAV15 | 13:11:04 | 13:16:04 | 300 | 18.65 | 100 | 10 | 144 | 135 | |

DATA LOG:
DATE: 08/17/92 TAPE NO. 3 EXPERIMENT: Piper Navajo

| FILENAME | START_TIME | FIN_TIME | DWELL (s) | Tx_FREQ (MHz) | PRF (Hz) | ST_RS | END_RS | TOTAL_RS | Comments |
|---|---|---|---|---|---|---|---|---|---|
| NAV16 | 15:01:24 | 15:06:24 | 300 | 10.62 | 100 | 10 | 144 | 135 | |
| NAV17 | 15:07:07 | 15:12:07 | 300 | 10.62 | 100 | 10 | 144 | 135 | |
| NAV18 | 15:13:30 | 15:18:30 | 300 | 10.62 | 100 | 10 | 144 | 135 | |
| NAV19 | 15:18:54 | 15:23:54 | 300 | 10.62 | 100 | 10 | 144 | 135 | |
| NAV20 | 15:24:12 | 15:29:13 | 300 | 10.62 | 100 | 10 | 144 | 135 | |
| NAV21 | 15:46:06 | 15:51:06 | 300 | 27.80 | 100 | 10 | 144 | 135 | Aircraft overhead at start |
| NAV22 | 15:51:17 | 15:56:17 | 300 | 27.80 | 100 | 10 | 144 | 135 | |
| NAV23 | 15:56:50 | 16:01:50 | 300 | 27.80 | 100 | 10 | 144 | 135 | |
| NAV24 | 16:02:51 | 16:07:51 | 300 | 27.80 | 100 | 10 | 144 | 135 | |
| NAV25 | 16:08:30 | 16:13:30 | 300 | 27.80 | 100 | 10 | 144 | 135 | |
| NAV26 | 16:14:06 | 16:19:06 | 300 | 27.80 | 100 | 10 | 144 | 135 | |
| NAV27 | 16:19:56 | 16:24:56 | 300 | 27.80 | 100 | 10 | 144 | 135 | |

DATA LOG:
DATE: 08/17/92 TAPE NO. 4 EXPERIMENT: 4.3 MHz Test Data

| FILENAME | START_TIME | FIN_TIME | DWELL (s) | Tx_FREQ (MHz) | PRF (Hz) | ST_RS | END_RS | TOTAL_RS | Comments |
|---|---|---|---|---|---|---|---|---|---|
| NOISE3 | 16:42:54 | 16:47:54 | 300 | 27.80 | 100 | 10 | 144 | 135 | TX off |
| TEST1 | 16:50:42 | 16:50:53 | 1 | 4.30 | 100 | 50 | 114 | 65 | |
| TEST2 | 16:59:04 | 16:59:15 | 6 | 4.30 | 50 | 50 | 110 | 61 | |
| TEST3 | 17:07:51 | 17:07:56 | 3 | 4.30 | 50 | 1 | 50 | 50 | |
| DATA1 | 17:08:33 | 17:13:33 | 300 | 4.30 | 50 | 50 | 324 | 275 | Tx. on |
| DATA2 | 17:14:56 | 17:19:56 | 300 | 4.30 | 50 | 50 | 324 | 275 | |
| DATA3 | 17:25:45 | 17:30:45 | 300 | 4.30 | 50 | 50 | 324 | 275 | System may not be locked |
| DATA4 | 18:03:53 | 18:08:53 | 300 | 4.30 | 50 | 50 | 324 | 275 | |
| DATA5 | 18:15:45 | 18:20:45 | 300 | 4.30 | 50 | 50 | 324 | 275 | |
| NOISE4 | 18:21:41 | 18:26:41 | 300 | 4.30 | 50 | 50 | 324 | 275 | Tx. off |

DATA LOG:
DATE: 08/18/92 TAPE NO. 1 EXPERIMENT: 4.3 MHz Test Data

| FILENAME | START_TIME | FIN_TIME | DWELL (s) | Tx_FREQ (MHz) | PRF (Hz) | ST_RS | END_RS | TOTAL_RS | Comments |
|---|---|---|---|---|---|---|---|---|---|
| RX4 | 09:20:38 | 09:25:38 | 300 | 18.65 | 100 | 10 | 144 | 135 | |
| 4MHZ1 | 09:34:58 | 09:38:18 | 200 | 4.30 | 100 | 50 | 254 | 205 | Tx @ different PRF |
| 4MHZ2 | 09:40:02 | 09:43:22 | 200 | 4.30 | 100 | 50 | 254 | 205 | |
| 4MHZ3 | 10:03:35 | 10:06:55 | 200 | 4.30 | 50 | 10 | 424 | 415 | |
| 4MHZ4 | 10:12:58 | 10:16:18 | 200 | 4.30 | 50 | 10 | 424 | 415 | |
| 4MHZ5 | 10:17:04 | 10:20:24 | 200 | 4.30 | 50 | 10 | 424 | 415 | |
| Q | 10:27:42 | 10:27:43 | 2 | 1.95 | 50 | 10 | 70 | 61 | aborted |
| MUX1 | 10:28:43 | 10:32:03 | 200 | 4.30 | 50 | 10 | 424 | 415 | 4 chan. multiplexed |
| MUX2 | 10:34:10 | 10:44:11 | 600 | 4.30 | 50 | 10 | 272 | 263 | |
| 4MHZ6 | 10:51:39 | 10:54:59 | 200 | 4.30 | 50 | 10 | 424 | 415 | Rx Gating + 10dB pre-amp |
| 4MHZ7 | 11:02:59 | 11:06:19 | 200 | 4.30 | 50 | 10 | 424 | 415 | No Gating, No pre-amp |
| 4MHZ8 | 11:08:02 | 11:11:22 | 200 | 4.30 | 50 | 10 | 424 | 415 | |
| 4MHX9 | 11:13:47 | 11:17:08 | 200 | 4.30 | 50 | 10 | 424 | 415 | |
| 4MHX10 | 11:21:10 | 11:31:10 | 600 | 4.30 | 50 | 10 | 424 | 415 | |

## Appendix B Detection of Half-Wavelength Thin Wires at 18.65 MHz

Figures B1-B7 are all similar to Figure 14 in the report, except that in Figures B1-B7 the spectral power in the Doppler interval of -2.20 to -1.20 Hz is shown for the range interval of interest only, i.e., for the range interval where the targets could be detected.

Three targets, BT1, BT2 and BT3, were detected from Figures B1-B7. BT1 was first detected in Figure B1 at the range of about 44 km, and it was seen moving away progressively throughout Figures B2-B7. It was last detected at the range of 66 km in Figure B7. BT2 was seen rising up at the range of 45 km in Figure B3 (reproduced in Figure 14). It was clearly detected throughout Figures B4-B5, but then the signal of the target became murky in Figures B6-B7 due to the launch of BT3. As shown in Figures B6-B7, BT2 and BT3 were effectively located within the same range cell from each other (i.e., 7.5 km).

The detection results are summarized below:

| Target | Ranges (RS#) | Data Files |
|---|---|---|
| BT1 | 28-46 | BL02-BL08 |
| BT2 | 28-39 | BL04-BL08 |
| BT3 | 28-35 | BL06-BL08 |

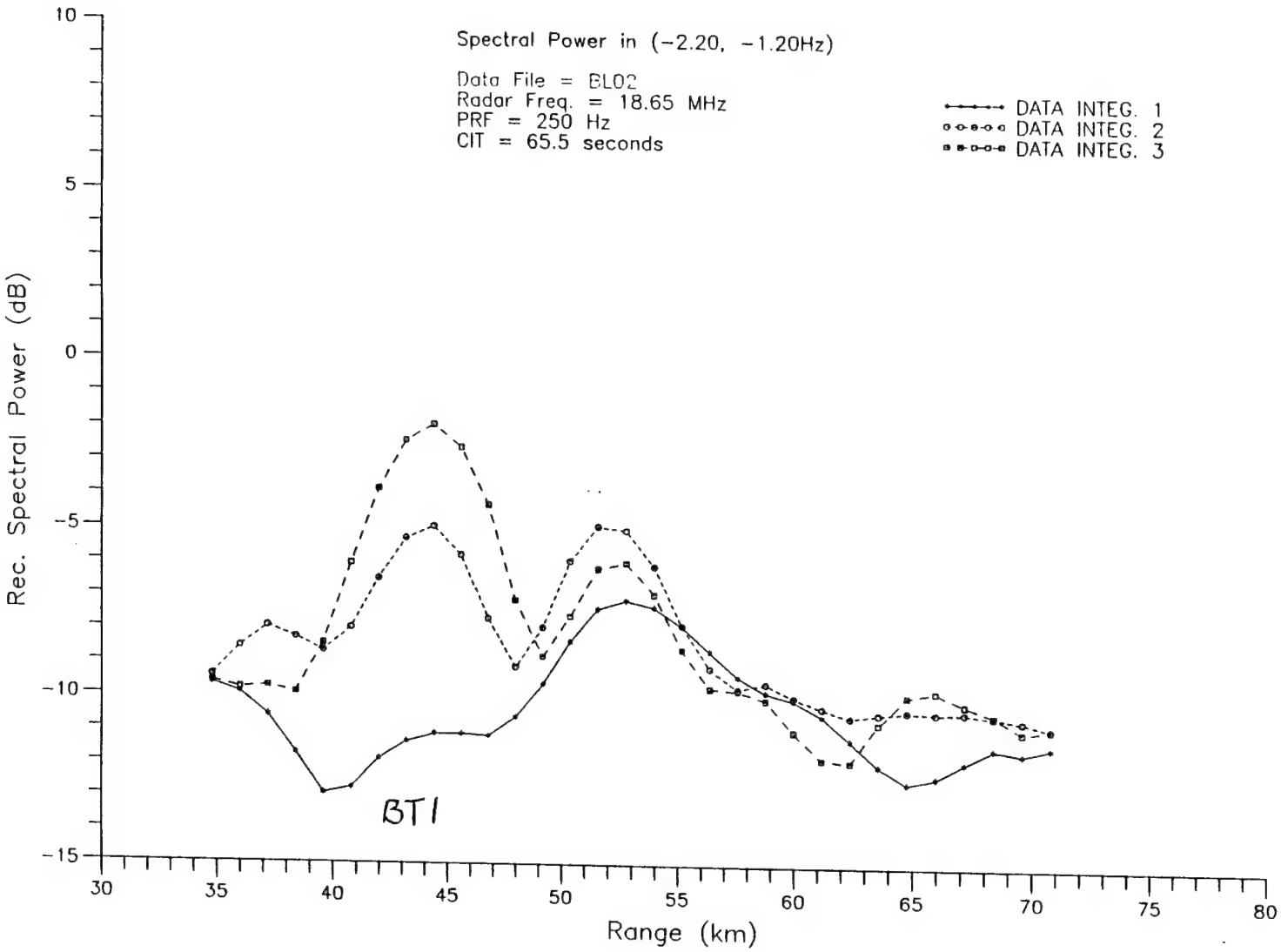


Figure B1 Detection of Half-Wavelength Long Copper Wire at 18.65 MHz

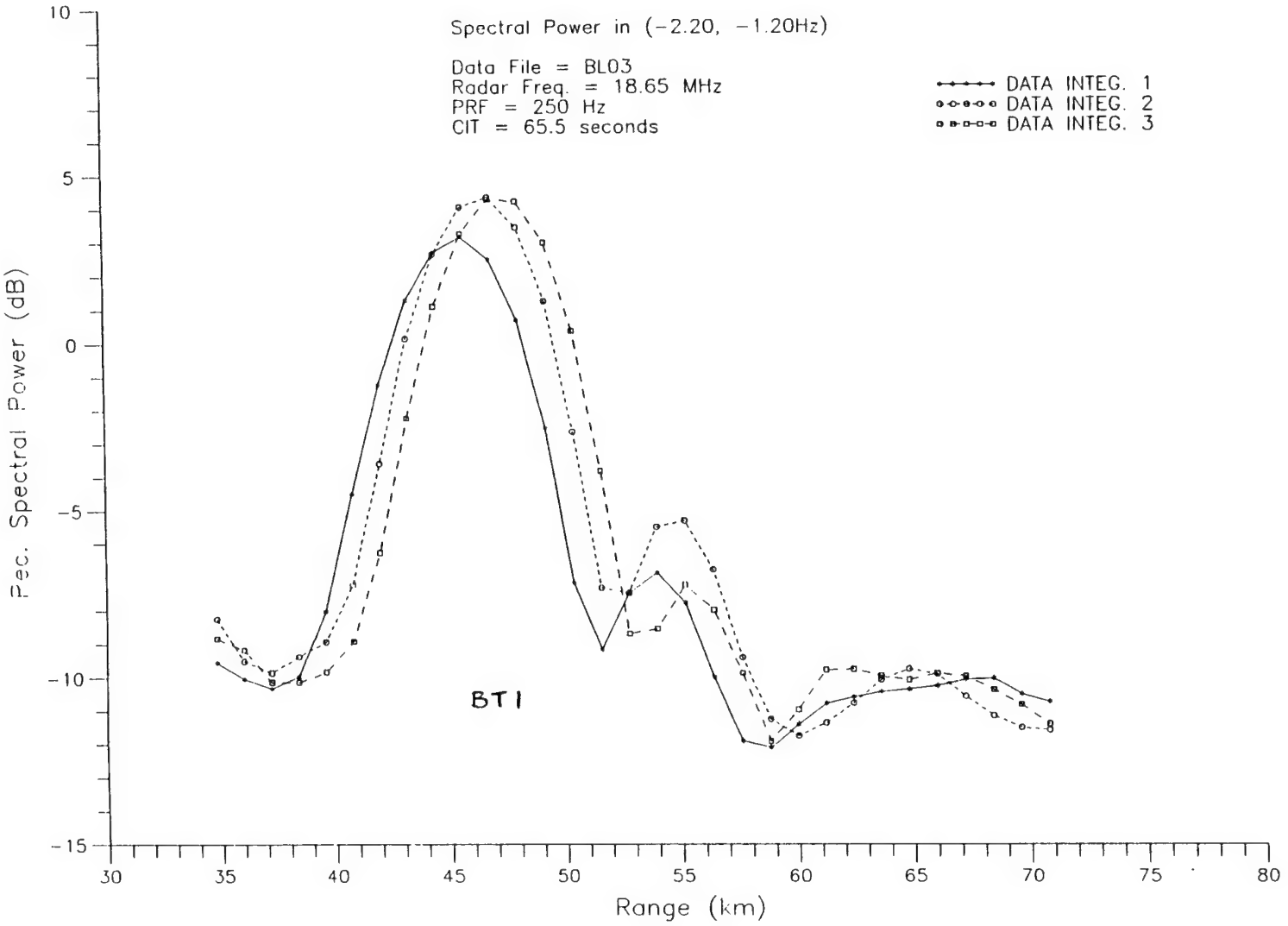


Figure B2 Detection of Half-Wavelength Long Copper Wire at 18.65 MHz

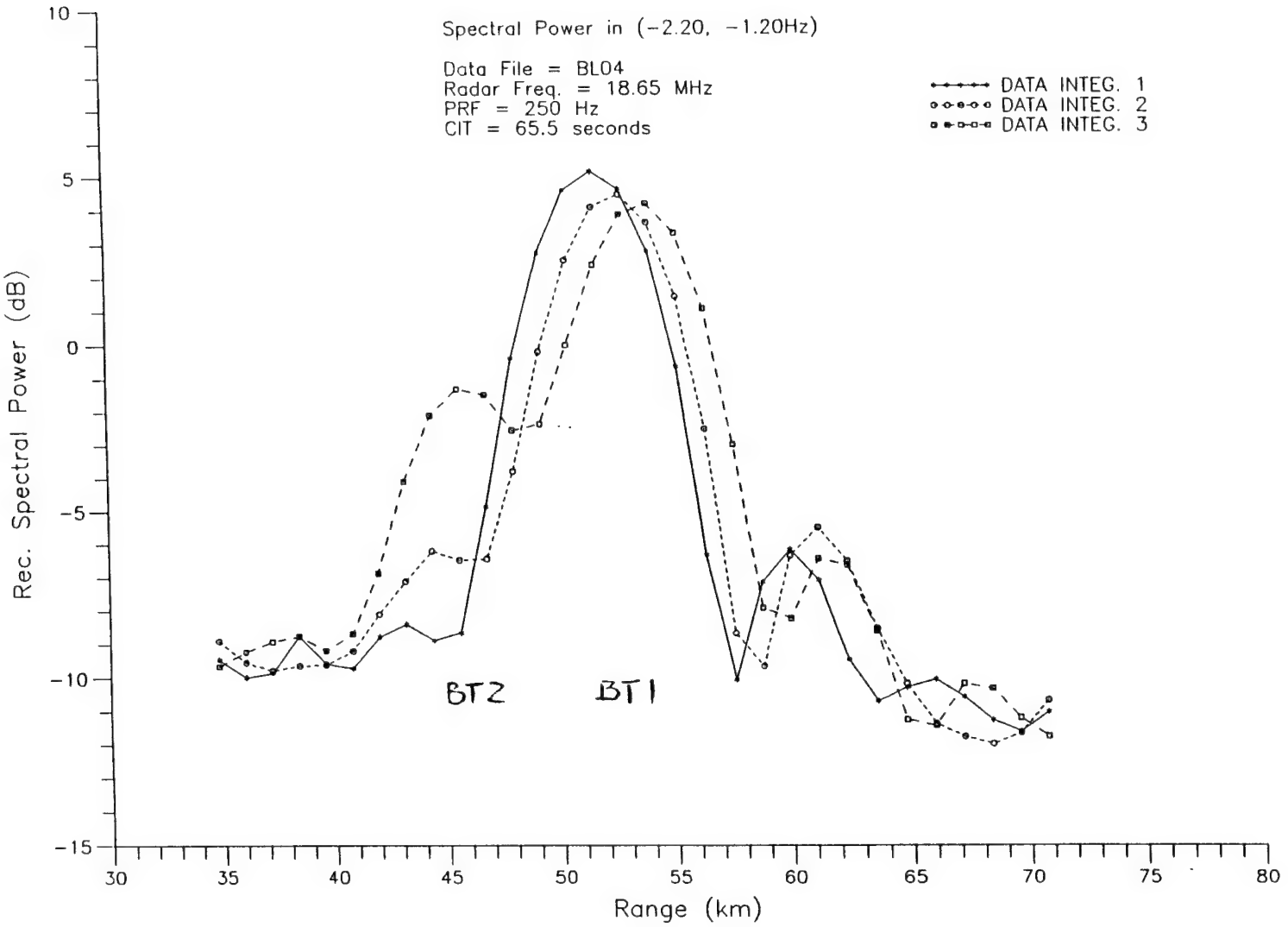


Figure B3 Detection of Half-Wavelength Long Copper Wire at 18.65 MHz

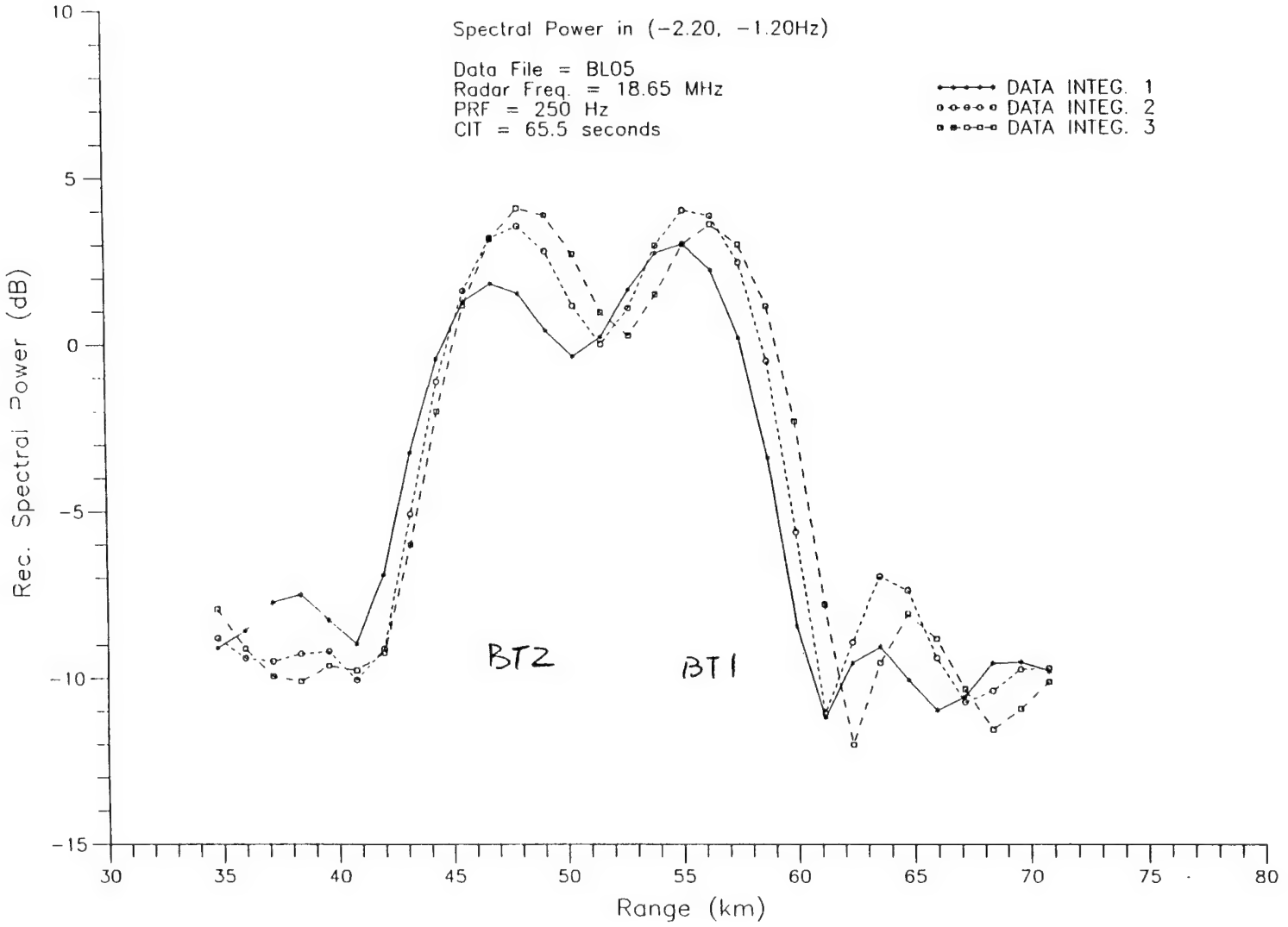


Figure B4 Detection of Half-Wavelength Long Copper Wire at 18.65 MHz

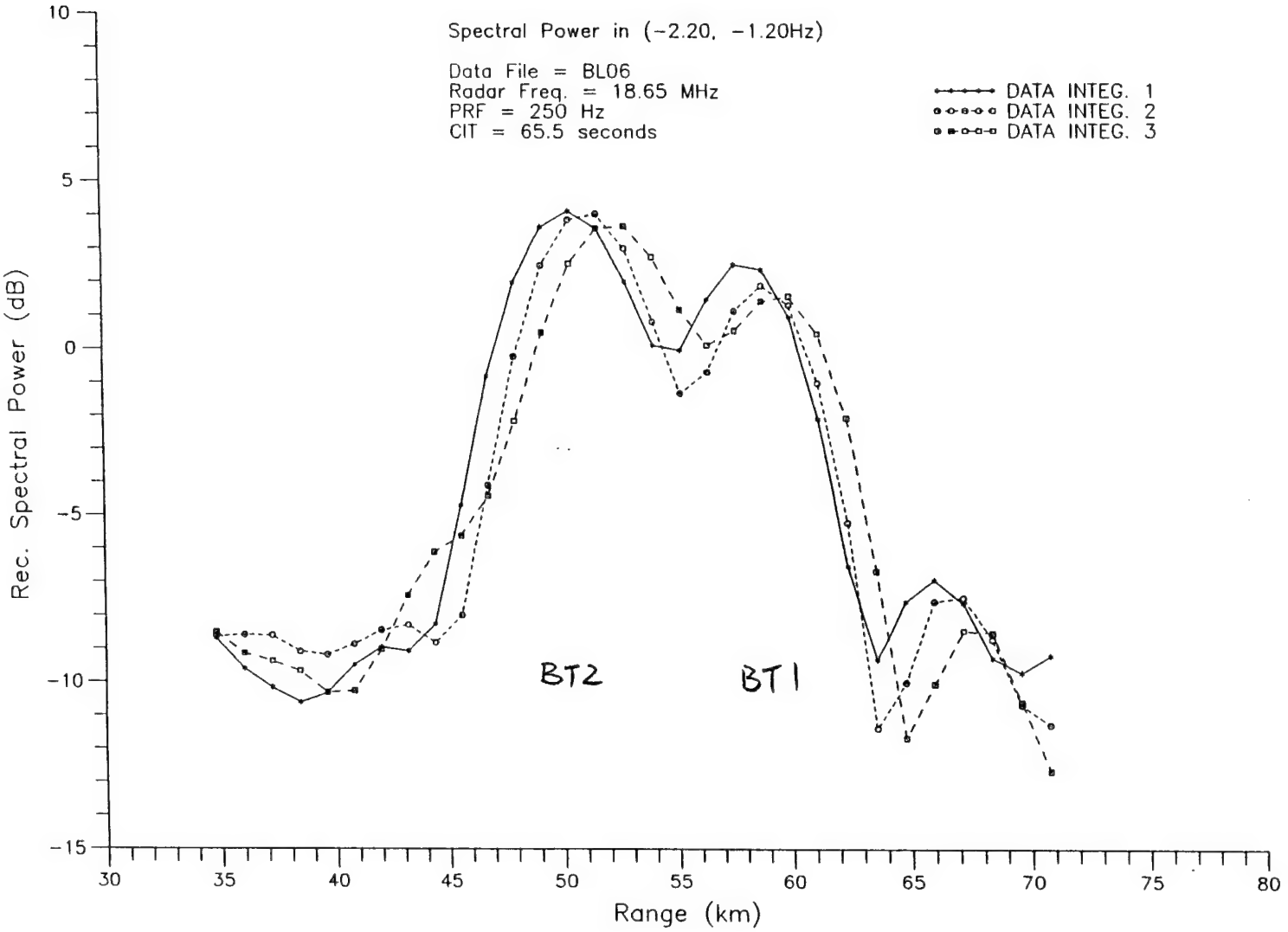


Figure B5 Detection of Half-Wavelength Long Copper Wire at 18.65 MHz

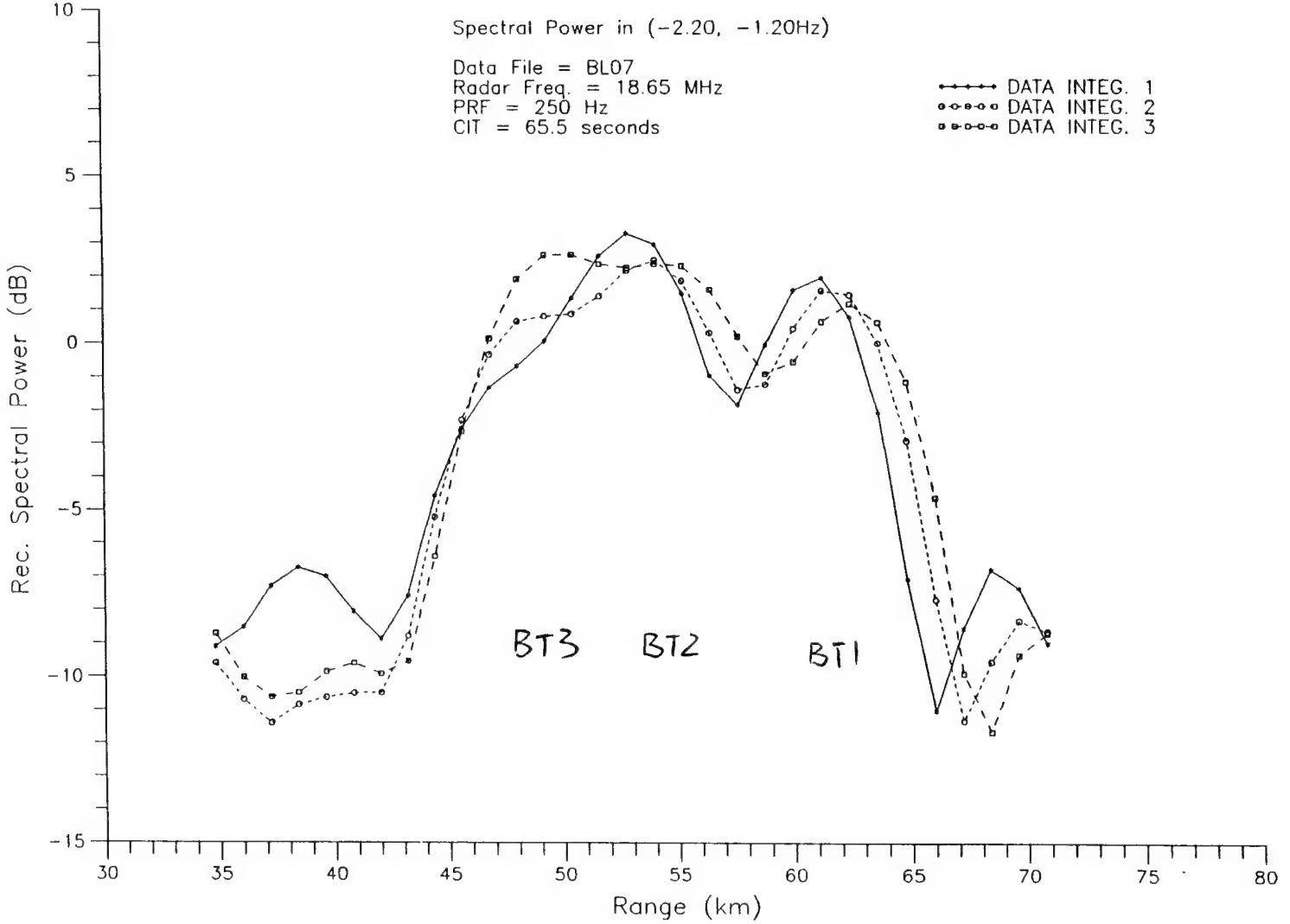


Figure B6 Detection of Half-Wavelength Long Copper Wire at 18.65 MHz

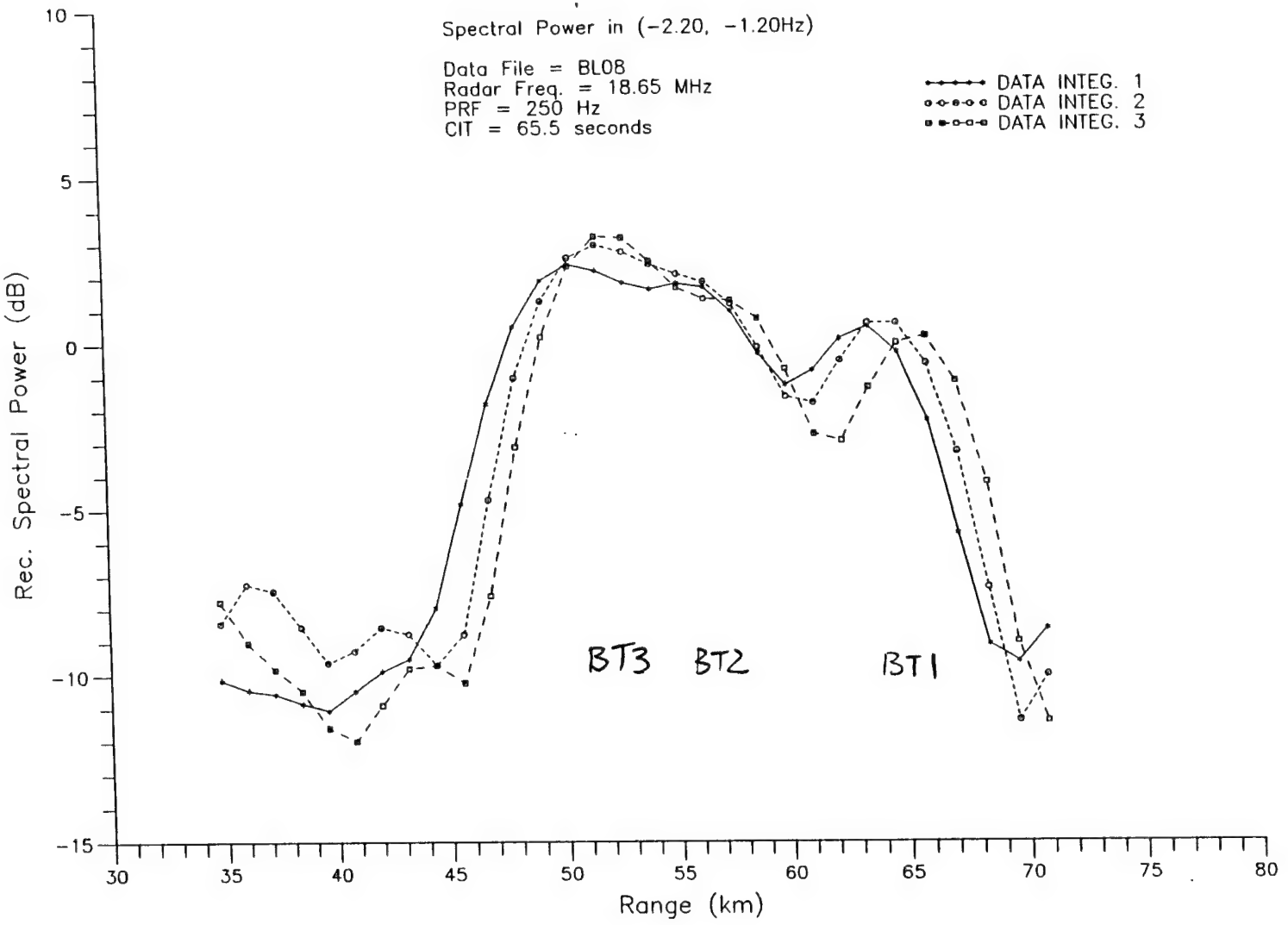


Figure B7 Detection of Half-Wavelength Long Copper Wire at 18.65 MHz

## Appendix C Detection of Half-Wavelength Thin Wires at 10.62 MHz

Figures C1-C10 are similar to Figure 13 in the report. Here the spectral power in the Doppler interval of -2.00 to -0.68 Hz is shown for the entire range of coverage of the radar.

BT4, BT5 and BT6 were detected from the curves in Figures C1-C10. BT4 corresponds to Balloon 4 in the data log. It was first detected in Figure C1, and was seen moving progressively away from the radar throughout Figures C2-C10. The target was last seen at the range of about 101 km. BT5 corresponds to Balloon 5. This target was first detected in Figure C2, and was tracked in Figures C3-C10 up to the range of about 82 km. Balloon 6, as labelled in the data log, seemed to be observable in Figures C3-C6. However, the target did not seem to move consistently away from the radar. Hence, we concluded that the target was not detected. BT6 corresponds to Balloon 7. It was first detected from the data in the file BL16, which was collected at about the same time as Balloon 7 was launched. BT6 was tracked throughout Figures C8-10 up to a range of about 67 km.

The detection results are summarized as below:

| Target | Ranges (RS#) | Data Files |
|---|---|---|
| BT4 | 36-75 | BL09-BL18 |
| BT5 | 36-64 | BL10-BL18 |
| BT6 | 42-47 | BL15-BL18 |

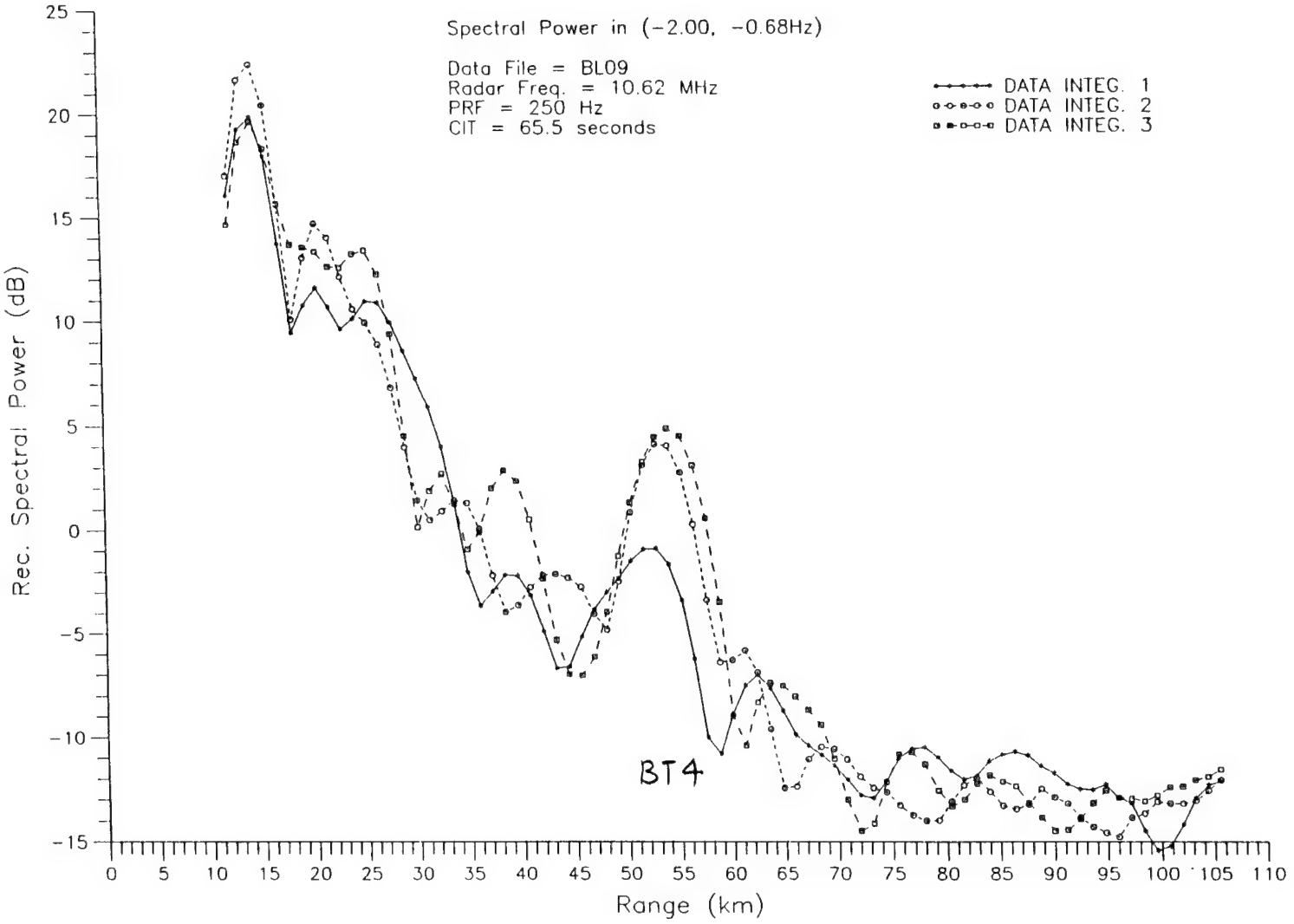


Figure C1 Detection of Half-Wavelength Long Copper Wire at 10.62 MHz

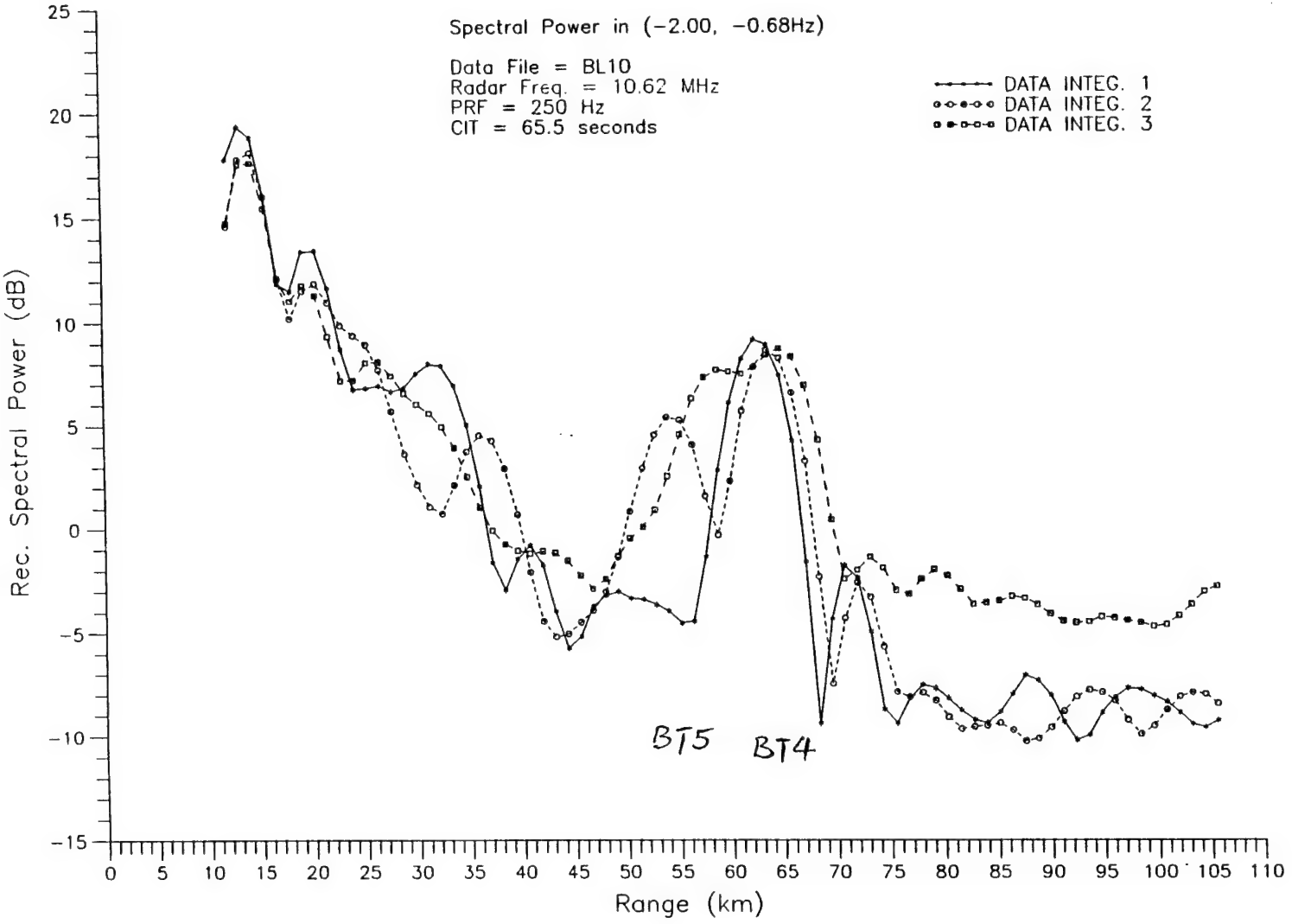


Figure C2 Detection of Half−Wavelength Long Copper Wire at 10.62 MHz

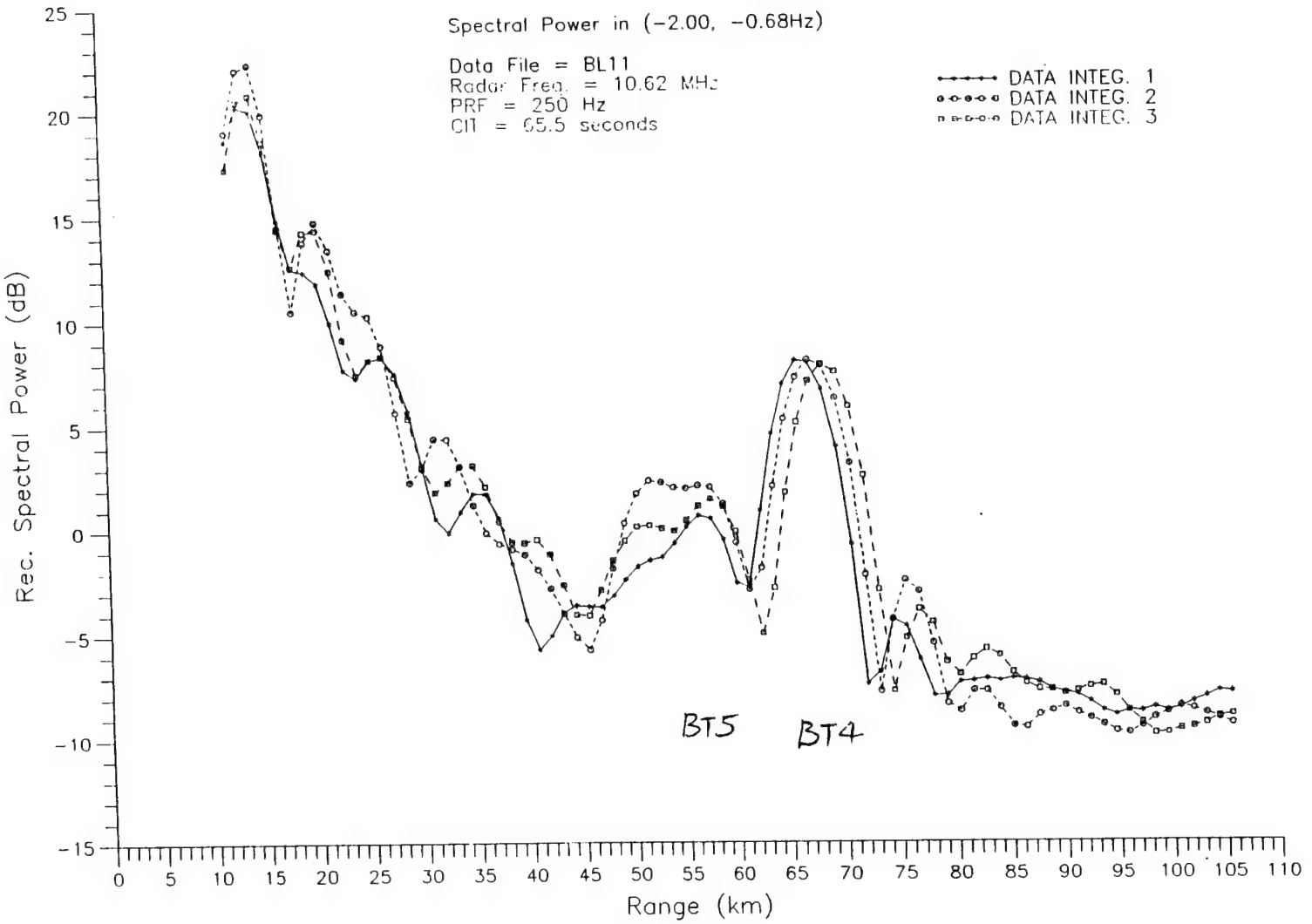


Figure C3 Detection of Half−Wavelength Long Copper Wire at 10.62 MHz

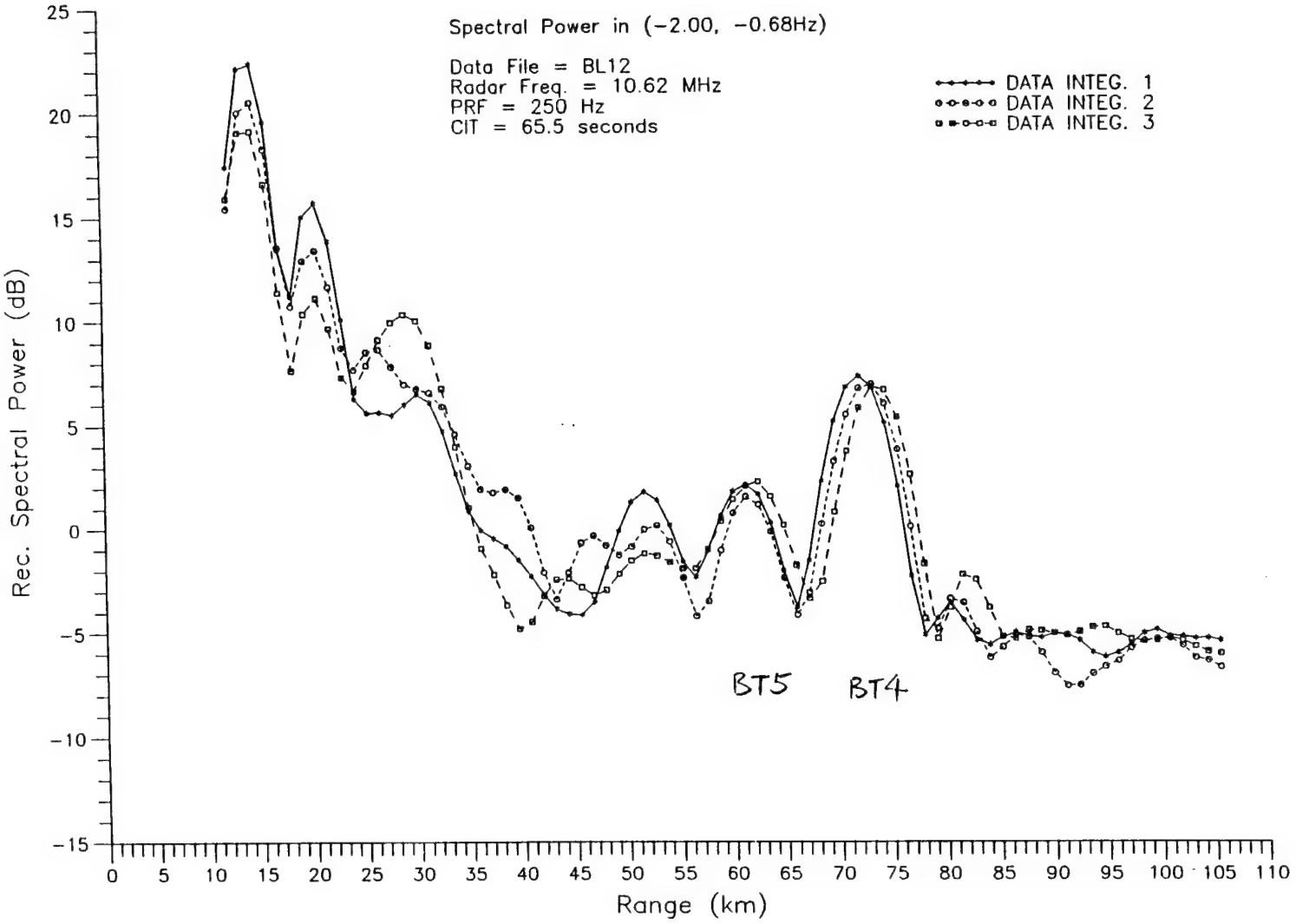


Figure C4 Detection of Half-Wavelength Long Copper Wire at 10.62 MHz

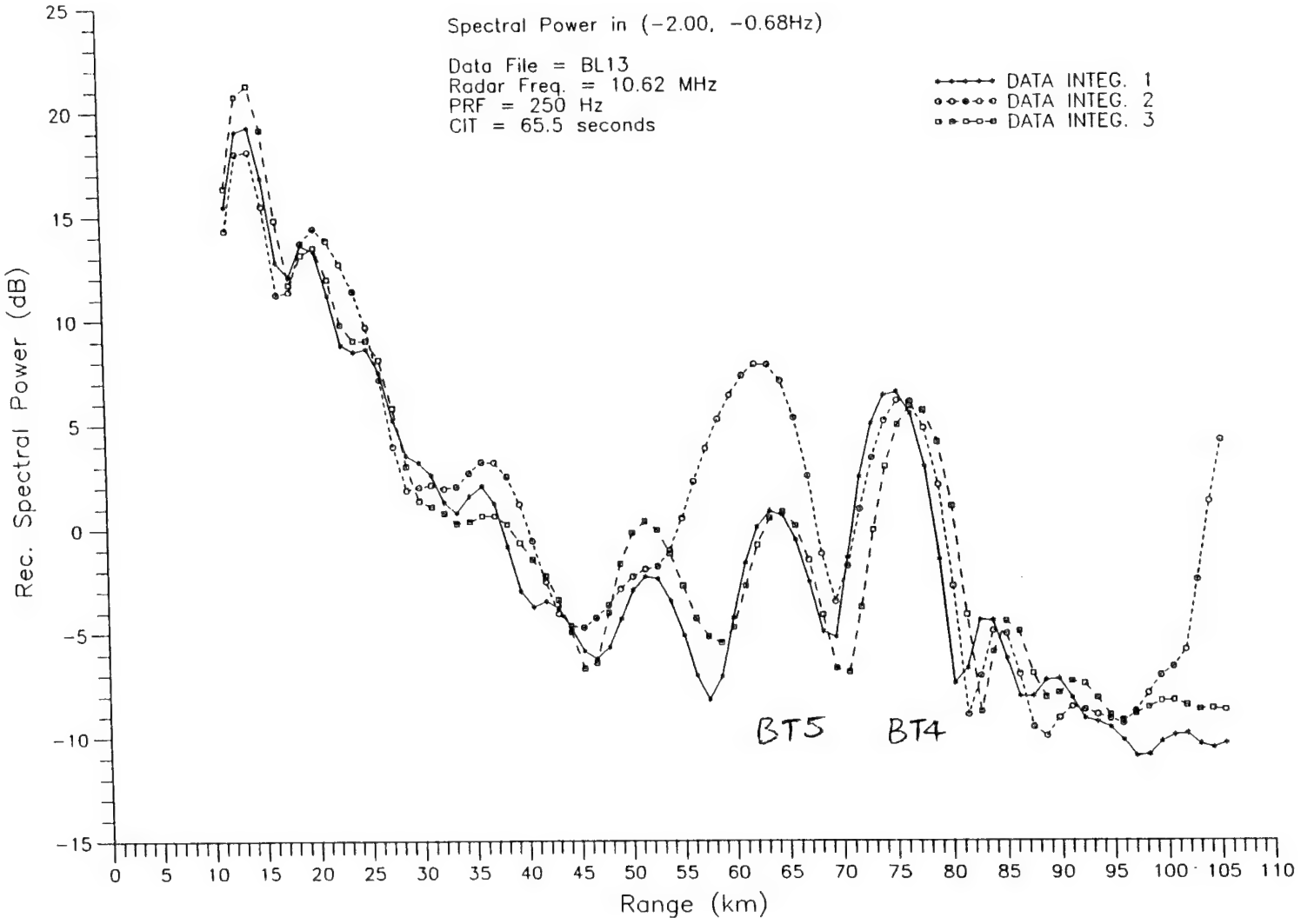


Figure C5 Detection of Half-Wavelength Long Copper Wire at 10.62 MHz

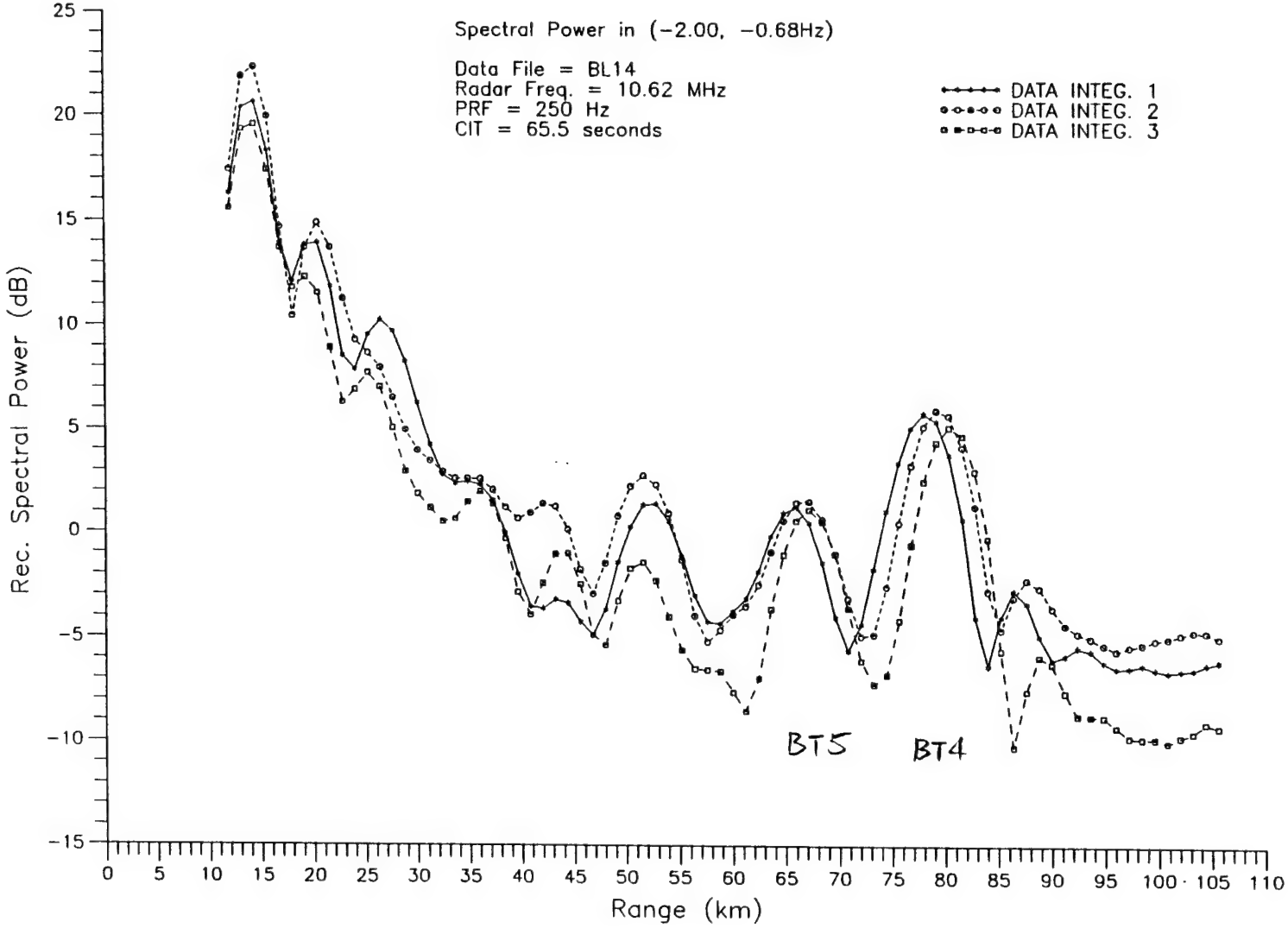


Figure C6 Detection of Half−Wavelength Long Copper Wire at 10.62 MHz

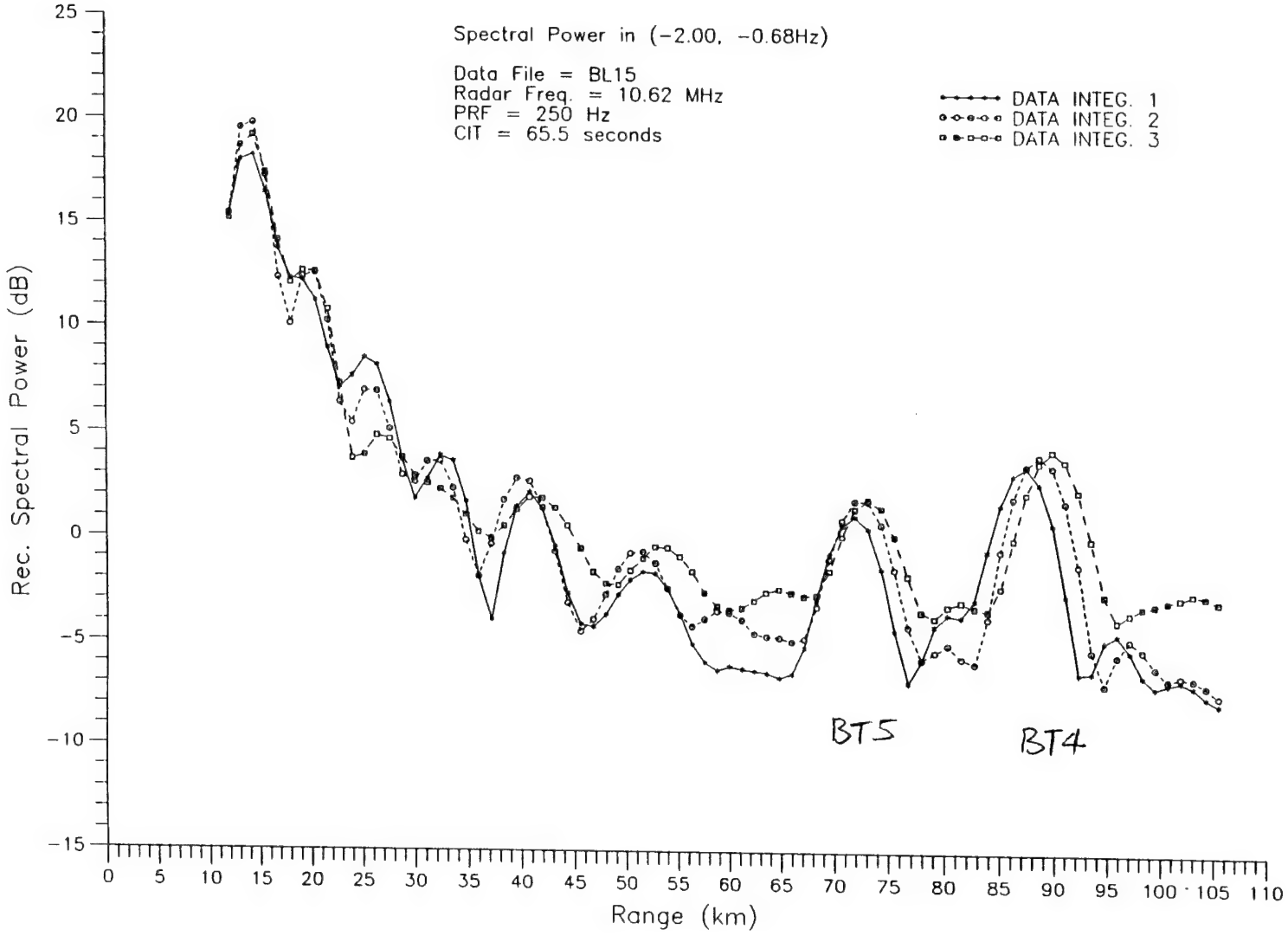


Figure C7 Detection of Half-Wavelength Long Copper Wire at 10.62 MHz

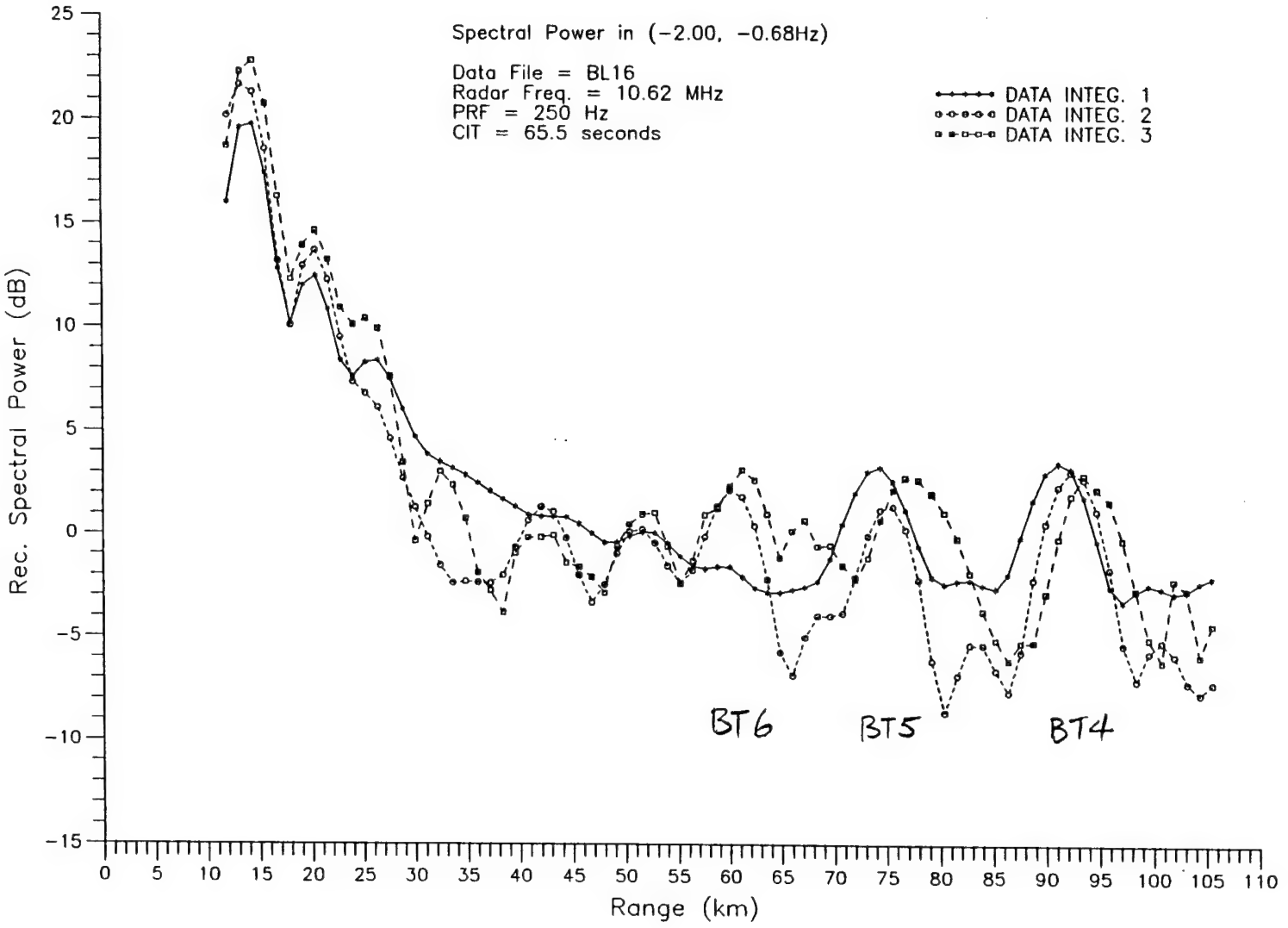


Figure C8 Detection of Half−Wavelength Long Copper Wire at 10.62 MHz

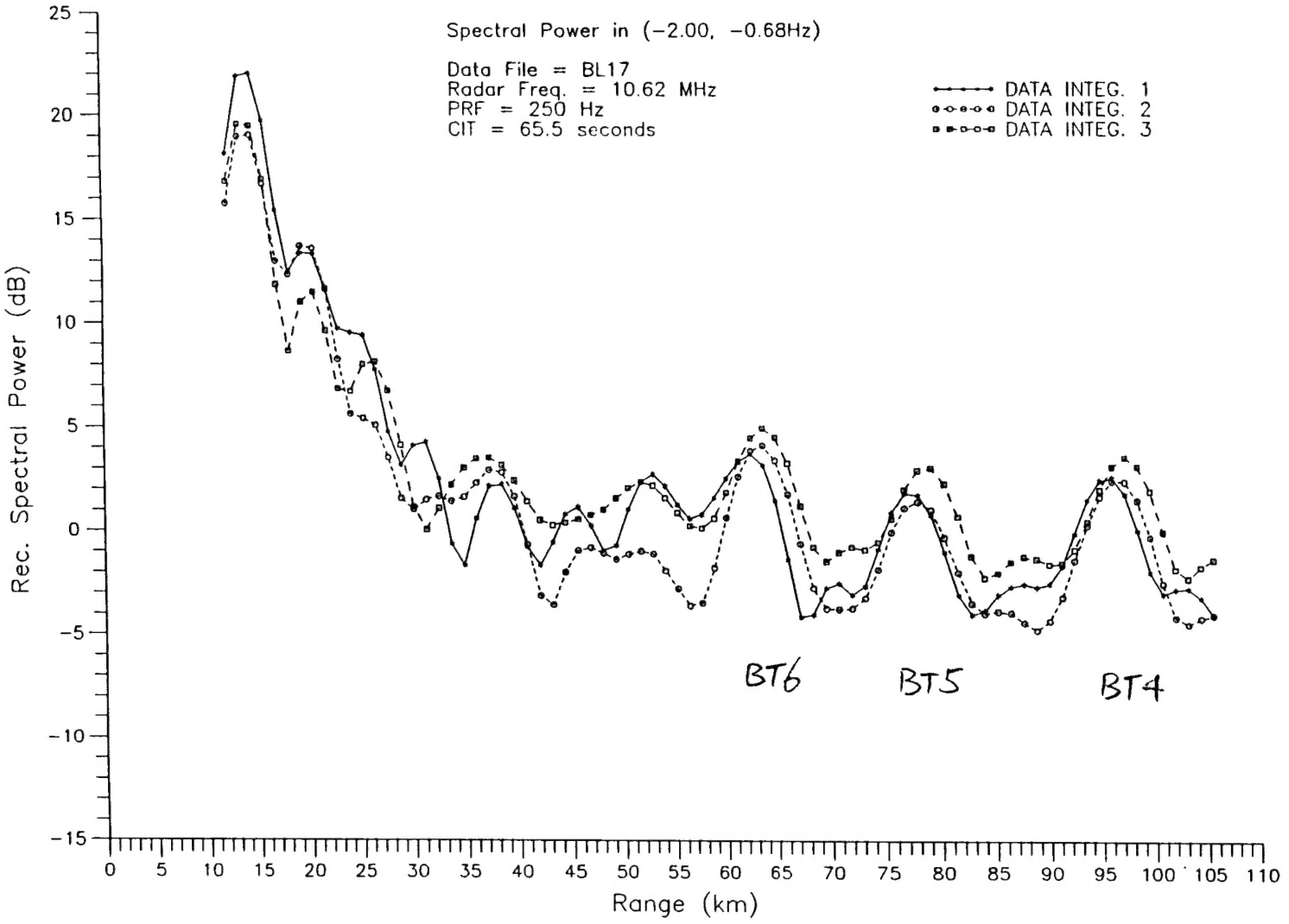


Figure C9 Detection of Half−Wavelength Long Copper Wire at 10.62 MHz

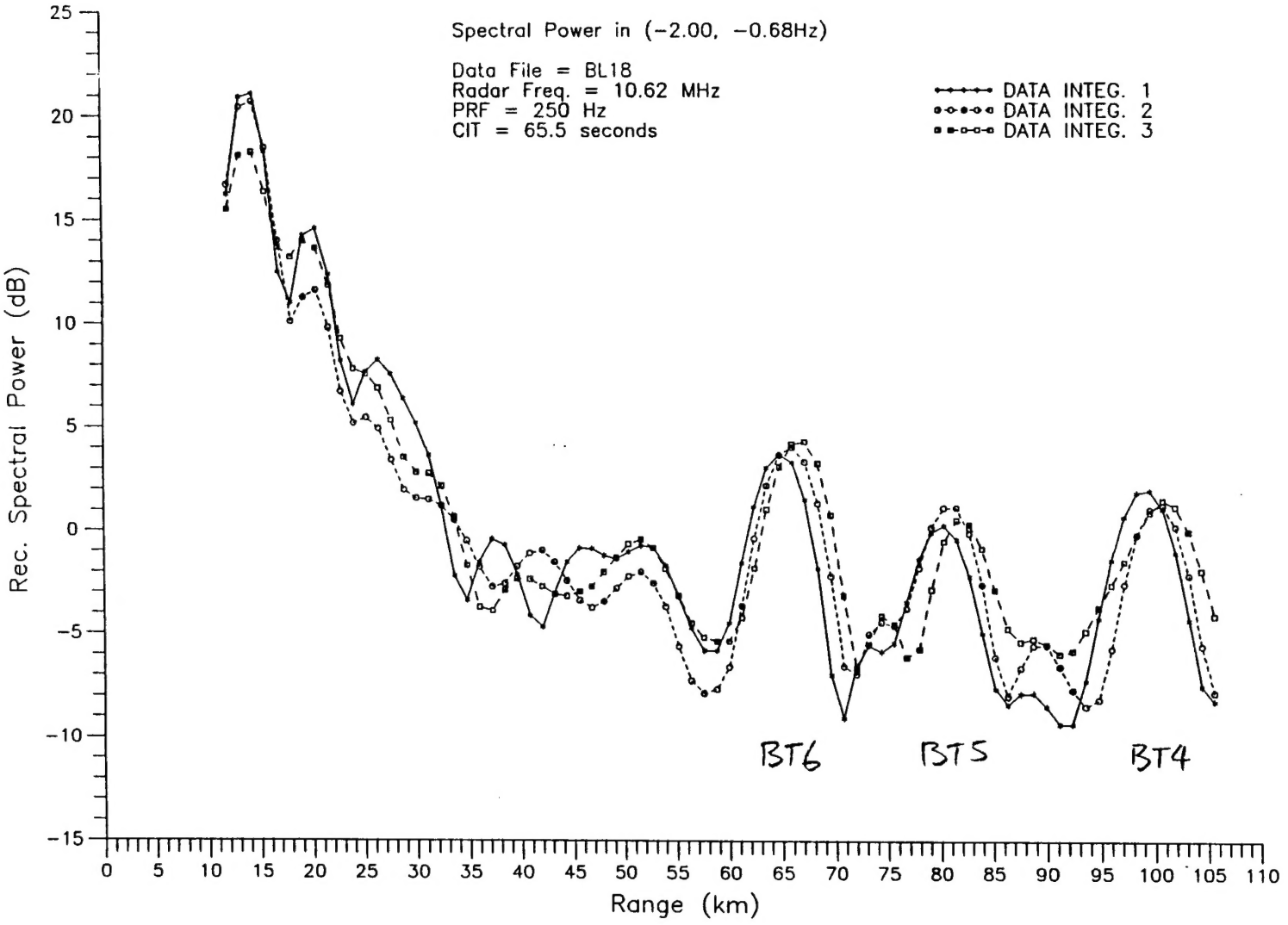


Figure C10 Detection of Half−Wavelength Long Copper Wire at 10.62 MHz

UNCLASSIFIED

SECURITY CLASSIFICATION OF FORM
(highest classification of Title, Abstract, Keywords)

## DOCUMENT CONTROL DATA

(Security classification of title, body of abstract and indexing annotation must be entered when the overall document is classified)

1. ORIGINATOR (the name and address of the organization preparing the document. Organizations for whom the document was prepared, e.g. Establishment sponsoring a contractor's report, or tasking agency, are entered in section 8.)

Defence Research Establishment Ottawa

2. SECURITY CLASSIFICATION (overall security classification of the document including special warning terms if applicable)

UNCLASSIFIED

3. TITLE (the complete document title as indicated on the title page. Its classification should be indicated by the appropriate abbreviation (S,C or U) in parentheses after the title.)

An Analysis of the Experimental Data Measured with the Modified HF Surface-Wave Radar at Cape Bonavista (U)

4. AUTHORS (Last name, first name, middle initial)

Leong, Hank W. H.

5. DATE OF PUBLICATION (month and year of publication of document)

July 1997

6a. NO. OF PAGES (total containing information. Include Annexes, Appendices, etc.)

75

6b. NO. OF REFS (total cited in document)

15

7. DESCRIPTIVE NOTES (the category of the document, e.g. technical report, technical note or memorandum. If appropriate, enter the type of report, e.g. interim, progress, summary, annual, or final. Give the inclusive dates when a specific reporting period is covered.)

DREO Technical Report

8. SPONSORING ACTIVITY (the name of the department project office or laboratory sponsoring the research and development. Include the address.)

DND - Defense Research Establishment Ottawa
Surface Radar Section
Shirley's Bay, Ottawa

9a. PROJECT OR GRANT NO. (if appropriate, the applicable research and development project or grant number under which the document was written. Please specify whether project or grant)

05AB11

9b. CONTRACT NO. (if appropriate, the applicable number under which the document was written)

10a. ORIGINATOR'S DOCUMENT NUMBER (the official document number by which the document is identified by the originating activity. This number must be unique to this document.)

DREO REPORT 1312

10b. OTHER DOCUMENT NOS. (Any other numbers which may be assigned this document either by the originator or by the sponsor.

11. DOCUMENT AVAILABILITY (any limitations on further dissemination of the document, other than those omposed by security classification)

( X ) Unlimited distribution
( ) Distribution limited to defence departments and defence contractors; further distribution only as approved
( ) Distribution limited to defence departments and Canadian defence contractors; further distribution only as approved
( ) Distribution limited to government departments and agencies; further distribution only as approved
( ) Distribution limited to defence departments; further distribution only as approved
( ) Other (please specify):

12. DOCUMENT ANNOUNCEMENT (any limitation to the bibliographic announcement of this document. This will normally correspond to the Document Availability (11). However, where further distribution (beyond the audience specified in 11) is possible, a wider announcement audience may be selected.)

UNLIMITED

13. ABSTRACT ( a brief and factual summary of the document. It may also appear elsewhere in the body of the document itself. It is highly desirable that the abstract of classified documents be unclassified. Each paragraph of the abstract shall begin with an indication of the security classification of the information in the paragraph (unless the document itself is unclassified) represented as (S), (C), or (U). It is not necessary to include here abstracts in both official languages unless the text is bilingual.)

This report presents the results of an analysis of the data measured with the experimental High-Frequency Surface-Wave Radar (HFSWR) at Cape Bonavista, after a major modification in the radar receiver. The radar was evaluated at four different radio frequencies (4.3, 10.62, 18.65 and 27.8 MHz) and a target was detected at each of the frequencies. Specifically, a low-flying Beechcraft Kingair was detected beyond the line of sight to a distance of about 110 km when the radar operated at 4.3 MHz with an average transmitter power of about 40 Watts. A low-flying Piper Navajo was detected within the line of sight up to a range of 26 km when the radar operated at 27.8 MHz. Half-wavelength long copper wires (#18 AWG) were used as test targets at the radio frequencies of 10.62 and 18.65 MHz. Each wire was attached to a helium balloon, which was then carried away by a strong outward wind. Some of these targets were tracked to a range of about 101 km at 10.62 MHz, and to a range of about 66 km at 18.65 MHz.

The detection of the Kingair by the HFSWR at 4.3 MHz was also studied by simulation. The simulation results showed that the radar could detect the Kingair up to a distance of 95 km. By comparing the simulation results with the experimental results at 4.3 MHz, we found that the measured performance of the radar agreed well with the theoretical performance in the range interval from 35 to 95 km, when the target was detected beyond the line of sight. The measured target signal-to-noise ratio (SNR) and the theoretical target SNR showed almost the same range dependence in the specified interval, with the measured SNR approximately proportional to $R^{-4.71}$, where R is the target range.

14. KEYWORDS, DESCRIPTORS or IDENTIFIERS (technically meaningful terms or short phrases that characterize a document and could be helpful in cataloguing the document. They should be selected so that no security classification is required. Identifiers, such as equipment model designation, trade name, military project code name, geographic location may also be included. If possible keywords should be selected from a published thesaurs, e.g. Thesaurus of Engineering and Scientific Terms (TEST) and that thesaurus-identified. If it is not possible to select indexing terms which are unclassified, the classification of each should be indicated as with the title.)

High Frequency (HF)
High Frequency Surface Wave Radar (HFSWR)
HFSWR Radar Receiver
Experimental Radar Data
Target Detection
Aircraft Targets
Half-Wavelength Copper Wires
Interference